



UNIVERSITÀ DEGLI STUDI DI PADOVA

DIPARTIMENTO DI INGEGNERIA DELL'INFORMAZIONE

SCUOLA DI DOTTORATO DI RICERCA IN INGEGNERIA DELL'INFORMAZIONE

INDIRIZZO IN BIOINGEGNERIA

XXVII CICLO

**TOWARDS THE APPLICATION OF MULTI-DOF
EMG-DRIVEN NEUROMUSCULOSKELETAL
MODELING IN CLINICAL PRACTICE:
METHODOLOGICAL ASPECTS**

ALICE MANTOAN

DIRETTORE DELLA SCUOLA: *Ch.mo Prof. Matteo Bertocco*

COORDINATORE D'INDIRIZZO: *Ch.mo Prof. Giovanni Sparacino*

SUPERVISORE: *Ch.mo Prof. Claudio Cobelli*

This work is dedicated to my *Family*,
who fills my life of love, joy and safety.

ABSTRACT

New methods able to assess the individual ability of patients to generate motion and adaptation strategies are increasingly required for clinical applications aiming at recovering motor functions. Indeed, more effective rehabilitation treatments are designed to be personalized on the subject capabilities. In this context, neuromusculoskeletal (NMS) models represent a valuable tool, as they can provide important information about the unique anatomical, neurological, and functional characteristics of different subjects, through the computation of human internal variables, such as muscle activations, muscle forces, joint contact forces and moments. A first possible approach is to estimate these values using optimization-based NMS models. However, these models require to make assumptions on how the muscles contribute to the observed movement. More promising are instead NMS models driven by electromyographic signals (EMG), which use experimentally recorded signals that can be considered a direct representation of the subject motor intentions. This allows to account for the actual differences in an individual neuromuscular control system, without making any preliminary assumptions. Therefore these models have the potentialities to provide the level of personalization that is essential for applications in the clinical field.

Although EMG-driven NMS models have been investigated in the literature, even for clinical purposes, they are mostly limited to one degree of freedom (DOF), and consider only the muscles spanning that DOF. Additionally, despite the promising results, they are still not introduced in the clinical practice; the main reason possibly being their complexity, that makes them not usable in clinical context, where standard and reliable procedures are required. The importance of EMG-driven NMS modeling for clinical applications would be even higher with the availability of multi-DOF models, as impairments usually compromise multiple joints. Nevertheless, even if a first multi-DOF EMG-driven NMS model for the lower limbs has been recently introduced in literature, its even greater complexity makes more difficult an analysis of its applicability in the clinical field.

This work represents a first effort towards a critical analysis of multi-DOF EMG-driven NMS models to evaluate their possible use in clinical practice. To achieve this objective, several issues and limitations have been addressed. In the specific, the attention has been focused on two aspects: (i) making the methodology usable, to foster its adoption by multiple laboratories and research groups, and to facilitate sensitivity analyses required to assess its accuracy; (ii) highlighting the effects of some methodological aspects related to data

acquisition and processing, and evaluating their impact on the accuracy of estimated parameters and muscle forces. This analysis is even more important for multi-DOF EMG-driven NMS model as it is still not present in the literature.

To accomplish the first goal, a software tool (MOtoNMS) has been developed and it is freely available for the research community. It is a complete, flexible, and user-friendly tool that allows to automatically process experimental motion data from different laboratories in a transparent and repeatable way, for their subsequent use with neuromusculoskeletal modeling software. MOtoNMS generalizes data processing methods across laboratories, and simplifies and speeds up the demanding data elaboration workflow. This simplification represents an indispensable step towards an actual translation of NMS methods in clinical practice.

The second part of the work has been, instead, dedicated to analyze the impact on model parameters and muscle forces prediction of different techniques for EMG data collection and processing that are feasible for clinical settings, in particular concentrating on EMGs normalization. Indeed, moving EMG-driven NMS modeling towards clinical applications that deal with multiple DOFs requires to carefully consider subject's motor limitations due to his/her mobility impairments. This results in a rethinking about the methodologies for data acquisition and processing. Therefore, the impact of using only data from walking trials on both calibration of model parameters and computing the maximum EMG values needed for the normalization step, has been assessed with two case studies. Moreover, a protocol for the collection of maximum voluntary contractions has been proposed. This protocol is suitable for multiple DOFs applications involving patients with reduced motor ability and it requires only low-cost and easy to acquire tools to make it applicable in any laboratory.

The research proposed in this thesis provides tools to simplify the use of multi-DOF EMG-driven neuromusculoskeletal models and proposes analyses and procedures to evaluate the accuracy and reliability of the obtained results with the aim of pursuing clinical applications.

SOMMARIO

Le applicazioni cliniche in ambito riabilitativo sono sempre più alla ricerca di strumenti che permettano di valutare la capacità individuale del paziente di generare il movimento ed eventuali meccanismi di compensazione, questo al fine di sviluppare delle strategie di intervento che risultino personalizzate e quindi più efficaci. In questo contesto, gli strumenti prodotti dalla ricerca sulla modellazione neuromuscoloscheletrica (NMS) sono di particolare interesse perché riescono a dedurre le caratteristiche anatomiche, neurologiche e funzionali specifiche di un soggetto, attraverso la stima di variabili dinamiche interne come le attivazioni e le forze muscolari, e le forze di contatto e i momenti ai giunti. Queste quantità possono essere stimate utilizzando modelli neuromuscoloscheletrici basati su tecniche di ottimizzazione, ma a patto di fare assunzioni a priori su come i muscoli contribuiscono al movimento che viene osservato. Più promettente è invece l'approccio della modellazione neuromuscoloscheletrica guidata dai segnali elettromiografici (EMG), che fa invece uso di segnali raccolti sperimentalmente che sono una diretta rappresentazione delle intenzioni motorie del soggetto. Questo permette di evitare assunzioni e di riuscire invece ad individuare le differenze nel comportamento del sistema neuromuscolare in diversi soggetti. Questa caratteristica li rende pertanto più adatti ad applicazioni in campo clinico, perché potenzialmente più adatte a fornire un maggior livello di personalizzazione.

La letteratura presenta diversi studi, anche in ambito clinico, che utilizzano modelli neuromuscoloscheletrici guidati da segnali EMG, ma la loro applicazione è di solito limitata a un grado di libertà e ai muscoli a questo collegato. Nonostante questi risultati, non sono ancora stati introdotti nella pratica clinica, e ciò è dovuto principalmente alla complessità insita nel loro uso, che li rende ancora non utilizzabili in un contesto in cui standardizzazione e affidabilità sono proprietà fondamentali. L'importanza della modellazione basata su segnali EMG in ambito clinico diventa ancora più importante se consideriamo modelli a più gradi di libertà, perché spesso le lesioni interessano più articolazioni. Purtroppo, anche se un primo modello a più gradi di libertà è stato da poco introdotto in letteratura, la sua maggiore complessità rende ancora più complicato analizzare la sua applicabilità in ambito clinico.

Questo lavoro rappresenta un primo sforzo per valutare, attraverso un'attenta analisi critica, la possibilità di introdurre nella pratica clinica modelli neuromuscoloscheletrici guidati da segnali EMG per sistemi a più gradi di libertà. Per raggiungere questo obiettivo, diver-

si problemi e limiti sono stati evidenziati ed affrontati. In particolare, l'attenzione si è focalizzata su due aspetti: (i) rendere la metodologia più facilmente applicabile, per semplificare la sua adozione da parte di diversi laboratori e gruppi di ricerca, e facilitare analisi di sensibilità necessarie a valutarne l'accuratezza; (ii) evidenziare la criticità di alcuni aspetti metodologici legati all'acquisizione e al processamento dei dati, e quantificarne gli effetti sull'accuratezza dei parametri stimati e sulle forze muscolari predette. Questa analisi si rende maggiormente necessaria per modelli a più gradi di libertà perché non ancora presente in letteratura.

Per raggiungere il primo obiettivo è stato sviluppato uno nuovo strumento software (MOtoNMS), che è ora disponibile alla comunità di ricerca con licenza gratuita. È uno strumento completo, flessibile, e facile da usare che permette di processare automaticamente, in modo trasparente e ripetibile, dati di movimento acquisiti sperimentalmente da laboratori con diversa strumentazione, preparandoli per il loro successivo uso con software di simulazione neuromuscoloscheletrica. MOtoNMS permette di uniformare i metodi di elaborazione dei dati tra laboratori, semplificando e velocizzando il lungo flusso di lavoro richiesto per generare i dati in ingresso ai software di modellazione. Questa semplificazione rappresenta pertanto un passo indispensabile per portare la modellazione neuromuscoloscheletrica nella pratica clinica.

La seconda parte del lavoro è stata invece dedicata ad analizzare tecniche per la raccolta e il processamento dei segnali EMG, con particolare riferimento alla loro normalizzazione, che possano essere proposte in ambito clinico, valutando la sensibilità dei parametri del modello e quindi della predizione delle forze muscolari. Portare la modellazione NMS guidata da segnali EMG verso applicazioni cliniche che coinvolgono più gradi di libertà richiede infatti attente considerazioni legate ai limiti motori del paziente dovuti alle diverse lesioni che può presentare. Questo comporta di ripensare la metodologia per l'acquisizione e l'elaborazione dei dati. Per questo si è valutato l'impatto di usare dati raccolti da sole prove di camminata sia per la calibrazione dei parametri che per la normalizzazione dei valori EMG. Inoltre è stato proposto un protocollo per la raccolta di massime contrazioni volontarie adatto ad applicazioni a più gradi di libertà, che coinvolgano pazienti con comportamento motorio parzialmente compromesso, e caratterizzato dall'utilizzo di sola strumentazione economica e facilmente reperibile per poter essere adottato in qualsiasi laboratorio.

La ricerca proposta in questa tesi fornisce strumenti per semplificare l'uso di modelli neuromuscoloscheletrici a più gradi di libertà guidati da segnali EMG, e propone analisi e procedure per valutare accuratezza e affidabilità dei risultati, ai fini di applicazioni in ambito clinico.

ACKNOWLEDGEMENTS

I would like to thank *Dr. Zimi Sawacha* for proposing me this research project and for letting me focusing on it. Thanks for have followed my path and for your comprehension in the most difficult moments. I would also like to acknowledge *Prof. Claudio Cobelli* for funding my research.

I am also grateful to *Dr. Monica Reggiani*, who introduced me to the computer science world, teaching me the many things I have learned during the way. Thanks for your patience and your constant support.

I would like to thank all my colleagues at the *Bioengineering of Human Movement Laboratory* of the University of Padova, for sharing with me these more than three years: *Fabiola Spolaor*, *Alessandra Scarton*, *Annamaria Guiotto*, *Martina Negretto*, and also *Silvia Del Din* and *Alberto Rigato*. Thanks for your friendship, for putting up with me and for making me smile even in the worst moments.

I would like to thank all the members of the *Rehabilitation Engineering Group* at the Department of Management and Engineering of the University of Padova, for making me part of your great group.

A special thanks is dedicated to *Michele Vivian*: thanks for being my mate since the beginning of this adventure and for the moments of work and the spare time we have shared abroad and during all the path.

A special thanks is for *Elena Ceseracciu*: without your guidance and constant suggestions (even from remote), I probably would have never ended this PhD.

I would like to dedicate a special thanks also to *Michela Riz*: it has been a pleasure to share these years with you. Thanks for being my friend and for all you have done for me: the breaks, the coffees, the cakes, and your support in any moment and situation, till the deadline of this thesis. These 3-years PhD would have not been the same without you.

Finally, I am also grateful to my dear *family*, for being my life.

CONTENTS

1	INTRODUCTION	1
1.1	Introduction to neuromusculoskeletal modeling	1
1.2	Clinical relevance of neuromusculoskeletal modeling applications	4
1.3	The Problem	7
1.4	Aims of the thesis	9
1.5	Thesis Outline	10
2	MULTI-DOF EMG-DRIVEN NMS MODELING	13
2.1	State of the Art of EMG-driven NMS models	13
2.2	The multi-DOF EMG-driven NMS model	16
2.2.1	Muscle Activation Dynamics	17
2.2.2	Muscle Contraction Dynamics	22
2.2.3	Moment Computation	23
2.2.4	Model Calibration	24
2.3	CEINMS: an EMG-driven NMS model implementation	27
2.4	Workflow	28
2.4.1	Data collection: motion analysis	28
2.4.2	Musculoskeletal modeling	30
2.4.2.1	Scaling	33
2.4.2.2	Inverse Kinematics	33
2.4.2.3	Inverse Dynamics	34
2.4.2.4	Muscle Analysis	34
2.4.3	EMGs processing	35
2.4.4	Input for the NMS model	35
2.5	Limitations	36
3	MOTONMS: A MATLAB TOOLBOX TO PROCESS MOTION DATA FOR NMS MODELING AND SIMULATION	39
3.1	Introduction	39
3.2	Aims	41
3.3	Toolbox Description	41
3.3.1	Data Elaboration	43
3.3.1.1	Dynamic Trials Elaboration	43
3.3.1.2	Static Trials Elaboration	43
3.3.2	Data Management	45
3.3.2.1	Input Data Loading	45
3.3.2.2	Output Data Generation	46
3.3.2.3	Data Storage Structure	46
3.3.3	System Configuration	46
3.4	Results	49
3.5	Discussion	52
3.6	MOtoNMS and the Open-Source approach	55
3.7	Conclusions and Future Works	56

4	THE NMS MODEL CALIBRATION: EMG NORMALIZATION	59
4.1	Introduction	59
4.2	Aims	65
4.2.1	Aim of the First Study	65
4.2.2	Aim of the Second Study	65
4.3	First Study	65
4.3.1	Data Collection	68
4.3.1.1	Subject and Experimental Setup	68
4.3.1.2	Manual MVC Protocol	68
4.3.2	Processing Workflow	70
4.3.2.1	Data preparation	70
4.3.2.2	Musculoskeletal modeling and simulation	71
4.3.2.3	EMG-driven NMS model calculations	71
4.3.3	Data Analysis Procedure	73
4.3.4	Results	75
4.3.4.1	EMG Analysis	75
4.3.4.2	Predicted Torque	76
4.3.4.3	Calibrated Muscle Parameters	84
4.3.4.4	Mean Muscles Forces	84
4.3.4.5	Muscle Contributions to the Net Joint Moments	86
4.3.4.6	Flexors and Extensors Contributions to the Net Joint Moments	86
4.3.5	Discussion	86
4.4	Second Study	98
4.4.1	Data Collection	99
4.4.1.1	Subject and Experimental Setup	99
4.4.1.2	Minimal MVC Protocol	99
4.4.2	Processing Workflow	102
4.4.3	Data Analysis Procedure	102
4.4.4	Results	102
4.4.4.1	EMG Analysis	102
4.4.4.2	Predicted Torque	105
4.4.4.3	Calibrated Muscle Parameters	105
4.4.4.4	Mean Muscles Forces	105
4.4.4.5	Muscle Contribution to the Net Joint Moments	113
4.4.4.6	Flexors and Extensors Contribution to the Net Joint Moments	113
4.4.5	Discussion	113
4.5	Conclusions and Future Works	125
5	CONCLUSIONS	129
	BIBLIOGRAPHY	133

INTRODUCTION

1.1 INTRODUCTION TO NEUROMUSCULOSKELETAL MODELING

Human movement is driven by neural commands, that stimulate the activation of many muscles on multiple joints. Muscles are force generators: as a response to the neural drive, they develop forces that are transmitted by tendons to the body segments to which they are attached, causing the generation of joint moments. These, in turn, result in acceleration of joints and segments, and thus into movement. In this, muscles in conjunction with tendons act as an interface between the central nervous system and the body segments. The mechanism they used to accomplish this role is complex, since multijoint movement requires the coordination of many muscles, that contribute to accelerate even joints they do not span (Zajac, 1993). But mostly, muscles can be activate by the nervous system with different strategies to produce the same prescribed joint moment and motion. This is a crucial property of our neuromusculoskeletal system, know as redundancy. Understand how muscles activate, generate force and coordinate the actuation of multiple joints simultaneously is essential to gain insights into the mechanisms underlying human movement, and is regarded as a great challenge in many fields, from biomechanics to motor control and rehabilitation.

Direct measurement of the individual muscle forces contribution to movement is not feasible in most cases, and therefore non-invasive methods based on models have to be developed. Two opposite approaches are generally used to investigate the biomechanics of human movement and attain predictions of muscle forces: forward dynamics and inverse dynamics (Buchanan et al., 2004; Erdemir et al., 2007; Chèze et al., 2012).

The latter starts by considering the position and the external forces acting on a body. It has been widely used due to the availability of joint kinematics data and ground reaction forces from gait analysis. These variables allow the estimation of joint moments, but each of them represents the resultant action of all muscles spanning the corresponding joint. Therefore, the contribution of each single muscle is not accounted. This approach yields two main limitations: firstly, the calculation of muscle forces from joint moments leads to a large set of possible solutions, as multiple muscles span each joint and can contribute differently. Secondly, information about co-contraction of agonist and antagonist muscles cannot be derived. In addition, supposing muscle forces can be determined, there is no current model

that enables the inverse transformation from muscle forces to muscle activations.

The problem of the redundancy of the neuromusculoskeletal system has been addressed by minimizing an objective function selected for the movement under investigation. Optimization methods, such as static optimization, combined with a model of the musculoskeletal geometry of the human body, have been applied for almost three decades to estimate muscle forces exploiting an inverse dynamics-based approach. These are closed-loop methods that continuously track the joint moments obtained from inverse dynamics calculations and apportion them to the individual muscles crossing a specific joint, under the assumption that each muscle contributes according to a pre-defined objective function. Therefore, muscle activations and forces are found so that they fit joint moments and/or joint angles, and assuming that the chosen criterion is generalizable across subjects and motor tasks. This gives rise to questions regarding the physiological validity of the objective function, as it makes a priori assumptions about how muscles are recruited to produce a given movement, that is, conversely, what we aim to understand. Moving to the clinical field, optimization-based techniques are even more questionable, since it has been shown that muscle excitations strategies are determined by the personal history of training and pathology of the subject (Lloyd and Buchanan, 2001). Furthermore, again the co-contraction of muscles cannot be accounted. This aspect cannot be underestimated: it can lead to a great inaccuracy in the predictions, as co-contraction of muscles is very common. For example, let us assume that the inverse dynamics calculations give a net knee flexion moment of 5 Nm. A static optimization method will probably estimate muscle forces for the hamstrings groups so that they generate a 5 Nm flexion moment. However, the same net knee moment can be achieved with the hamstrings generating a 25 Nm flexion moment, and at the same time the quadriceps generating a 20 Nm extension moment. In such case, the actual contribution of knee flexors muscles will result six time greater than that estimated with static optimization. Thus, an inverse dynamics-based optimization approach, although widely used, cannot reflect the actual differences in an individual neuromuscular control system, especially when motor impairments lead to abnormalities in the muscle activations patterns. It is therefore not recommended to ascertain how muscle contributes to the observed movement of body joints and segments (Zajac, 1993; Buchanan et al., 2004, 2005).

On the opposite site, the problem can be addressed exploiting a forward dynamics approach. In this case, the input is a measure or estimate of the neural drive, which is transformed through a three-step process to obtain joint moments. Firstly, a model of the underlying *muscle activation dynamics* transforms the neural signal into a

time varying measure of the muscle activation ranging from zero to one. Then, a model of the muscle that accounts for the *muscle contraction dynamics* allows the transformation of the muscle activation into muscle force. The tendon, coupled with the muscle, transfers the developed force from the muscle to the bone. For this reason, we will refer to this force as *musculotendon* force, and to the coupling of a muscle with a tendon as *musculotendonous unit* (MTU). The third step is about joint moments computation. A moment for each degree of freedom (DOF) is obtained as the sum of all the musculotendon forces that contribute to that moment, multiplied by their respective moment arms. A model of the musculoskeletal geometry and information about joint angles are required to determine the muscles moment arms (that change as a function of joint angles). Once joint moments are attained, joint movements can be derived through the equations of motion. The process herein described is meant to reproduce how the body actually generate movement, that is the steps by which the neuromusculoskeletal system transforms the neural commands into movement, in terms of joint moments. For this reason, forward dynamics models characterized by these three fundamental blocks (i. e., *muscle activation dynamics*, *muscle contraction dynamics*, *moment computation*) are also referred to as neuromusculoskeletal (NMS) models.

A key-point of this approach is that it requires to provide estimates of the neural commands. These can be obtained still exploiting optimization methods, however the same drawbacks of an inverse dynamics approach occurs in this case. An alternative strategy is to use surface electromyography (EMG) data experimentally recorded as an individual estimate of the neural drive, rather than attempting to predict how muscles are activated to produce a given movement. EMGs are small electrical signals generated in the muscles that induce contraction according to the neural stimulation, and thus they have the potential to reveal the actual activated muscles. They can be detected on the surface of the skin through sensors attached on the body. The term *EMG-driven* is used to indicate that a forward dynamics NMS model uses EMG signals as neural input. Differently from the other approaches, these models implicitly account for individual muscle activation patterns. This strategy allows to overcome the indeterminacy of the neuromusculoskeletal system while accounting for co-contraction and without the need to make any assumption on how the forces applied to a joint are partitioned to surrounding muscles, ligaments and articular surfaces, or the need to satisfy any constraints imposed by a single objective function. This is of extreme relevance to fully understand how the nervous system controls human movement in both healthy and impaired subjects, and to establish a scientific basis for rehabilitation treatment of pathological movements.

EMG-driven forward dynamics models have also been used in combination with an inverse dynamics approach to estimate muscle forces

across a series of joints. Several authors exploit this hybrid approach for the *model calibration*, that is to tune the set of parameters to a subject (Lloyd and Buchanan, 1996; Lloyd and Besier, 2003; Buchanan et al., 2004, 2005). Each of the step defining a NMS model is indeed characterized by complex and non linear relationships, that involve a large number of physiological parameters. These parameters are difficult to be obtained and vary across people (Chèze et al., 2012; Hicks et al., 2015). The musculoskeletal geometry is usually reconstructed using medical imaging techniques and then adjusted to different subjects exploiting scaling procedures (Delp et al., 2007). Most of muscle parameters have been initially defined in the literature from cadaveric studies (Delp et al., 1990), while some authors have proposed they own methods to replace values from literature with individual estimates (Winby et al., 2008; Menegaldo and De Oliveira, 2009; De Groote et al., 2010; De Oliveira and Menegaldo, 2010). Other parameters, such as those that describe the muscle activation dynamics, are even more difficult to be determined (Manal and Buchanan, 2003). Using an hybrid approach, joint moments are obtained from the EMG-driven forward dynamics model and using inverse dynamics. The parameters in the NMS model are determined comparing the joint moments derived from the forward dynamics calculations with the results from inverse dynamics. Since these should be the same, parameters are adjusted until the error between these two is minimized. After the calibration, the NMS model is used in a forward fashion to predict joint moments and muscle forces during novel tasks, that were not used to minimize the model error. This method contributes to account within the model for differences in the neuromusculoskeletal system among subjects, and was found to improve the match between external (inverse dynamics-based) and net muscle moments if compared to the use of parameters from literature (Lloyd and Buchanan, 1996; Lloyd and Besier, 2003). A subject-specific definition of model parameters is therefore of great importance for an actual and more precise representation of the neuromusculoskeletal system.

Models able to accurately reproduce the behavior of the neuromusculoskeletal system of an individual represent a valuable tool to achieve a deeper understanding of the neuromuscular dynamics during human movement both in normal and pathological conditions.

1.2 CLINICAL RELEVANCE OF NEUROMUSCULOSKELETAL MODELING APPLICATIONS

Overcoming limitations of optimization approaches, either forward or inverse, is even more important in the clinical field, for studying pathological movements.

The neuromusculoskeletal system governs our capacity to move. When it is impaired, a number of conditions (e.g., cerebral palsy, stroke,

spinal cord injury, knee osteoarthritis) occurs, and all of them are associated with a decreased ability to perform daily motor activities, such as walking, stair climbing, etc. . . . Rehabilitation treatments play a central role in restoring normal life conditions.

Currently, standard treatment options are available for different mobility impairments. The difficulty in defining a rehabilitation plan stands in the selection among the available techniques, and in determining the optimal values for the parameters associated with the selected therapy (e. g., the level of assistance, the amount and frequency of stimulation, the tasks to promote learning strategies). It is often the case that the treatment is not customized to reflect the uniqueness of the patient, because it is difficult to assess differences among subjects showing similar external behavior, to discover the causes of gait anomalies, to identify where to focus the attention of rehabilitation procedures. Current clinical practice is indeed based mainly on static anatomical data (e. g., x-rays), dynamic functional tests or measurements (e. g., gait analysis), and visual inspection of patients motor abnormalities. Although some of these abnormalities are related to primary observable impairments, others are likely to reflect compensatory activity that is used to optimize the motor patterns in the presence, for example, of muscular weakness, reduced coordinate control or pain. An analysis of the subject baseline characteristics, therefore, do not appear to be sufficient to account for these inner mechanisms. Moreover, clinicians make use of the available information to select the proper intervention based on their subjective experience, rather than consider objective predictions of post-treatment outcomes. This means that, starting from the same clinical data, different clinicians may take different decisions for a particular patient. This general and subjective process of clinical decision making results in treatment outcomes less effective than desired.

It is an evidence that current rehabilitation strategies do not always succeed in recovering motor functions of impaired subjects: sometimes the achievements in relation to the efforts are not satisfying, some others there are no improvements at all. This is mainly due to the large variability among patients, that is becoming essential to take into account. Experiments show that for many treatments *one size fits none* (Fregly et al., 2012), i. e., standard solutions are not effective, since recovery of motor function is specific, that is, the different and unique anatomical, neurological, and functional characteristics of every patient can significantly impact the optimal treatment. An effective rehabilitation plan should therefore include different techniques and therapies that should be combined and personalized based on patient anatomical, neurological, and functional characteristics.

It is conceivable that assessing the ability of individuals to generate motion and adaptation strategies, and achieving a deeper understanding on the relations among the impairments, the original causes of

abnormalities and the clinical outcomes of the treatment could lead to targeted interventions, thus resulting in better clinical outcomes. In that, EMG-driven NMS models have great potential. They can provide important information about the unique anatomical, neurological and functional characteristics of the subjects through the computation of human internal variables, such as muscle activations, muscle forces, joint contact forces and moments, from an individual neural signal. These can be used to identify the target of the rehabilitation program, to predict outcomes of different treatments, or the effect of different parameters within the treatment, based on patient-specific characteristics.

Prediction of muscle forces have already been used for example to identify compensatory strategies for muscle weakness (Neptune et al., 2001; Jonkers et al., 2003), to quantify knee joint contact forces for individuals with osteoarthritis, or to improve kinematics in order to diminish loads on painful knee (Fregly et al., 2007). In the neurological field, muscle excitations were used to compare contributions of paretic and non paretic muscles to body weight support in post-stroke gait (Higginson et al., 2006). Although potentially interesting, these applications relied on optimizations methods. Due to the subsequent lack of subject specific solutions, they are far from being used to prescribe therapeutic interventions.

By now, it is worldwide recognized the immense impact that an accurate and subject-specific model of the human neuromusculoskeletal system could exert over the design of medical interventions and technology (Reinkensmeyer et al., 2012). The use of experimentally recorded EMG signals as estimates of the actual neural input, in combinations with procedures for a subject-specific determination of muscle parameters, can provide the level of personalization required for the applications of NMS models in clinical practice.

At present, there are few studies applying an EMG-driven NMS model to clinical cases. We can mention the work of Besier et al. (2009), in which the authors examined muscle forces at the knee joint during walking and running in patellofemoral pain patients, and the recent investigations on joint contact forces to prevent joint loadings and degeneration in the presence of anterior cruciate ligament rupture (Gardiner et al., 2012, 2013) and knee osteoarthritis (Manal et al., 2010; Kumar et al., 2012; Manal and Buchanan, 2013). A neurological disorder, such as stroke, was also considered by Shao et al. (2009) and Higginson et al. (2012). The first predicted the ankle joint moment during stance for four patients following stroke, suggesting that EMG-driven NMS modeling can provide objective and quantitative information on abnormalities in the muscle activation patterns of post-stroke subjects. Higginson et al. (2012) used instead an hybrid approach: they combined the EMG-driven capability to capture the true neural drive and to provide subject specific parameters, with a forward dynamic sim-

ulation based on optimization to compensate for the limited set of available EMGs. Despite the simulation was about the whole body movement, EMG-driven estimation of muscle activations was provided only for ankle dorsi and plantar flexors muscles.

In the literature, studies exploiting EMG-driven NMS models, either for normal or pathological conditions, are limited to describe movement about a single joint, or more precisely, about a single-DOF. In a clinical context, however, the movement of the whole body, or of a whole limb or side of the body, is usually compromised, and focusing on a single joint, or mostly, on a single-DOF only, is somehow limited. An EMG-driven multi-DOF NMS model able to describe the overall movement of the lower extremities have been developed (Sartori et al., 2012a). However, to date, it has not been applied to pathological conditions.

EMG-driven models that can account for more complex movement, such as those that are typical of daily life activities (i. e., walking), should have an even greater relevance in a clinical context. Enhancing the impact of clinical interventions on the real life of individuals is an essential component of physical medicine and rehabilitation, and personalized NMS models represent a valuable tool to accomplish this goal, despite nor single or multi-DOF models have yet been extensively applied in clinical practice.

1.3 THE PROBLEM

Despite the promising potential, EMG-driven NMS modeling has yet to be introduced in clinical practice. Single-DOF models have been applied in research and for clinical studies, but they have not impacted in the clinical routine, while EMG-driven multi-DOF models have not been investigated at all.

Given these evidences, two are the questions that can be risen up: (i) which are the implications of bringing this approach into clinical practice? that is, which are the barriers that need to be overcome to see an actual adoption of EMG-driven NMS modeling in clinical contexts? (ii) which are the implications of moving from single to multi-DOF models? And mostly, which are those that contribute to limit their applicability?

Two factors are typically determinant when trying to translate research methods into real clinical applications: the possibility of assessing the accuracy and reliability of results, and the availability of tools that make them usable in practice and in different contexts.

A first problem, recognized by many authors, is the difficulty of validating results about muscle forces, due to the impossibility of directly measuring their values (Fregly, 2009; Chèze et al., 2012; Hicks et al., 2015). NMS models validation is currently based on assessing their ability to reproduce joint moments that match those derived from

experimental ground reaction forces and inverse dynamics computations. However, such approach can not guarantee the correctness of estimated muscle forces. Moreover, personalization is crucial for a successful application of NMS models to clinical problems, and it can be achieved by an accurate tuning of parameters, besides the use of EMG signals. Nevertheless, calibration of model parameters is also mostly based on minimizing the error in the prediction of joint moments.

Few sensitivity studies have been proposed to assess the influence of both input data (Oliveira and Menegaldo, 2012) and parameters (Menegaldo and De Oliveira, 2009) on model outcomes, but they are still very limited. The scarcity of this kind of analyses is largely due to the complexity of the problem, which involves a high number of parameters and variables. The modeling workflow is indeed long and elaborate: it requires sophisticated data acquisition sessions and the implementation of procedures for the processing of the data through several steps. Each of them must be performed with accuracy, extensively tested and verified, as it can strongly influence the final results (Hicks et al., 2015). This means that it is not sufficient to look at the model results, especially only in terms of joint moments, but it is instead necessary to go through the whole process to validate and assess the quality of results.

Standard procedures, that allow reproduction and comparison of results obtained at each step and in different conditions would be highly beneficial. Usually, a methodology can be extensively verified and validated for its use in practice if: (i) it can be generalized, that is it does not depend on the instrumentation used for the data acquisition, on software that are not openly available or on custom-made tools constrained to specific conditions, (ii) the contributions of operators do not greatly affect results, (iii) the same acquisition strategy may be used with any subject. In this way, results obtained by different research groups can be transparently compared and more easily assessed. Unfortunately, current state of art of NMS modeling is far from this scenario. In the literature, efforts that attempt to simplify the whole modeling workflow, and towards the creation of tools that allow generalization and standardization across laboratory and groups of the process can not be found.

The complexity implicit in the use of EMG-driven NMS models, not only prevents wider studies and sensitivity analysis, as well as extensive testing to prove accuracy, but also it makes them completely not usable in clinical contexts, where simplified, fast and standard procedures are the only that can actually be adopted.

The introduction of multi-DOF models just exacerbated these aspects. Considering multiple joints means combining the behavior of more muscles, each of those should be accurately described by subject-specific parameters to account for more complex movements. The

number of these parameters, and of the variables that can influence the results inevitably increase. Therefore, can we apply the same acquisition and processing strategies used for single-DOF models, or do we need to adjust them? How should we account for the increased complexity? Are calibrated parameters still an actual representation of the neuromusculoskeletal system of that particular subject? A critical evaluation of muscle forces and parameters obtained from a multi-DOF model is not present in the literature yet. To answer the questions above more investigations are necessary and consequently, the need for tools able to simplify, speed up and standardize the process is even more indispensable.

Finally, trying to exploit EMG-driven NMS models for clinical purposes means having to consider and deal with the limitations due to mobility impairments of pathological subjects. This is more evident when multijoints movements are involved, and may required to redesign the acquisition and calibration strategies. Few attempts to make EMG-driven NMS models feasible in clinical practice accounting for such constraints have been made (Doorenbosch et al., 2005; Gerus et al., 2010), however they are restricted to single-DOF models. Similar investigations for a multi-DOF model, as well as more in-depth analysis, are demanding but still highly required and should be fostered, since not enough efforts have been pursued until now to make this model clinically applicable, despite the great impact it would have on clinical practice.

1.4 AIMS OF THE THESIS

The overall aim of the research conducted during the PhD was to attempt the translation of EMG-driven NMS modeling methods into clinical practice. In order to accomplish this objective, the main limitations that prevent their extensive and reliable application have been addressed.

The work focused on two main aspects:

- (i) making the methodology *usable*, to foster its adoption by multiple laboratories and research groups, and to facilitate sensitivity studies necessary to assess its accuracy.

In the specific, the purpose was to:

- create tools and design methods to generalize and standardize the whole procedure, allowing repeatability and reproduction of results;
- create tools to simplify and speed up the effort-intensive phases of the modeling workflow;
- making these tools flexible and freely available, to satisfy the widest spectrum of requests and contribute to advancements in the field within the research community;

- making these tools user-friendly to be possibly used by clinicians;
- (ii) highlighting and quantifying the effects of some methodological aspects on the *accuracy* of parameters and muscle forces estimation when using a multi-DOF EMG-driven NMS model, that were not addressed in the relative literature before.

In the specific, the focus was on:

- facing methodological issues related to data acquisition and processing to account for pathological conditions and multijoint movements;
- analyzing the sensitivity of model parameters and muscle forces predictions to modeling hypothesis related to EMGs processing, in particular to EMGs normalization;
- designing and testing an alternative method to that applied by Sartori et al. (2012a) for the calibration of the multi-DOF NMS model, characterized by being clinically applicable and laboratory-independent;

The performed research contributes to improving the current state of the art of multi-DOF EMG-driven neuromusculoskeletal modeling by providing instruments that can facilitate its use in practice and further testing the multi-DOF EMG-driven model, which has been previously validated only on one healthy subject and based on the error in the prediction of joint moments, without arguing about the correctness of model parameters resulting from calibration (Sartori et al., 2012a). Other studies applying a multi-DOF EMG-driven model starting from experimental data were not done before. Furthermore, limitations imposed by clinical applications and the influence of some required methodological decisions on calibrated parameters and predicted muscle forces were still not investigated in the literature. This represents, therefore, a first attempt to fill the gaps that prevent multi-DOF EMG-driven NMS modeling from entering the daily and clinical practice.

1.5 THESIS OUTLINE

The research presented in this thesis is organized in four chapters:

Chapter 2 - introduces the multi-DOF EMG-driven model used within this work. Firstly, it presents the current state of the art of EMG-driven models, and then it explains the theoretical background behind the considered multi-DOF model, evidencing its peculiarities with respect to the other single-DOF models available in the literature. The complete workflow that leads to its application is also described,

and the chapter ends highlighting its major limitations.

Chapter 3 - focuses on the first set of objectives. With the intent to facilitate the adoption of NMS modeling techniques by multiple laboratories and research groups, and to encourage their introduction into clinical practice, it presents a software tool, MOtoNMS, developed to standardize and simplify the processing of experimental data for their integration into musculoskeletal software already available (Delp et al., 2007).

Chapter 4 - is related to the second part of the work. It comprises two studies, that aim at evaluating the effects of different EMGs normalization strategies on the calibration of the EMG-driven NMS model. For each of them, the whole methodology used to apply the multi-DOF EMG-driven NMS model and the corresponding results are presented. In particular, besides the estimated joint moments, muscle forces and parameters obtained from calibration are shown.

Chapter 5 - summarizes the results and the novelty of this research, delineating the conclusions and the future research paths.

Neuromusculoskeletal (NMS) models are intended to reproduce the mechanism by which the neuromusculoskeletal system gives rise to movement starting from the subject motor intention. They represent, in a mathematical way, the transformations that take place from a neural excitation, to muscle activation, and then to the subsequent generation of muscle forces and joint moments. EMG-driven NMS models are characterized by the use of experimentally recorded EMG signals as estimate of the individual neural drive, and can be exploited to predict muscle forces and joint moments about either a single or multiple degrees of freedom (DOFs).

2.1 STATE OF THE ART OF EMG-DRIVEN NMS MODELS

The use of EMGs signals into a forward dynamics model to account for different muscle recruitment patterns was pioneered by Hof and van den Berg (1981). Afterwards, EMG-driven NMS models have been developed by several research groups to estimate individual muscle forces throughout a wide range of tasks and at different anatomical locations, such as ankle (Shao et al., 2009; Menegaldo and De Oliveira, 2009; Gerus et al., 2010), knee (White and Winter, 1992; Lloyd and Buchanan, 1996; Lloyd and Besier, 2003), lower back (McGill, 1992; Granata and Marras, 1995; Nussbaum and Chaffin, 1998), elbow (Manal et al., 2002; Buchanan et al., 2004; Koo and Mak, 2005), wrist (Buchanan et al., 1993), and shoulder (Laursen et al., 1998). Due to difficulties in measuring muscle forces, the accuracy of EMG-driven models is usually assessed by comparison with joint moments computed by applying an inverse dynamics approach to ground reaction forces and kinematics experimentally measured. Early EMG-driven models were unable to achieve a satisfying level of agreement between the predicted joint moments and those calculated via inverse dynamics.

First attempts to model calibration

Several different methods were proposed to improve the accuracy of models predictions. McGill (1992), for instance, introduced an error term, called *gain*, as a mean to guarantee the matching. An alternative approach was that of altering the values of specific parameters within the model, regarded as *calibration parameters*, so that the estimated muscle moments match the external joint moments resulting from inverse dynamics computations. Implicit to an EMG-driven model indeed, are models for the muscle activation dynamics, the muscle

contraction dynamics, and for the musculoskeletal geometry, which entails a large set of parameters that can condition the behavior of the model. Initially, most of them were assigned based on cadaver measurements, and thus did not account for variations among subjects. Hatze (1981) and Van den Bogert et al. (1993) were the first to use non linear least-squares optimization to determine the muscle parameters from different subjects that minimize the error in the prediction of joint moments. This method was then extended by Lloyd and Buchanan (1996) to assess the loading of muscles and soft tissues at the knee. They found that the prediction error could be reduced using this technique, even if other possible sources of error were recognized and discussed.

Lloyd's EMG-driven model

EMG-driven models were used in static/isometric tasks, or for a limited set of dynamic tasks, until the work of Lloyd and Besier (2003), who successfully tested their knee model across a wide range of tasks and dynamic conditions (i. e., approximately 30 tasks performed on a Biodex dynamometer or within a gait laboratory, including running). The outcome of this study represented a significant advancement for EMG-driven modeling techniques, enlarging the set of movement tasks for which they could be used. In order to be able to account for many different dynamic conditions, the authors stressed the importance of assigning an anatomical and physiological basis to the model parameters, and of adjusting them to subject-specific values within a calibration process, which they implemented using a nonlinear least squares optimization, as in Lloyd and Buchanan (1996).

Winby et al. (2008) proposed to distinguish between anthropometric scaling, which can be accomplished using analytical methods to scale parameters from initial generic values to the size of an individual, and functional scaling, that accounts for the different muscle operating conditions in several movements, and that can be better performed with an optimization process after anthropometric adjustment. Some others authors used scale factors based on anthropometry to fit parameters available in the literature to specific individuals (Menegaldo and De Oliveira, 2009), or attempted to exploit more sophisticated techniques such as ultrasound (De Oliveira and Menegaldo, 2010), without involving optimization procedures. They argued that optimization strategies prevent to assess the influence of model and input processing inaccuracies on the results (Oliveira and Menegaldo, 2012). Nevertheless, their models were only used in static/isometric conditions.

Lloyd and Besier (2003) model experienced a significant diffusion and this is likely due to its possibility to investigate dynamic tasks with reasonable accuracy, while allowing a subject-specific estimation of model parameters. It indeed made possible the application of EMG-

driven NMS modeling to the study of human movement. Moreover, this model is one of the few in the literature that accounts for the non linearity among the recorded EMGs and the muscle activation (Potvin et al., 1996; Manal et al., 2002; Manal and Buchanan, 2003; Buchanan et al., 2004). Many researchers, indeed, assume that EMG and muscle forces are linearly related, despite this is not the case, as shown by Heckathorne and Childress (1981) and Woods and Bigland-Ritchie (1983)

Finally, differently to other models in the literature, a unique feature of Lloyd and Besier (2003) model is the introduction of a relationship that describes the coupling between muscle activation and optimal fiber length, which was previously reported by Huijing (1995) and Guimaraes et al. (1994).

Applications based on Lloyd's EMG-driven model

Several studies on human gait have been carried on based on this EMG-driven NMS mode, both on healthy (Buchanan et al., 2005; Lloyd et al., 2005; Winby et al., 2009b) and pathological populations. Neurological disorders involving alteration of muscle activation and movement patterns are of main interest. Knowledge of how muscles are activated and contribute to the altered movement can impact the design of more effective rehabilitation strategies based on the identification of the original causes of gait abnormalities (Shao et al., 2009; Higginson et al., 2012). A second area of applications is orthopedics. The EMG-driven model has been used to estimate joint contact forces and altered joint loading conditions in patients with knee osteoarthritis (Manal et al., 2010; Kumar et al., 2012; Manal and Buchanan, 2013) and ACL deficiency (Gardinier et al., 2012, 2013), in order to understand the mechanical factors that may be involved in the progression of joint degeneration. This would allow the design and the analysis of different rehabilitation interventions to reduce the joint internal loads.

However, all the applications mentioned above, rely on a model that accounts only for one selected DOF of the human limbs, and for the muscles spanning that specific DOF (*single-DOF* models). In this, the activity of the associated muscles is constrained to satisfy the joint moment or motion for the only considered DOF. Consequently, the model predicts muscle forces crossing one joint and the moment about that single DOF. This represents a significant limitation, since it is questionable if the estimated muscle forces are truly representative of the real muscle behavior. Indeed, human movement requires the coordination of many muscles that span multiple joints and develop forces that satisfy multiple DOFs. Single joint models do not account for the possibility that muscles can accelerate joints they do not span (Zajac, 1993). To achieve a deeper understanding of the neuromuscular dynamics during human movement, this aspect cannot be

neglected and moving to multijoints models is crucial. These should allow constraining the operation of muscles so that the forces they produce satisfy the joint moments simultaneously generated at multiple DOFs.

To our knowledge, only one multi-DOF EMG-driven NMS model can be found in the literature, and it has been developed starting from the original single-DOF model of Lloyd and Besier (2003). Two studies proposed its application: Barrett et al. (2007) and Sartori et al. (2012a). The second one focuses on demonstrating that the multi-DOF model solutions provide a prediction of the actual muscle behavior that is more accurate than those possible with the previously applied single-DOF models, and that pursue this technique is essential to better address the important and different scientific questions previously approached using single-DOF EMG-driven modeling. Barrett et al. (2007), instead, showed the importance of a multijoints model directly describing the effect of eight major muscles on hip, knee and ankle kinematics during swing, but concluded that a clinical application of multi-DOF EMG-driven modeling needs to be further and extensively investigated.

Prior to follow this recommendation, attempts to use this multi-DOF model in combination with optimization (Sartori et al., 2014) or using muscle synergies as input (Sartori et al., 2013) have been tested very recently on a healthy population of five subjects, mainly to overcome limitations related to EMG signals acquisition and processing. If compared to the single-DOF model, therefore, the applications of a real EMG-driven multi-DOF EMG-driven NMS model are still limited to only two studies, that involved, in one case, data from Winter (2009), while in the second a single healthy subject.

To date, other studies analyzing the feasibility and the accuracy of the application of a multi-DOF EMG-driven NMS model both in research and clinical practice, have not been made yet and should be strongly encourage.

2.2 THE MULTI-DOF EMG-DRIVEN NMS MODEL

This section reviews the theoretical background of EMG-driven NMS models, firstly describing the common structure, and then characterizing each component as part of the first, and actually the only, multi-DOF EMG-driven NMS model that has been presented in the literature to estimate muscle forces and joint moments in the lower limbs. This model has been proposed by Sartori et al. (2012a), who extended to multiple DOFs the previously published and extensively validated single-DOF model developed by Lloyd and Besier (2003). It differs in that it allows to constrain muscles to produce forces that satisfy the joint moments simultaneously generated at multiple DOFs in multiple joints, including the hip, knee, and ankle joints.

Lloyd and Besier (2003) model estimated the forces of 13 musculotendon units (MTUs) crossing the knee joint to predict the knee flexion-extension moment, while in Sartori et al. (2012a), the NMS model was able to use EMG signals from 16 muscles groups to drive 34 MTUs and satisfy the resulting joint moments simultaneously produced about hip adduction-abduction (HipAA), hip flexion-extension (HipFE), knee flexion-extension (KneeFE), and ankle plantar-dorsi flexion (AnkleFE), during different motor tasks.

The main structure of any EMG-driven NMS model is composed of three main parts: (i) muscle activation dynamics, (ii) muscle contraction dynamics, and (iii) moment computation (Fig. 1). Lloyd and

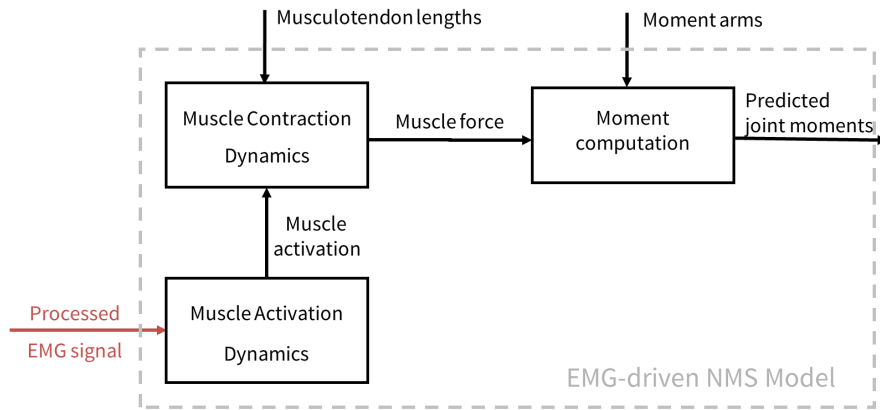


Figure 1: Schematic structure of an EMG-driven NMS model.

Besier (2003) model involves a fourth step for the calibration of parameters, which has been inherited by all its subsequent applications, including this multi-DOF model. The main structure is indeed defined as in Lloyd and Besier (2003), and it will be here described. Peculiarities of the multi-DOF model will be highlighted.

2.2.1 Muscle Activation Dynamics

Muscle activation dynamics is the process of transforming normalized linear envelopes, $(e(t))$, previously obtained from raw EMG signals into an estimate of how much a muscle is activated towards the generation of force (Fig. 2). This step is necessary since the smooth EMG percentage profile resulting from low pass filtering, rectification and normalization of the experimentally recorded EMG signal does not provide an appropriate representation of muscle activation values. A first reason is that it exists a delay between the time of the EMG and that of the corresponding force generation, known as electromechanical delay (Corcos et al., 1992), that is not accounted. Secondly, it was observed that processed EMG signals have a shorter duration than the resulting forces, and that muscle activation is a function of its

recent history (Zajac, 1989). Van Ruijven and Weijs (1990) suggested to include a model of the muscle twitch response to consider these aspects in the modeling and better describe the whole process. According to Milner-Brown et al. (1973), the twitch response can be modeled as a critically damped second-order differential system, that can be expressed in a discrete form and solved as a recursive filter (Thelen et al., 1994; Lloyd and Besier, 2003). This is given by:

$$u_j(t) = \alpha e_j(t - d) - \beta_1 u_j(t - 1) - \beta_2 u_j(t - 2) \quad (1)$$

where $e_j(t)$ is the filtered, rectified, and normalized EMG of muscle j at time t ; $u_j(t)$ the neural activation (as defined in Buchanan et al. (2004)) of muscle j at time t ; α the gain coefficient for muscle j ; β_1 , β_2 the recursive coefficients for muscle j that determine the second order dynamics; and d the electromechanical delay. Thus, the normalized EMG values, $e(t)$, are mapped to the neural activation values, $u(t)$ (Fig. 2), according to Eq. 1 and through four parameters (d , α , β_1 , β_2). A set of constraints are required to ensure a positive stable solution

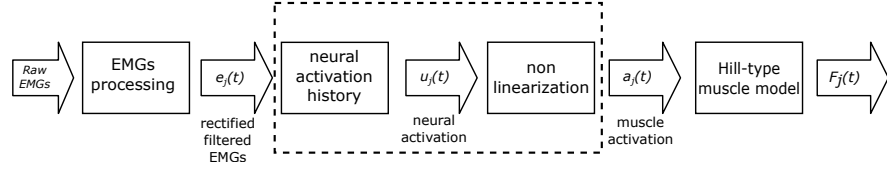


Figure 2: Schematic representation of the steps involved when estimating muscle forces from EMG signals. The transformations from $e(t)$ to $a(t)$ that characterize the muscle activation dynamics are illustrated by the dashed rectangle. The subscript j indicates an individual muscle.

(Eq. 2) and a unit gain for the filter (Eq. 4), so that neural activation does not exceed 1:

$$\begin{aligned} \beta_1 &= C_1 + C_2 \\ \beta_2 &= C_1 \cdot C_2 \end{aligned} \quad (2)$$

where

$$\begin{aligned} |C_1| &< 1 \\ |C_2| &< 1 \end{aligned} \quad (3)$$

and

$$\alpha - \beta_1 - \beta_2 = 1 \quad (4)$$

The values of C_1 and C_2 determine the impulse response of the second-order filter. If they are both positive, the result is an underdamped response, while if they assume negative values or they have different sign, with $|C_1| > |C_2|$, the filter has a damped response.

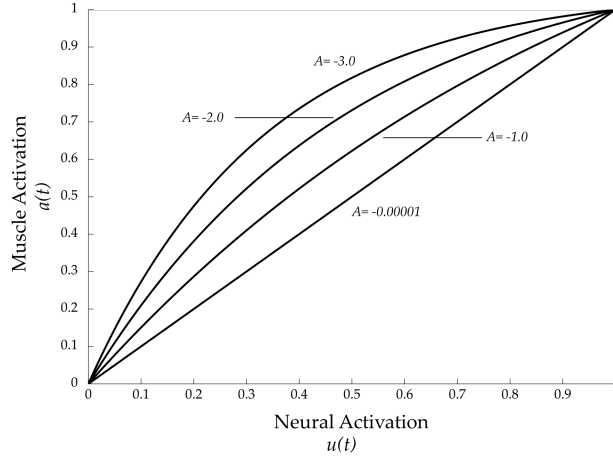


Figure 3: Nonlinearization of neural activation, $u(t)$, to muscle activation, $a(t)$, according to Eq. 5. A is the nonlinear shape factor, constrained to $-3 < A < 0$.

This damped second-order response stretches the duration of the processed EMG, thus accommodating the issue of the shorter duration of EMG with respect to the resulting force. Moreover, the electromechanical delay is included in the equation (d in Eq. 1), allowing for a better synchronisation between activation and force production. In addition, this model can even implicitly account for the tissue filtering characteristics (Lloyd and Besier, 2003).

However, still $u(t)$ is not the most reasonable approximation of the muscle activation, $a(t)$. It has been shown, indeed, that activation is nonlinearly related to EMG, especially at lower forces (less than 30%). Manal and Buchanan (2003) formulated a logarithmic relationship for forces less than 30% and linear for higher values. Lloyd and Besier (2003) used instead an alternative exponential formulation:

$$a(t) = \frac{e^{A \cdot u_j(t)} - 1}{e^A - 1} \quad (5)$$

where $a_j(t)$ is the activation of muscle j , $u_j(t)$ the neural activation of muscle j at time t (from Eq. 1), and A the nonlinear shape factor, constrained to vary between -3 and 0 , with $A = -3$ being highly exponential and $A = 0$ being a linear relationship (Fig. 3). Eq. 5 is similar to that proposed by Potvin et al. (1996), and can be found also in Manal et al. (2002).

The transformations described above (Fig. 2) are used to estimate the activation of each MTU included in the musculoskeletal model. In order to do that, the experimentally recorded EMG signals are usually allocated to the considered MTUs. The more MTUs are included in the model, the more this mapping is a prerequisite for the muscle activation dynamics step, as a consequence of the low resolution of surface electromyography.

JOINTS	MUSCULOTENDON ACTUATORS
Hip	addbrev, addlong, addmag1, addmag2, addmag3, gmax1, gmax2, gmax3, gmed1, gmed2, gmed3, gmin1, gmin2, gmin3, illiacus, psoas
Knee	vasint, vaslat, vasmed, bicfemsh
Ankle	perbrev, perlong, perter, sol, tibant
Hip, Knee	bicfemlh, semimem, semiten, gra, recfem, sar, tfl
Knee, Ankle	gaslat, gasmed

Table 1: The 34 musculotendon actuators included in the musculoskeletal model and the joints they span.

In the case of the multi-DOF model, to account for 4 DOFs, the lower limb model was composed of 34 MTUs (Tab. 1). The EMGs were recorded from 16 muscles and distributed to the 34 MTUs as shown in Fig. 4. EMG signals that could be experimentally recorded from those muscles that were modeled as a single wire (Delp et al., 2007), were assigned to their respective MTU. This is the case of: Vastus Lateralis, Vastus Medialis, Soleus, Tibialis Anterior, Tensor Fasciae Latae, Rectus Femoris, Sartorius, Gracilis, Gastrocnemius Lateralis and Gastrocnemius Medialis. EMGs from the remaining MTUs are usually difficult or impossible to be measured experimentally. The rationale behind the proposed allocation scheme was the location of the muscle innervation zones and the functional role played by the muscles, i. e., two muscle groups that share the same innervation zone and contribute to the same action were assumed to have equivalent EMG patterns. Therefore, EMG signals recorded from those muscles that were modeled as a multi wire complex were assigned to all the MTUs that composed each muscle group. That is, Adductor Magnus was used to drive addmag1, addmag2, addmag3. Besides, since they share the same innervation zone, Adductor Magnus was used to drive also addbrev and addlong. Similarly, the EMG from Gluteus Maximum drove gmax1, gmax2 and gmax3, as well as the Gluteus Medius drove gmed1, gmed2 and gmed3. Moreover, it was used to drive also the gmin MTUs. EMG from the Medial Hamstrings was distributed to both the semimem and the semiten, while the Lateral Hamstrings was used for the bicfemsh and the bicfemlh. A single signal from the Peroneous muscle group drove the corresponding 3 MTUs: perbrev, perlong and perter. The activity of the vasint MTU was instead obtained as the mean between the Vastus Lateralis and Vastus Medialis EMGs. Finally, the Iliacus and Psoas muscles were not driven by EMG signals as they are located too deeply and do not share innervation points with other superficial muscles whose EMGs signals were experimentally recorded. Consequently, the model can not account for the active force produced by these muscles. However, they

are included in the model setting the corresponding MTUs activation to zero, as they significantly contribute to the hip flexion with the generation of passive forces (Section 2.2.2). Nevertheless, this distribution of EMG signals did not account for all muscles in the lower extremities. Some deep muscles were excluded as they are supposed to not contribute significantly to joint moments generation due to their small physiological cross-sectional area. These were: Pectineus and Periformis at the hip, Plantaris and Plopiteus at the knee, Extensor hallucis and digitorum longus, Flexor hallucis/digitorum longus at the ankle. According to Sartori et al. (2012a), considering the HipAA, HipFE, KneeFE and AnkleFE moment arms, the MTUs included in the model accounted for the 91%, 87%, 95%, and 80% of the total physiological cross-sectional area respectively, and thus the exclusion of those muscles should not compromise the results to a large extent. Finally, the presented distribution of experimental EMGs was assumed to be uncorrelated from the kind of movement performed, and thus constant.

2.2.2 Muscle Contraction Dynamics

Once obtained the muscle activations, these are input for a model that accounts for the muscle contraction dynamics to determine muscle forces (Buchanan et al., 2004). A Hill-type muscle model is traditionally used when multijoints systems are involved (Zajac, 1989). Each musculotendon unit is therefore modeled as a muscle fiber in series with an elastic or viscoelastic tendon (Fig. 5A). The muscle fiber also is described as the parallel of a contractile and an elastic component (Fig. 5B).

The contractile element is the active part of the muscle, that generates active force in response to the activation, while the parallel elastic element represents a passive part that applies a resistive force when stretched beyond a resting length. The total force developed by the muscle fiber, F^m , is the sum of the active (F_λ^m) and the passive (F_p^m) components. The tendon is also a passive element, that generates a force proportional to the distance it is stretched, when it is above the tendon slack length, L_s^t , while it does not carry any load below. As proposed by Zajac (1989), both in the single and multi-DOF model, it is modeled with a nonlinear function, normalized to L_s^t and $F^{m^{ax}}$, the maximum isometric muscle force. Since the tendon is in series with the muscle fiber, the force developed in the muscle passes through the tendon and viceversa, and they are related by the pennation angle as follow:

$$F^t = F^m \cos(\varphi) \quad (6)$$

where φ is the pennation angle, that is the angle between the tendon and the muscle fiber. For many muscles this angle is negligible, but

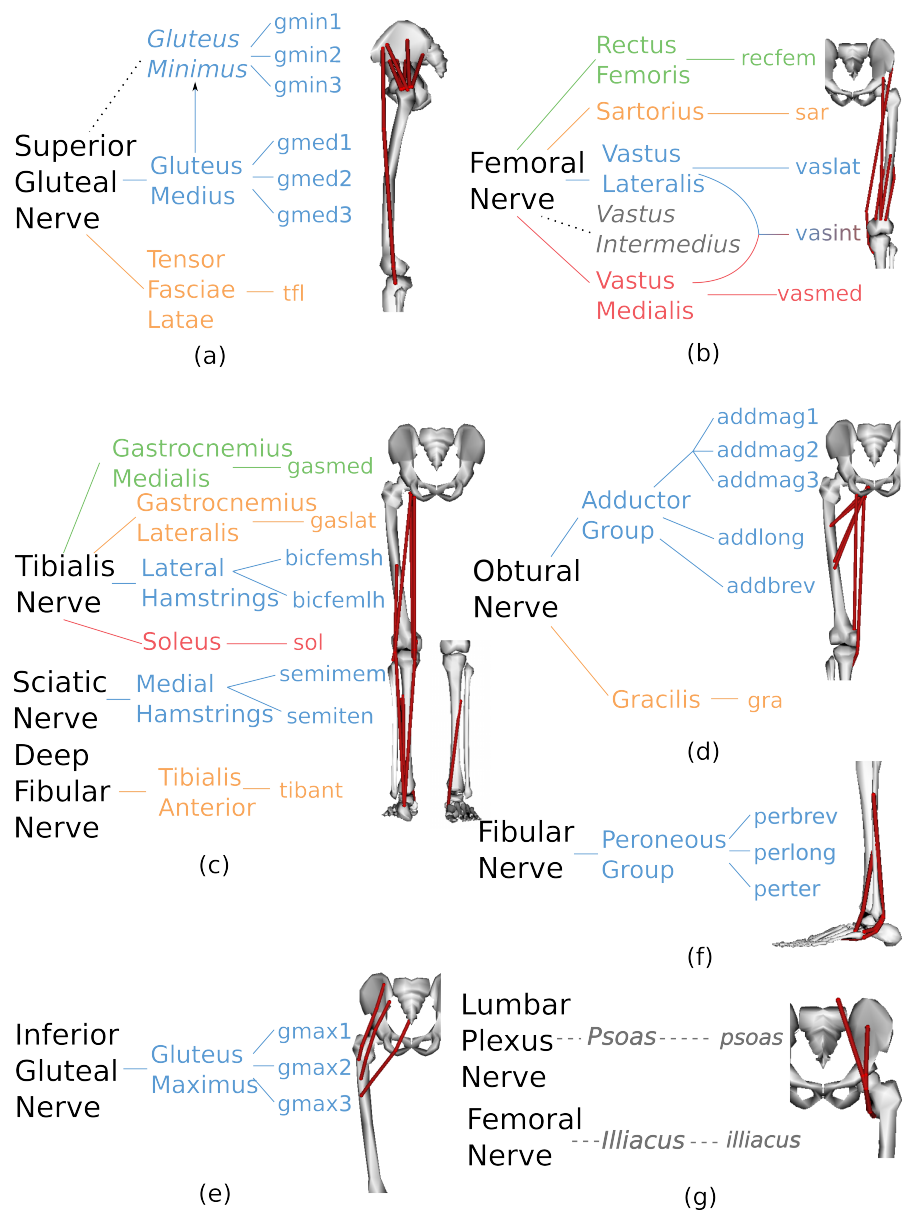


Figure 4: **Allocation of the 16 experimental EMG signals to the 34 musculotendon units (MTUs).** Innervation zones are represented by the nerve name at the first level of each tree. Eighteen muscle groups that are innervated from the corresponding innervation zone, are represented by the full muscle name at the second level. MTUs are represented by the shortened names at the third level. A dotted line connected to an *italic-style* full muscle name means the corresponding EMG signal could not be recorded (a,b, and f). A MTU name written in *italic-style* means it is not driven by EMG signals, and therefore it only produces passive force (f). Within each tree, branches have different color referring to different recorded EMG signals (source Sartori et al. (2012a)).

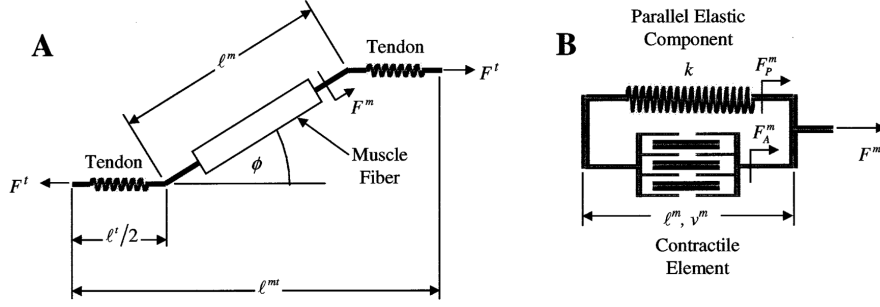


Figure 5: **Hill-type muscle model** (A) Schematic representation of the musculotendon unit as a muscle fiber in series with the tendon. (B) Schematic representation of the muscle fiber, composed by a contractile element and a parallel elastic component. The force produced by the contractile element is a function of l^m and v^m . The total muscle fiber force, F^m , is the sum of F_A^m and F_P^m (source Buchanan et al. (2004)).

for those with large pennation angles (i. e., greater than 20°), it can have a significant effect on the computation of tendon force. Pennation angle also changes as a function of muscle fiber length. Assuming that the muscle has constant thickness and volume as it contracts, the equation used to calculate the pennation angle at time t is:

$$\varphi(t) = \arcsin\left(\frac{L_0^m \sin(\varphi_0)}{L^m(t)}\right) \quad (7)$$

where $L^m(t)$ is the muscle fiber length at time t , L_0^m the optimal fiber length, that is the fiber length at which the force reaches its higher value and φ_0 the pennation angle at optimal fiber length.

The force produced by the musculotendon unit, $F^{mt}(t)$, equals the force in the tendon, and in its general form is given by:

$$\begin{aligned} F^{mt}(\theta, t) &= F^t = F^m \cos(\varphi) = (F_A^m + F_P^m) \cos(\varphi) \\ &= F^{max} \cdot [f_A(l) \cdot f(v) \cdot a(t) + f_P(l)] \cdot \cos(\varphi) \end{aligned} \quad (8)$$

This equation is complex and highly non linear. The musculotendon force is a function of the activation, obtained from the previous step, and the musculotendon kinematics. It has been shown that the force generated by a muscle is a function of its fiber length and of its fiber contraction velocity (Hill, 1938; Zajac, 1989). These relations are expressed using generic force-length, $f_A(l)$, force-velocity, $f(v)$, and passive elastic force-length, $f_P(l)$ curves, which are shown in Fig. 6. They are normalized to maximum isometric muscle force (F^{max}), optimal fiber length (L_0^m), and maximum muscle contraction velocity (v^{max}). The force-length relationship for the contractile element, $f_A(l)$, was derived by cubic spline interpolation of the experimental points on the force-length curve obtained by Gordon et al. (1966). Moreover, Huijing (1995) and Guimaraes et al. (1994) showed that the optimal

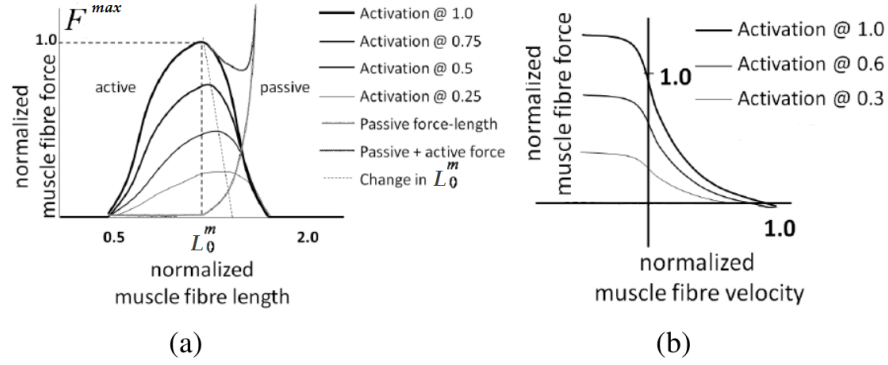


Figure 6: **Force-length and force-velocity curves.** (a) Active and passive force length curves. Values are normalized by F^{max} and L_0^m with 1.0 being 100% activation. Optimal fiber length was scaled with activation by the relation experimentally determined in Huijing (1995). (b) Normalized force-velocity relationship.

fiber length increases as activation decreases (Fig. 6). Lloyd and Besier (2003) have introduced a relationship that account for this coupling between the activation and the optimal fiber length:

$$L_0^m(t) = L_0^m (\gamma(1 - a(t)) + 1) \quad (9)$$

where γ is the percentage change in optimal fiber length, L_0^m the optimal fiber length at maximum activation, $L_0^m(t)$ the optimal fiber length at time t and activation $a(t)$.

The passive elastic muscle force, $f_p(l)$ is characterized by small values when the muscle fibers are shorter than their optimal fiber lengths, L_0^m , but it rises greatly thereafter. This was described with an exponential relation by Shutte (1992). The force-velocity relationship, $f(v)$, instead was introduced by Schutte et al. (1993).

The resulting formulation of the musculotendon force (Eq. 8) is a non-linear first-order differential equation, which is solved by numerical integration using a Runge-Kutta-Fehlberg algorithm (Buchanan et al., 2004).

2.2.3 Moment Computation

Musculotendon lengths and moment arms for each MTU are computed exploiting a musculoskeletal model (Delp et al. (2007), Section 2.4.2. These models account for the way they change as a function of joint angles, and include essential information about the geometry of the musculoskeletal system required for their estimation (e. g., origin and insertion of MTU, joint centers).

Once muscle forces and moment arms are provided, this block computes the joint moments generated about all the DOFs of each joint included in the model. This is done by multiplying each muscle force

for its corresponding moment arm, and then summing the contributions of all the muscles that caused that particular moment:

$$M_i(\theta, t) = \sum_j (ma_{ij}(\theta) \cdot F_j^{mt}(\theta, t)) \quad (10)$$

where M_i is the joint moment about the i -th DOF, ma_{ij} is the moment arm of j -th muscle respect to the i -th DOF, and F_j^{mt} is the force produced by the j -th musculotendon unit, resulting from Eq. 8.

2.2.4 Model Calibration

All the equations presented above, involve physiological parameters that characterize the muscle properties for each individual, and allow to scale the equations to model different muscles. These parameters are determined within a calibration process based on nonlinear optimization and on a set of calibration trials. A simulating annealing algorithm is used to alter the values of an initial set of parameters taken from literature or previously scaled with analytical method (Winby et al., 2008). Parameters are constrained to vary within predefined boundaries to ensure a physiological behavior of the muscle, and adjusted to track the external joint moments obtained for the calibration trials from inverse dynamics calculations. The calibration is an iterative process that, at each step, evaluates the difference between the joint moments estimated by the EMG-driven model and those derived from inverse dynamics during multiple calibration trials (Fig. 7). The subject-specific parameters for each muscle are refined in order to minimize an objective function defined as follows:

$$f = \sum_t^{nt} \sum_d^{nd} E_{t,d} \quad (11)$$

where

$$E_{t,d} = \frac{1}{n_r} \sum_{r=1}^{n_r} \frac{\left(M_{t,d,r}^{estimated} - M_{t,d,r}^{external} \right)^2}{\text{var}(M_{t,d,r}^{external})} \quad (12)$$

$E_{t,d}$ is relative to the t -th trial and to the d -th DOF. It represents the total sum of squared differences between estimated and external moments (from inverse dynamics), normalized by the number of acquired points (n_r) and the variance of the trial.

Parameters adjusted during this calibration process are:

- C_1 and C_2 , the recursive filter coefficients (Section 2.2.1). They are bounded by stability criteria ($|C_1|, |C_2| < 1$) and assumed to be global parameters (i. e., the same for all muscles);
- A , the nonlinear shape factor, describing the nonlinear relation between neural excitation and muscle activation. Using Eq. 5, by definition it is comprised between -3 and 0;

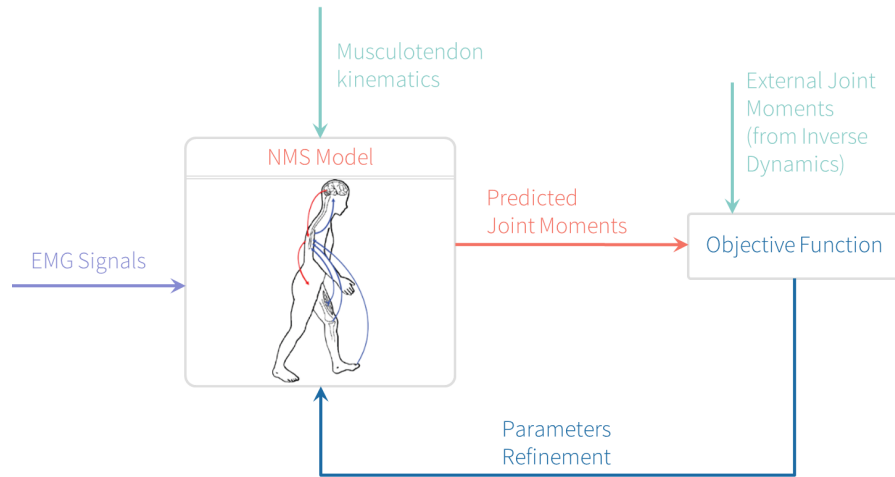


Figure 7: Schematic representation of the model calibration procedure. The NMS model is started with an initial set of uncalibrated parameters taken from literature or previously scaled with analytical method (Winby et al., 2008). The parameters are refined using an optimization algorithm to minimize the error between the estimated and the measured joint moments.

- L_s^t , the tendon slack length: the length at which the tendon begins to generate force. It is the most difficult to be determined experimentally among the parameters of the muscle contraction model. According to Sartori et al. (2012a), initial values were obtained after anthropometrical scaling of values taken from literature (Yamaguchi et al., 1990; Delp et al., 1990; Lloyd and Buchanan, 1996; Lloyd and Besier, 2003), exploiting the seventh analytical method proposed by Winby et al. (2008). The parameters were then allowed to vary within $\pm 5\%$ of their adjusted initial value;
- L_0^m , the optimal fiber length: the fiber length of maximum activation. This parameter, in Lloyd and Besier (2003), was fixed to values reported by Delp et al. (1990), while in the multi-DOF it has been introduced within the calibration process. Similarly to the L_s^t , it was firstly adjusted with anthropometrical scaling (Winby et al., 2008) and then constrained to $\pm 2.5\%$ of the initial value.
- *strength coefficients*: multiplicative factors for F^{\max} . The parameter F^{\max} corresponds to the maximum force a muscle can produce at its optimal fiber length, and it is related to its physiological cross sectional area (PCSA, i.e., the amount of sarcomeres in parallel). The strength coefficients allow to scale F^{\max} in order to account for differences in muscles PCSA. They have been introduced to reduce the total number of calibrated pa-

rameters in the optimization procedure. Using these strength coefficients, instead of calibrating directly F^{\max} for each muscle, it is indeed possible to keep it fixed and calibrate a reduced number of strength coefficients, that can be shared by multiple muscles. Lloyd and Besier (2003), for example, used two flexor and extensor strength coefficients (φ and δ). In the multi-DOF model, the MTUs were gathered into 11 groups according to their functional action. During calibration, the same strength coefficients were assigned to MTUs belonging to the same group. These were: uniarticular hip flexors, uniarticular hip extensor, hip adductors, hip abductors, uniarticular knee flexors, uniarticular knee extensors, uniarticular ankle plantar flexors, uniarticular ankle dorsi flexors, biarticular quadriceps, biarticular hamstrings, and biarticular calf muscles (Sartori et al., 2012a). Regardless the functional group, strength coefficients were varied between 0.5 and 2. In Lloyd and Besier (2003), instead, the two global coefficients φ and δ , were constrained to $\pm 50\%$ of F^{\max} , where F^{\max} for the muscles were determined from the average of the data presented in Yamaguchi et al. (1990).

Despite the majority of parameters in the multi-DOF model is calibrated, there are still some that are not included in this process. These are:

- d , the electromechanical delay (Section 2.2.1), known to range from 10 to 100 msec (Buchanan et al., 2004). Different values have been used in the literature for this parameter, and sometimes it has also been calibrated (Besier et al., 2009). Lloyd and Besier (2003) fixed it equal to 40 ms;
- γ , the percentage change in fiber length in Eq. 9. In Lloyd and Besier (2003), it was assumed to be a constant of 15%;
- φ_0 , the pennation angle at optimal fiber length. In Lloyd and Besier (2003), it was set to values reported by Delp et al. (1990).

These parameters values are not specified in Sartori et al. (2012a).

Once the calibration process is completed and subject-specific parameters are determined, it is possible to use the EMG-driven NMS model in a forward and open-loop mode to predict muscle forces and joint moments about multiple DOFs on a novel set of trials. If properly calibrated, the model should be able to track novel data without the need for optimization and tracking of external joint moments.

2.3 CEINMS: AN EMG-DRIVEN NMS MODEL IMPLEMENTATION

CEINMS (Calibrated EMG-Informed NeuroMusculoSkeletal modeling toolbox) is the software tool that implements the presented multi-DOF EMG-driven NMS model (Lloyd et al., 2014). It is currently being

developed by the Rehabilitation Engineering Group, at the Department of Management and Engineering of the University of Padua, and the Center For Musculoskeletal Research at the Griffith University. CEINMS is the result of an interdisciplinary collaboration among the biomechanics and the computer science worlds. It collects and integrates in a unique software all the algorithms and codes that were developed by Lloyd and colleagues (Lloyd and Buchanan, 1996; Lloyd and Besier, 2003; Sartori et al., 2012a, 2013, 2014). For example, it implements two different models to describe the nonlinear relation between the neural and the muscle activation: the piecewise function proposed by Manal and Buchanan (2003), and the exponential one introduced by Lloyd and Besier (2003). It also includes three models for the tendon (Sartori et al., 2012b). Moreover, given the appropriate anatomical and physiological data, CEINMS can be configured to operate with any number of DOF and MTU. This is possible thanks to its modular and generic design that allows the independent selection of different operation modes.

CEINMS is also written to be flexible and extremely configurable. It makes use of several XML files to handle the large number of parameters involved in NMS simulations, to select and store the input and output files, and to support the multiple available execution choices. This enables, for example, to easily define the set of parameters to be calibrated and the ranges within they are allowed to vary during the calibration process (Fig. 8).

The software is written in C++ and can be run to any platform.

2.4 WORKFLOW

This section examines the processing workflow that leads to the application of an EMG-driven NMS model. Input data are not directly available and need to be properly acquired and prepared. Three main steps can be recognized: (i) collection of experimental motion data, (ii) musculoskeletal modeling, and (iii) NMS modeling.

The NMS model was presented before. As part of the workflow, in this section we describe how the collected EMG signals are processed to obtain the normalized linear envelope required for the transformations involved in the muscle activation dynamics within the NMS model (Section 2.2.1). For each part, the state of the art of current methods is presented. Finally, the last subsection summarized the input that must be provided in order to calibrate and run forward simulations with the EMG-driven NMS model.

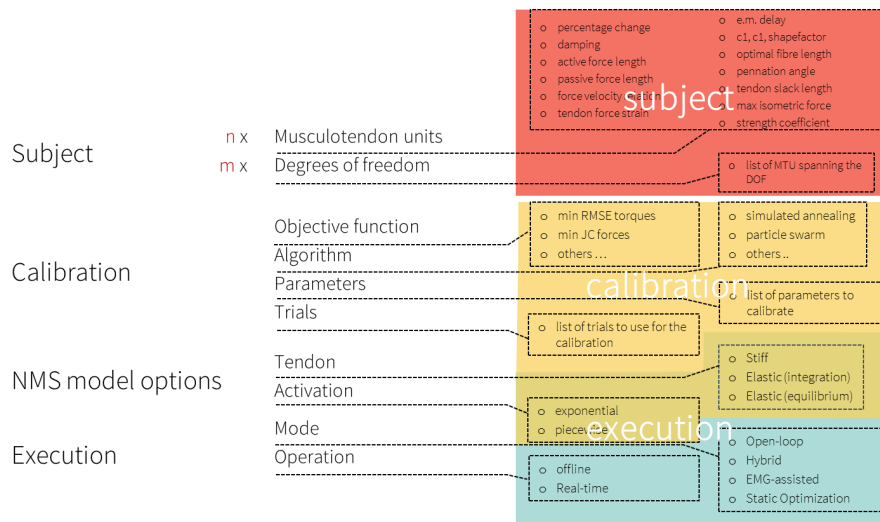


Figure 8: An overall overview on parameters that can be configured in CEINMS. XML files are defined to gather either the initial or the calibrated subject-specific parameters, that characterize the musculotendon properties and their association with the joints and DOFs, and the configuration choices that can be selected by the user during the calibration (e.g., set of calibration trials, constraints for each parameter) and execution (e.g., nonlinear relation among neural and muscle activation, the model for the tendon) procedures.

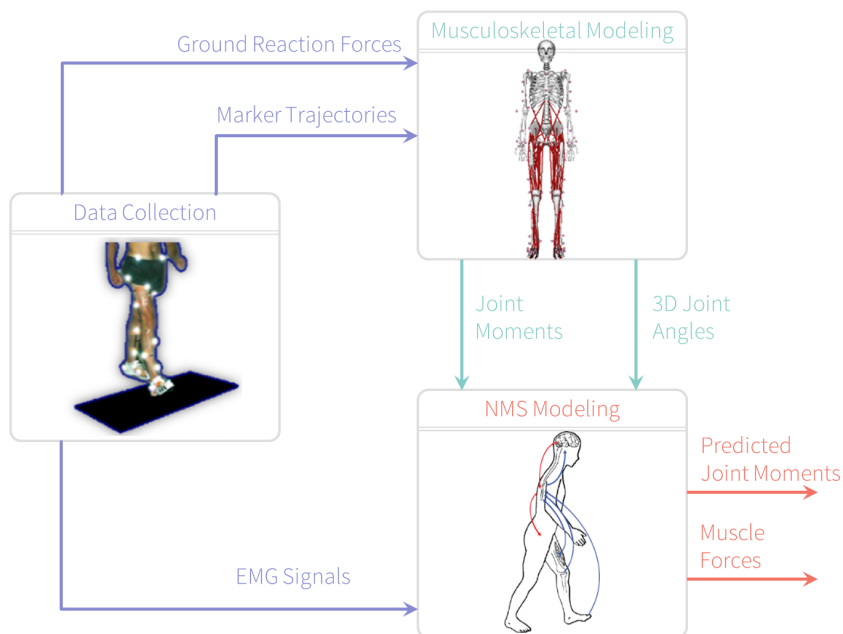


Figure 9: Schematic representation of the processing modeling workflow. Motion data are collected to drive a musculoskeletal model and obtain the information required for the application of an EMG-driven NMS model.

2.4.1 *Data collection: motion analysis*

The first step in the workflow is the collection of experimental motion data in a gait laboratory, where motion capture technology, force platforms and surface electromyography are available.

Stereophotogrammetric systems capture the trajectories of markers attached to the body of a subject, that allow the reconstruction of the 3D movement and the computation of joint angles. Force platforms provide foot-ground reaction forces (GRFs) that are necessary for the computation of joint moments via inverse dynamics. These are then used either to calibrate or validate the NMS model. Previous single-DOF and static applications, involving isometric tasks, exploited isokinetic dynamometers to obtain joint moments data. However, this solution is not feasible when studying dynamic tasks such as walking.

EMG-driven models require the acquisition of the electromyographic activity of muscles. EMG signals from sixteen lower limb muscles have been acquired until now for multi-DOF EMG-driven applications (Sartori et al., 2012a). Modifications in the EMG acquisition protocol impact the EMG distribution to MTUs (Section 2.2.1), and must be carefully evaluated based on the DOFs considered in the particular study.

It should be mentioned that these motion data needs to be acquired synchronously.

A minimum of two distinct dataset must be collected: a set of trials for the calibration of the NMS model, and a different one for its execution in open-loop. Calibration dataset should include tasks that encompass different activation strategies and contractile conditions of the muscle, as recommended by Lloyd and Besier (2003), and later addressed by Gerus et al. (2010). Different methods have been used to gather calibration trials, especially when moving from single to multi-DOF NMS models. A combination of dynamic movements and both isometric and isokinetic contractions on isokinetic dynamometers is the preferred solution for single-DOF models (Lloyd and Besier, 2003; Lloyd et al., 2005; Winby et al., 2009a; Gerus et al., 2010). Sartori et al. (2012a) used instead four different motor tasks, such as walking, running, sidestepping and crossover. Since the work of Lloyd and Besier (2003), most of applications aims at determining knee or ankle moments during walking or running. Nevertheless, trials used to calibrate the model are never used for validation purposes, thus requiring the acquisition of a second dataset.

Moreover, normalization of processed EMG signals (Section 2.4.3) often requires the acquisition of dedicated data. To allow comparison among different subjects, or among different acquisition sessions, EMGs must be normalized, and the estimates of the neural drive ($e(t)$ in Section 2.2.1) provided in a percentage scale. Some authors ex-

ploited the entire set of already recorded trials (Sartori et al., 2012a), some others collected maximal voluntary contraction (MVC) trials just for normalization purposes (Lloyd and Buchanan, 1996; Lloyd and Besier, 2003; Buchanan et al., 2004; Koo and Mak, 2005; Shao et al., 2009).

Finally, a static standing pose of the subject must be acquired to allow the scaling of a generic musculoskeletal model to match the anthropometry of each individual (Section 2.4.2.1). The use of functional joint axes have also been proposed to enhance the model scaling procedure (Sartori, 2011). However, this requires the additional acquisition of swinger trials and a tool to compute functional joint centers starting from these movements.

The whole data acquisition process, therefore, is fundamental, as the better data we have, the better model outcomes we can achieve. However, it can result complex and very time consuming, and it must be planned carefully.

Once data have been acquired, they need to be properly processed for their integration in musculoskeletal software. This step is usually performed exploiting acquisition devices proprietary software in conjunction with costum-made MATLAB codes.

2.4.2 *Musculoskeletal modeling*

Several software tools exists to model and simulate the movement of musculoskeletal systems (e. g., SIMM, AnyBody, OpenSim, MSMS). Among them, the freely available OpenSim software (Delp et al., 2007) has seen a widespread adoption and it is often exploited for NMS applications. It is indeed a repository of musculoskeletal models that allow the calculation of musculotendon lengths and moment arms over a wide range of body positions. These models include a geometric representations of the bones, a kinematic descriptions of joints, and the definition of the Hill-type muscle model for a variable number of MTU (Fig. 10 a). These properties are fundamental for the accuracy of results but vary among models, as shown by Wagner et al. (2013), who recently compare commonly available generic musculoskeletal models. Therefore, the first step when approaching musculoskeletal modeling is usually to choose the more appropriate musculoskeletal model among those available, being aware of its limitations.

To be used in NMS modeling simulations, the model must include all the muscles and DOFs of interest. Muscles are defined as complexes of MTUs, where muscle fibers and tendons are represented together. Most of them are composed by a single MTU, while others are made of multiple MTUs. The single MTU is a wire-like component, modeled as a line segment path constrained to an origin and an insertion point. Wrapping surfaces and internal via points are included when

the muscle line of action is constrained by bones or deeper muscles (Fig. 10 b).

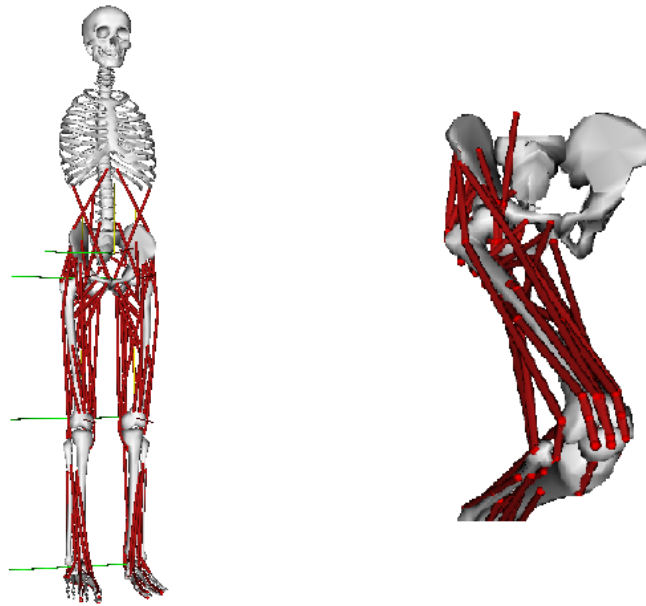


Figure 10: (a) Generic musculoskeletal model including a representation of bones, joint axes and muscles. (b) Muscle-tendon geometry definition within the musculoskeletal model. MTU paths are represented as line segments defined by insertion, origin and intermediate via points.

OpenSim software provides also a library of tools and algorithms that can be run manually through a graphical user interface or implementing batch processing scripts to automatize the procedure. In this section, a brief explanation is given of the processing steps that can be performed within the OpenSim modeling software in order to obtain joint moments for the NMS model calibration, and the musculotendon lengths and moment arms required respectively for the muscle contraction dynamics and moment computation blocks involved in a forward simulation (Fig. 11).

For additional information on the musculoskeletal models and OpenSim built-in tools, the reader can refer to the Delp et al. (2012).

2.4.2.1 *Scaling*

In the absence of subject-specific musculoskeletal models, generated for example starting from imaging techniques (Blemker et al., 2007), it is common practice to scale generic models to obtain a subject-specific representation of the musculoskeletal system. This means that the antropometry of a generic model, i. e., length of each bone and muscle, mass of each segment, is altered so that it matches a particular subject as closely as possible. This is a fundamental step that has a

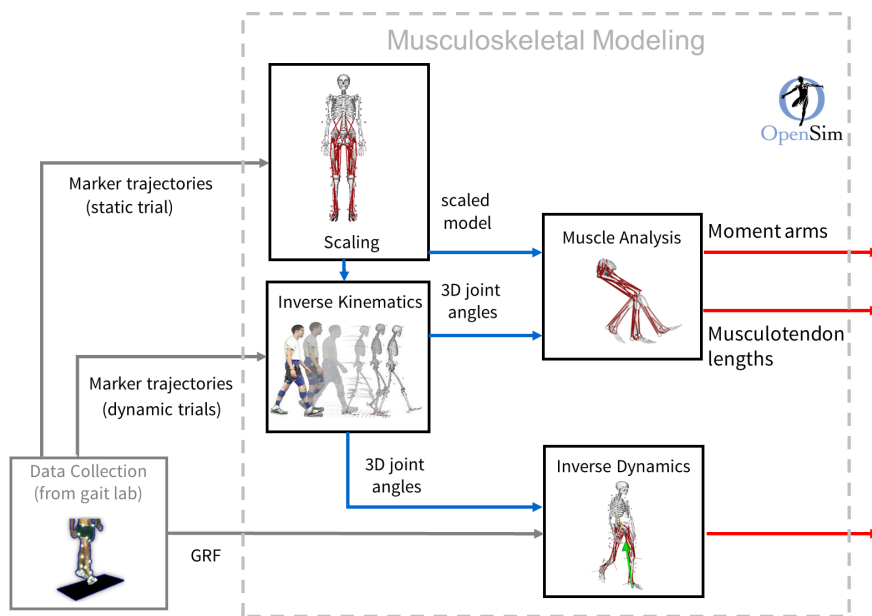


Figure 11: Flowchart of steps in the Musculoskeletal Modeling part. Data collected (in grey) are inputted to the OpenSim software, where tools are used to scale the generic model to the subject (Scaling), compute joint angles (Inverse Kinematics), joint moments (Inverse Dynamics) and the musculotendon kinematics (Muscle Analysis). Output of this modeling block are in red.

great impact on modeling outcomes, since it influences the estimation of musculotendon lengths and the inertial properties involved in the inverse dynamics computations. However, it is often an approximate process, that has not univocal solution and can depend on user experience. Therefore, attention must be paid when performing this step.

Lengths and mass are scaled linearly, and the scale factors are obtained computing the ratio between the segment mass and dimension of the subject and those of the generic OpenSim model. While the unscaled model has predefined weight, height, inertia and position of center of mass for each segment, the dimensions of subject segments are estimated by computing the distance between virtual markers specified by the users and placed on the model based on the location of the experimental markers. Markers trajectories from static trials are indeed used to adjust the position of the associated virtual markers. Markers that correspond to anatomical landmarks and joint centers can be exploited for a more accurate estimation of segments dimensions (Delp et al., 2012). For instance, the length of the femur can be calculated by computing the distance between hip and knee joint centers (Sartori, 2011).

To overcome limitations of the OpenSim linear scaling, analytical methods have also been proposed (not implemented within the OpenSim software framework) to further adjust muscle parameters (Winby et al., 2008; Menegaldo and De Oliveira, 2009).

2.4.2.2 *Inverse Kinematics*

Markers trajectories acquired during dynamic trials are then used to drive the scaled musculoskeletal model. The OpenSim Inverse Kinematics Tool (IK) can compute the generalized coordinates, usually corresponding to three-dimensional joint angles. This is done by minimizing the difference between the experimentally recorded marker positions and the virtual markers placed on the model and adjusted during the Scaling step. Joint angles are required to determine musculotendon kinematics during each task, through Muscle Analysis (Section 2.4.2.4), and for the estimation of joint moments from the external loads applied to the subject and inverse dynamics-based calculations.

2.4.2.3 *Inverse Dynamics*

Inverse dynamics solves the equations of motion in an inverse sense, that is starting from the kinematics (e. g., estimated through IK) and the kinetics information recorded during motor tasks (i. e., the GRFs measured through force platforms), to obtain the net moments at each joint, that are responsible for the given moment. This process is imple-

mented in another built-in tool of OpenSim software (ID Tool) (Delp et al., 2012).

It has been shown that a critical parameter of this procedure is the cut-off frequency by which filtering input data (Roewer et al., 2014; McCaw et al., 2013; Bezodis et al., 2013). Joint moments are used to calibrate the model, thus they can strongly influence the estimation of subject-specific parameters within the NMS model (Lloyd and Besier, 2003). Joint moments from dynamometers have been preferred to avoid inaccuracies in the estimation of joint moments (Herzog, 1988). However, with dynamic and multi-DOF tasks, alternatives to inverse dynamics seem not feasible. Some recommendations for kinematics and kinetics filtering can be found in the literature (Van den Bogert and De Koning, 1996; Edwards et al., 2011; Kristianslund et al., 2012). However, while the OpenSim software allows the setup of any value for the cut-off frequency, an heavy filtering (usually around 6 Hz) is also suggested, since noise is amplified by differentiation (Delp et al., 2012). This problem has been a point of discussion within the biomechanics community (see BIOMCH-L discussion on Isokinetics and Inverse Dynamics by Devita, P., 1999), it was highlighted by Lloyd and Besier (2003) since the beginning of their work on the NMS model, and it is currently object of debate (see BIOMCH-L discussion on Filtering kinematics and kinetics for inverse dynamic parameters- what is best practice?, by Liew, B., 2014). Nevertheless, in the field of NMS applications, it is often underestimated, as it is proven by the lack of details about inverse dynamics analysis, and, mostly, of sensitivity studies to evaluate the impact on the NMS model calibration of filtering kinematics and kinetics for the inverse dynamics computations. Moreover, worth of note is that this aspect is even exacerbated in the case of multi-DOF models.

Alternatively to the ID Tool, Residual Reduction Analysis (RRA) Tool can also be used to estimate joint moments (Delp et al., 2012; Sartori, 2011; Sartori et al., 2012a), but with the same implications related to the filtering issues.

2.4.2.4 *Muscle Analysis*

Muscle analysis aims at reporting the state of the muscles during the execution of a given movement. The scaled musculoskeletal model and the 3D joint angles are used to determine instantaneous estimates of the lengths of MTUs, and of their moment arms with respect to each considered DOF. The analysis can be performed by configuring properly the OpenSim Analyze Tool (Delp et al., 2012). A subset of muscles, as well as of DOFs, can be specified to reduce computation time and the number of output files.

2.4.3 EMGs processing

Prior to be inputted to the muscle activation dynamics step (Section 2.2.1), raw EMGs must be processed to obtain normalized EMG linear envelopes (Fig. 2). This preliminary processing step has been largely described, often as part of the NMS model, within the muscle activation dynamics (Lloyd and Besier, 2003; Buchanan et al., 2004, 2005). We decide to keep the description separate to reflect the actual processing workflow. A NMS model usually has a software implementation (e.g., CEINMS), that starts accounting for the neural activation history (Fig. 2), thus requiring to pre-process the EMGs separately. This is typically done by means of custom-made MATLAB scripts.

EMGs signals must be firstly high-pass (or band-pass) filtered to eliminate low-frequency noise components, with cut-off frequency in the range of 5-30 Hz (and 300-500 Hz), rectified and then low-pass filtered to obtain the linear envelope. Cut-off frequencies for the low-pass filtering are found to vary between 4 Hz (Manal et al., 2002; Buchanan et al., 2004; Shao et al., 2009; Manal and Buchanan, 2013) and 8 Hz (Buchanan et al., 2005), with Lloyd and Besier (2003) using 6 Hz, as even Besier et al. (2009) or Gardinier et al. (2013). A zero-phase fourth order recursive Butterworth filter is usually recommended to avoid shifts of the EMG signals in time (Buchanan et al., 2004).

Finally, normalization is required to scale results between 0 and 1, thus allowing comparison among different subjects and acquisition sessions (Buchanan et al., 2004).

Despite this step may appear well-delineated, many authors have recognized in the EMGs processing one of the main source of error for NMS models (Koo and Mak, 2005; Chèze et al., 2012; Menegaldo and Oliveira, 2012; Oliveira and Menegaldo, 2012), and investigated the effects of different EMG filtering strategies to improve estimates of muscle forces (Potvin and Brown, 2004; Staudenmann et al., 2007). Reviews on methodological aspects related to EMG recordings for muscle force estimation have also been proposed (Disselhorst-Klug et al., 2009; Staudenmann et al., 2010).

Within this thesis work, Chapter 4 will address some issues related to EMG normalization.

2.4.4 Input for the NMS model

This subsection summarizes the input quantities that are necessary to run an EMG-driven NMS simulation from experimental data with the CEINMS software. Those are:

- *musculotendon lengths*, for the muscles in the NMS model, calculated by means of an anatomical musculoskeletal model of the subject;

- *moment arms*, for the muscles that insist on each joint, calculated by means of an anatomical musculoskeletal model as a function of joint angles;
- *normalized EMG linear envelopes*, that are obtained by processing EMGs signals.

To calibrate a NMS model to a subject on individual experimental data, for each trial of the calibration dataset the following data are also required:

- *joint moments*, at the joints of interest, usually estimated by means of inverse dynamics.

2.5 LIMITATIONS

This section aims at highlighting limitations in the presented workflow. Several steps are included: from the collection of experimental data to the process of simulating the movement of a musculoskeletal system, and the processing of EMG signals. The accuracy and reliability of EMG-driven NMS model simulations are greatly dependent on the quality at each of these steps, as they inevitably determine the affidability of NMS model input data. Therefore, it is essential to decompose, examine, and address limitations and issues at each phase of modeling to fully comprehend and interpret NMS model results.

The workflow starts with the collection of experimental data, which requires not trivial procedures. We have seen that different dataset are necessary in addition to that used for the simulations: for the calibration of the NMS model, for the normalization of EMGs, that often involved additional acquisitions, for the computation of functional joint centers, if they are used in the scaling procedure. Moreover, each dataset should include several tasks, to encompass different muscle activation strategies and contractile conditions, or to obtain MVCs from all muscles of interest, or joint centers for multiple joints. The experimental setup and acquisition procedure, therefore, may result long and complex. This without accounting the number of EMG sensors that have to be attached to the body of a subject, whose position influence the acquired signals, and whose number increases for multi-DOF models. When planning the acquisition protocol, it is indeed fundamental to consider also restrictions due to the acquisition environment, the available instrumentation and the physical capacities of the subject. For example, Biodex isokinetic dynamometers have been often exploited to obtain MVCs for the normalization of EMGs, or for isometric and isokinetics trials that are used for the calibration process. However, such instrument is often not available in clinics or minor research laboratories. Moreover, moving towards clinical applications of EMG-driven NMS modeling means carefully consider

and deal with the limitations due to the mobility impairments of a pathological population. For instance, functional trials for the computation of joint centers to be used in the scaling procedure of the musculoskeletal model (Sartori, 2011) can not be part of a routine practice with pathological subjects. In addition, the multi-DOF NMS model has been calibrated exploiting trials of multiple motor tasks, including running, fast walking, cross over and side stepping (Sartori et al., 2012a), that cannot be performed by impaired and older people. EMG normalization was also based on the same dynamic movements. Finally, a protraction in the acquisition time is critical with patients, who can incur in fatigue.

These factors may possibly explain why there are no extensive studies about the application of a multi-DOF model, neither in research nor in a clinical context (only one work with experimental data, and on one healthy subject), and even the fact that single-DOF models, despite more investigated, have not entered the clinical practice yet. Nevertheless, limitations are not restrained to the initial step of data collection.

The subsequent integration of the recorded data into musculoskeletal modeling software (e. g., OpenSim), as well as processing of EMG signals, is usually performed by means of proprietary software and/or custom-made codes, that prevent the reproduction and repeatability of procedures and results among research groups. Each laboratory, indeed, replicates the processing pipeline according to its acquisition setup, software and methodologies, creating scripts and tools to accomplish the same objective, but that can not be generalized across laboratories. The lack of standard procedures and tools that facilitate comparison of results obtained in different contexts and speed up the processing workflow represents a strong limitation for the establishment of NMS modeling techniques, both in research and clinical practice (Reinbolt et al., 2011).

Similarly, the OpenSim built-in tools are run manually through the user graphical interface, or by batch processing scripts that are not freely available and usually customized by the users. One consequence is that processing parameters are often omitted by the authors, as well as considerations on intermediate results obtained during the musculoskeletal modeling part. Nevertheless, the influence of processing techniques and parameters in the accuracy of results must be evaluated at each step for a critical interpretation of the final outcomes. Filtering frequency cut-off, for instance, may greatly influence the content of information that can be extracted from the processed data. If not properly defined, it can lead to results too smooth and to a loss of important information. This is more crucial in clinical applications, where small deviations in the data shape may reveal abnormalities that characterize different pathological conditions. A reasonable

choice of frequency cut-off, as well as other processing parameters, should be carefully sought, especially in the inverse dynamics step. Extensive studies and sensitivity analysis, necessary to evaluate the accuracy, the reliability, and the repeatability of simulations, would be encouraged by open-source tools able to automatize and speed up the whole procedure, while precisely tracing the used parameters and intermediate results (Hicks et al., 2015). A well-organized storage of data, parameters, and results may help managing large dataset, that are usually required for clinical studies and applications. These can also be supported by making these tools user-friendly (Erdemir et al., 2007).

Scaling of the musculoskeletal model is another potential source of errors, that can affect accuracy of the overall NMS model results. Several approaches can be followed to set the measurements for the computation of the scale factor for each segment within the OpenSim Scaling Tool (Delp et al., 2012). Those measurements are usually decided by the user, but it is an evidence that small variations in the configuration yield to different scaled models. Lots of work is going on within the research community to obtain a more accurate and subject-specific representation of the geometry of the musculoskeletal system (Blemker et al., 2007; Fregly et al., 2012). The creation of subject-specific musculoskeletal models are even more recommended (Scheys et al., 2008), but in most occasions it is not feasible. The procedure involved is indeed still expensive, for the use of imaging techniques, and extremely time consuming, despite tools have been recently developed to facilitate this task (Valente, 2013). Analytical methods have been also proposed to provide more accurate estimates of muscle parameters linearly scaled with the OpenSim Scaling Tool (Winby et al., 2008). A freely availability of tools that implements such methods would help in obtaining more accurate initial values for the calibration parameters of NMS models.

All the mentioned aspects made the use of NMS models complex in the research field, even before than in clinical practice.

The work presented in this thesis aims at addressing these limitations and developing the basis for future wider studies, including sensitivity analysis, larger dataset, and clinical cases, possibly in clinical settings.

Chapter 3 presents a new software tool, MOTOtoNMS, that has been developed to overcome limitations related to the pre-processing of experimentally recorded motion data for their integration in musculoskeletal software such as OpenSim. It goes in the direction of simplify and standardize the initial part of the workflow.

A tool for the batch processing of the musculoskeletal part within the OpenSim software, from IK onward (Mantoan and Reggiani, 2014c), has also been developed and made freely available to the community. It automatizes the procedure and allow the storing of setup and log

files and the plotting of results for their visual inspection and analysis.

Chapter 4 is instead an example of investigation that must be pursued to attain the required accuracy for clinical applications. It faces issues mainly related to the data acquisition, when expensive instruments are not available or impaired people are involved, and the influence of different EMG normalization strategies on the NMS model calibration.

MOTONMS: A MATLAB TOOLBOX TO PROCESS MOTION DATA FOR NMS MODELING AND SIMULATION

3.1 INTRODUCTION

Neuromusculoskeletal modeling and dynamics simulation have recently emerged as powerful tools to establish the causal relation between the neuromusculoskeletal system function and the observed movement. They estimate human internal variables, such as neural signals and muscle dynamics, that could not be derived by experimental measures and conventional motion analysis (Pandy, 2001; Zajac et al., 2003; Jonkers et al., 2003; Piazza, 2006; Fregly, 2009). This provides a key contribution to fully understand human locomotion in healthy subjects and to establish a scientific basis for rehabilitation treatment of pathological movements (Zajac et al., 2003; Fregly, 2009; Fregly et al., 2012).

In the latest years, several software tools (e. g., SIMM, AnyBody, OpenSim, MSMS) were released to automate and facilitate the complex and time-consuming process of modeling and simulate the movement of musculoskeletal systems (Delp and Loan, 1995; Damsgaard et al., 2006; Delp et al., 2007; Khachani et al., 2007). Among them, the freely available OpenSim software has seen a widespread adoption with a growing network of research applications (Piazza, 2006; Steele et al., 2010; Hamner et al., 2010; Reinbolt et al., 2011; Donnelly et al., 2012).

Regardless the applications and the final objective of the study, these software tools require as input the simultaneous recordings of heterogeneous motion data acquired with different devices: three-dimensional markers trajectories, foot ground reaction forces (GRFs), and, often, surface electromyography (EMG). Before the recorded raw data can actually be used as input for the simulation software, several pre-processing steps are required depending on the objective of the study (Winter, 2009; Chiari et al., 2005). Among them, filtering is usually performed and is one of the most critical (Kristianslund et al., 2012; Edwards et al., 2011). In addition, simpler steps as transformations among coordinate systems of the acquisition devices and the musculoskeletal modeling software still require to be carefully defined. Finally, the integrated and pre-processed motion data must be stored using the file format of the chosen simulation software.

While mature tools are available for the analysis of biomechanical data (Barre and Armand, 2014), there is still a lack of a robust tool

for the pre-processing of experimental recorded data for optimal integration in neuromusculoskeletal modeling and simulation software. This represents a major factor limiting the translation of neuromusculoskeletal studies into daily practice, as highlighted by several researchers (Kaufman, 1998; Erdemir et al., 2007; Reinbolt et al., 2011).

The main cause holding back the development of such a tool is probably the large number of commercially available motion analysis devices and proprietary softwares (Kaufman, 1998; Reinbolt et al., 2011; Benedetti et al., 2013). It is therefore difficult to handle all data seamlessly and with unified procedures. As a recognized problem, the biomechanics community proposed a standard file format (C3D - Coordinate 3D, Motion Lab Systems (2014)) to store all the heterogeneous motion data: raw coordinate of 3D points, raw analog data from synchronized devices, force plates calibration, analog channels configuration, sample rates, and quantities computed by the acquisition software (joint angle, joint moment, joint power, ...).

Despite the maturity of C3D, its use is still limited. Most of the companies provide acquisition systems that record information using different file formats and proprietary software tools that mainly process data with their own format. The consequence is that researchers develop a proliferation of custom tools and codes that perform similar processing pipeline, but might differ for the input data format and for the use of procedures and proprietary software specific to an acquisition system. As the latter are usually not openly available, it becomes difficult to reproduce the same data processing procedures in a consistent and repeatable way across different laboratories (Kaufman, 1998; Paul and Wischniewski, 2012).

Over the last years, the problem escalated as emerging biomechanics research challenges require multidisciplinary knowledge stimulating multicenter collaborations (Davis et al., 2000; Gorton et al., 2009). Thus, the definition of shared and standard procedures for biomechanical data collection, management, and processing is increasingly required (Kaufman, 1998; Paul and Wischniewski, 2012).

This work presents MOtoNMS (matlab MOtion data elaboration TOolbox for NeuroMusculoSkeletal applications), a software toolbox that directly addresses this problem. MOtoNMS is an open source software that has been already successfully used to process and share data from different laboratories, each one with its own gait analysis instrumentation and methodologies, for their use in neuromusculoskeletal analyses and applications.

The procedures implemented in MOtoNMS include: (i) computation of centers of pressure and torques for the most commonly available force platforms (types 1 to 4, including Bertec, AMTI, and Kistler); (ii) transformation of data between different coordinate systems; (iii) EMG filtering, maximum EMG peak computation, and EMG normalization; (iv) different procedures for gait events detection; (v) joint

centers computation methods for hip, knee, ankle, elbow, shoulder, and wrist; (vi) support for OpenSim file formats and possibility to configure new output formats.

While MOtoNMS already provides a library of modules for the most commonly required steps, its architecture is designed to be open to new contributions in instrumentations, protocols, and methodologies. The choice of MATLAB, the most widespread language among biomechanists, goes also in the direction of simplifying the sharing of procedures within the community.

In this chapter, we describe the toolbox structure and modules and then introduce the testing procedure. Finally, we point out MOtoNMS key features and main advantages. Motion data and results are freely available online (Mantovan and Reggiani, 2014a), showing that MOtoNMS can handle experimental data collected in motion analysis laboratories with different setups and can process them to provide inputs for OpenSim (Delp et al., 2007) and CEINMS (Section 2.3), the software implementing the multi-DOF EMG-driven NMS model (Lloyd and Besier, 2003; Sartori et al., 2012a).

3.2 AIMS

This work aims at developing a software to fill the current lack of robust tools for the processing of experimental motion data for their use in neuromusculoskeletal software. This represents the first attempt towards the standardization and simplification of the whole processing workflow that leads to the application of EMG-driven NMS models (Section 2.4). The more general intent is to facilitate the adoption of NMS modeling techniques by multiple laboratories and research groups, and to encourage their introduction into clinical practice.

In doing that, the software is called to answer the following requirements:

- be general enough to account for different instruments, software, laboratories setups, acquisition protocols and methodologies;
- uniforming the procedure, identifying and implementing the commonly required processing steps;
- be flexible and highly configurable, making the standard processing modules customizable by the user according to its data and purposes;
- keep trace of the parameters configuration set for each performed elaboration, allowing reproduction of results;
- be user-friendly, to be accessible to a wide spectrum of users;
- automate the procedure, speeding up the processing workflow;

- manage large dataset, automatically storing output data with a uniquely defined structure, facilitating information retrieval, sharing of data and the development of utility or batch processing scripts.

3.3 TOOLBOX DESCRIPTION

The MOtoNMS toolbox is implemented in MATLAB (The MathWorks, USA) and is intended to be accessible to a wide spectrum of users, from researchers to clinicians, who are interested in pre-processing experimental motion data to be used in neuromusculoskeletal simulations. The selection and setup of procedures is available through a set of graphical user interfaces, thus not requiring end-users to have advanced computer skills. Current MOtoNMS release works with MATLAB R2010b and later versions, and runs on the major operating systems (Windows, Linux, and MacOS X).

Fig. 12 presents the toolbox organization. MOtoNMS comprises several blocks that are grouped in three main functional areas: *Data Elaboration*, with the procedures for the data processing pipeline, *Data Management*, responsible for the input data loading and the output data generation and storing, and *System Configuration*, supporting the user in the configuration of the elaboration through user friendly graphical interfaces. The structure of the software, with the distribution of modules in three well-defined areas, simplifies the integration of other functionalities and algorithms.

3.3.1 *Data Elaboration*

Data Elaboration is the toolbox core with the two blocks of Dynamic Trials Elaboration and Static Trials Elaboration. These are responsible for processing EMG, GRFs, and marker trajectories for dynamic and static trials.

3.3.1.1 *Dynamic Trials Elaboration*

This block (Fig. 13) handles motion data recorded from dynamic trials. It supports the different GRF data structure generated by the most common force plate (FP) types (Motion Lab Systems, 2008), with no constraints on the number and position of FPs in the laboratory. Depending on the FP type and its output (Table 2), MOtoNMS correctly computes plate moments and centers of pressure (CoP). Three-dimensional marker trajectories undergo piecewise cubic interpolation to fill any possible gap caused by markers occlusions during the acquisition. Then, the pre-processed marker data and raw GRFs are filtered with a zero-lag second order low pass Butterworth filter at customizable cut-off frequencies.

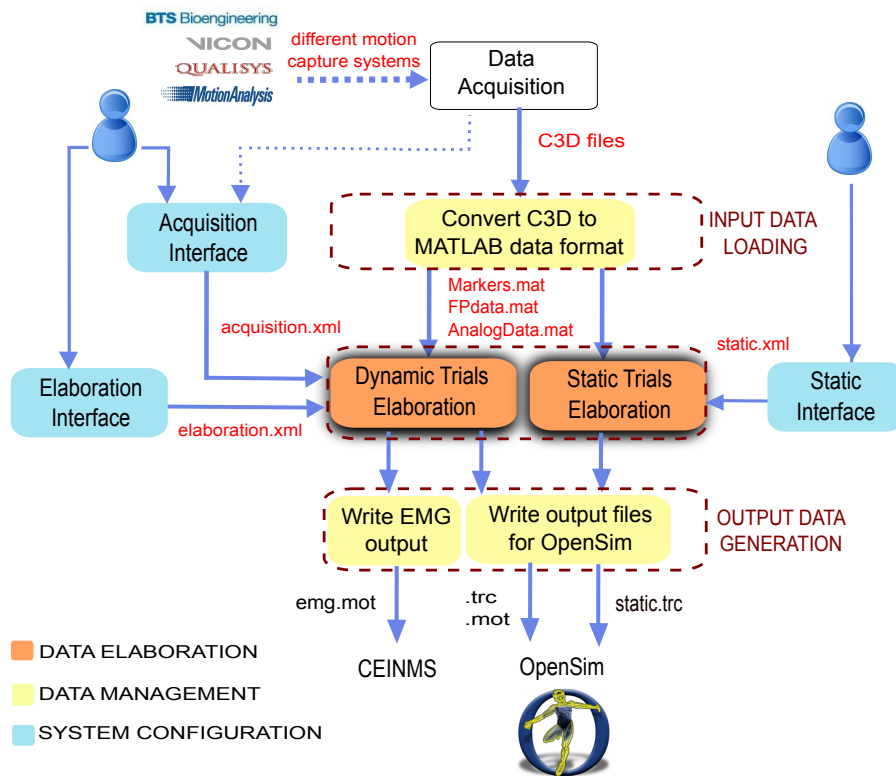


Figure 12: **MOtoNMS overview schema.** *Data Elaboration* is the toolbox core, processing data according to the user's choices selected during the *System Configuration* steps. *Data Management* defines storing and management of input and output files.

The analysis window definition sub-block (Fig. 13) enables selecting the data segments to be processed. Frames of interest can be selected based on events, when available in the input C3D file. Alternatively, a thresholding algorithm based on GRF data is implemented for automatic detection of heel strike and toe off events (Rueterbories et al., 2010). Lastly, a manual selection of start and stop frames is also possible. Processed GRFs are then used to compute FP free torques (Gordon Robertson et al., 2004) based on filtered forces, moments, and CoP for the selected frames. Finally, marker and GRF data are transformed from laboratory or FP reference systems to the global reference system of the selected musculoskeletal application, i.e. OpenSim. Required rotations depend on the laboratory setup described in the dedicated configuration file (Section 3.3.3).

When available, raw EMG signals are processed by high-pass filtering, rectification, and low-pass filtering (Lloyd and Besier, 2003). Resulting EMG linear envelopes are then normalized. For each muscle, the maximum EMG peak is identified by extracting the maximum instantaneous value from the subset of trials selected by the user. The user can enable the plot of the computed values (i.e., raw and pro-

cessed EMG, raw and filtered GRFs, CoPs, and moments), stored to files in dedicated folders for visual inspection.

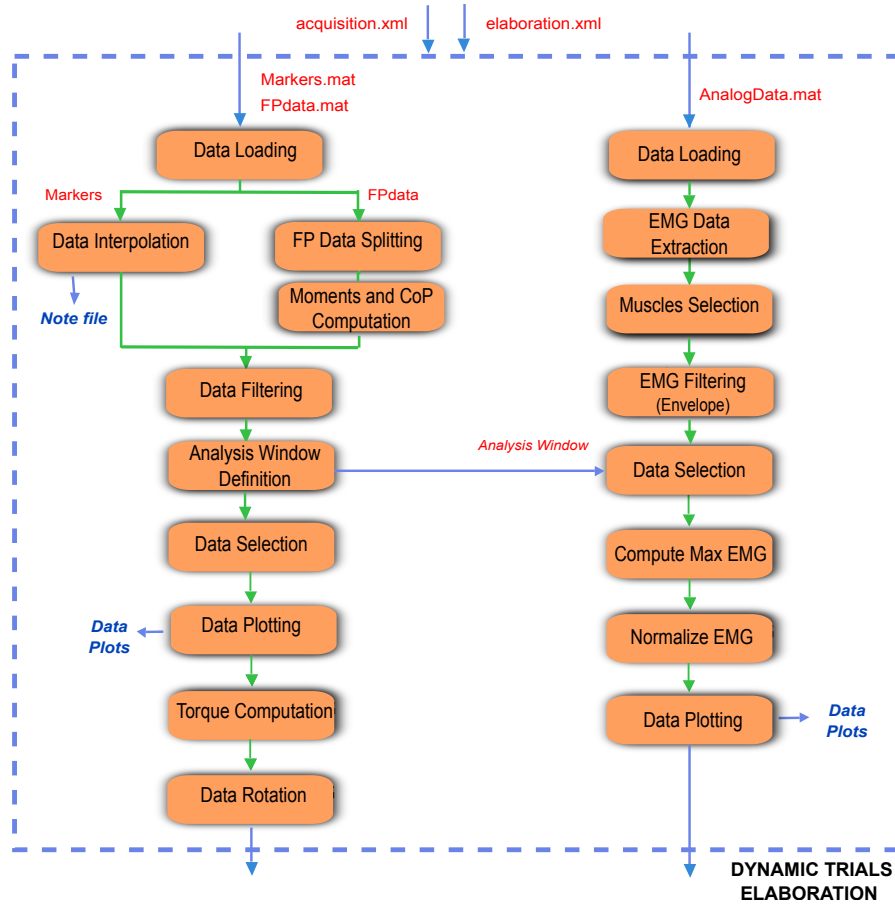


Figure 13: **Dynamic Trials Elaboration.** Flowchart of the Dynamic Trials Elaboration block.

3.3.1.2 Static Trials Elaboration

The Static Trials Elaboration block computes subject-specific joint centers from data recorded during static standing trials. These estimates improve the scaling of generic musculoskeletal models to match an individual’s anthropometry (Delp et al., 2007). This block is designed to accommodate different algorithms for the joint centers estimation. Users can include their own procedures for the joints of interest. Currently, MOtoNMS provides joint centers computation methods for hip, knee, ankle, elbow, shoulder, and wrist. Hip joint center is estimated through Harrington method (Harrington et al., 2007), while the others are computed as the mid points between anatomical landmarks specified by the user.

	Type-1	Type-2	Type-3	Type-4
Channel (1,i)	Force _x	Force _x	Force _x ^{1,2}	Force _x
Channel (2,i)	Force _y	Force _y	Force _x ^{3,4}	Force _y
Channel (3,i)	Force _z	Force _z	Force _y ^{1,4}	Force _z
Channel (4,i)	CoP _x	Moment _x	Force _y ^{2,3}	Moment _x
Channel (5,i)	CoP _y	Moment _y	Force _z ¹	Moment _y
Channel (6,i)	FreeMoment _z	Moment _z	Force _z ²	Moment _z
Channel (7,i)	n/a	n/a	Force _z ³	n/a
Channel (8,i)	n/a	n/a	Force _z ⁴	n/a

Table 2: **Force platform signals by TYPE.** The type of a FP defined the type of its output signals. There are four main types of FP. The table shows the assignment of analog channel numbers to FP output data for each of them, where i indicates the force platform number. The FP outputs may be connected to any convenient analog input channel, in any order that is convenient to the user. The assignment of FP signals to analog channels is usually stored in the C3D file. For example, if Moment_z of FP number 2 is connected to analog channel 15, then Channel(6,2) in the C3D file will contain the entry 15. The type 3 of force platform, differently from the others, has eight analog outputs, which are combinations of the Force_x, Force_y, and Force_z measured at the corners of the FP. The superscript numbers, in this case, refer to the sensors location at the corresponding numbered FP corners (source: Motion Lab Systems (2008)).

3.3.2 *Data Management*

Data Management (Fig. 12) deals with input and output data, supporting an easy integration of new file formats and inducing a clear and uniquely defined organization of the files. This is achieved also through a complete separation between Data Management and Data Elaboration.

3.3.2.1 *Input Data Loading*

Input data are extracted from C3D files and stored in MATLAB structures. This avoids continuous and computationally expensive access to C3D files. The extracted data include: marker trajectories, FP characteristics, GRFs, EMG signals, other data from analog channels, and events. Two implementations for data extraction are available: using C3Dserver software (Motion Lab Systems, 2014), limited to MATLAB 32 bit on Window platforms, or exploiting the Biomechanical Toolkit (BTK, (Barre and Armand, 2014)). Users can choose between the two alternatives according to the system requirements, with the second one enabling cross-platform execution.

3.3.2.2 *Output Data Generation*

The processed marker trajectories and GRFs are stored in .trc and .mot files (OpenSim file formats). The EMG linear envelopes are exported by default to .mot files (SIMM and OpenSim motion format), compatible also with the CEINMS toolbox (Lloyd et al., 2014). Alternative file formats can be selected by the user, such as .sto (OpenSim storage) and text formats. The support of new file formats for other musculoskeletal modeling software requires only to implement new output blocks without any significant change in the Data Elaboration step (Fig. 12).

3.3.2.3 *Data Storage Structure*

With MOtoNMS, users are expected to follow few simple rules in the organization of experimental data. This enables MOtoNMS to automatically generate output directories with a well defined structure, providing the required consistency for information retrieval and sharing of results among research teams (Fig. 14).

3.3.3 *System Configuration*

The high configurability of MOtoNMS results in a high number of parameters. These are not set directly in the code as it would make the system hard to maintain. Instead, MOtoNMS can be fully configured through configuration files without modifying the underlying MATLAB code. Moreover, the use of configuration files guarantees

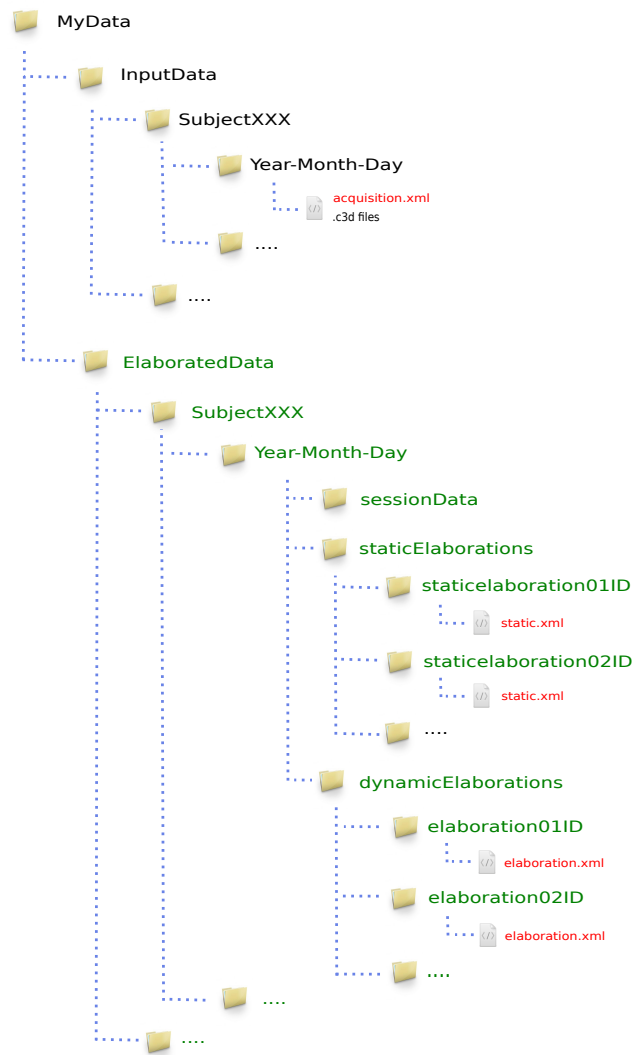


Figure 14: **Data Folders Organization.** Folders in black store input data. The picture presents the structure suggested by MOtoNMS authors: a folder for each subject that includes a set of directories, each one for a different acquisition session. All subjects must be grouped in a `InputData` folder. Red files are the configuration files, while green folders are for the output generated by the toolbox. These folders are automatically created and mirror the structure of the `InputData` folder. MOtoNMS reads C3D files and saves the extracted data in the `sessionData` subfolder. `staticElaborations` and `dynamicElaborations` subfolders include the output respectively of the Static Trials Elaboration and the Dynamic Trials Elaboration blocks. Finally, the results of multiple executions of these two parts, with different configurations for the same input data, are stored in different subfolders, each one named with an identifier chosen by the user through the graphical interface.

the reproducibility of the data processing. Parameters are defined in three files: (1) *acquisition*, including information about the acquisition session (i.e., number of FP, coordinate system orientations, marker

sets, and EMG setups), (2) *elaboration*, including parameters that univocally define the execution of the Dynamic Trials Elaboration block (i.e., selected trials, cut-off frequencies, markers list for output file, . . . , Lst. 1), and (3) *static*, including additional parameters for the elaboration of static trials (i.e., joint centers of interest). MOtoNMS stores a copy of the configuration files together with the output to keep a trace of performed elaborations (Mantoan and Reggiani, 2014b). The chosen language for these files is XML (eXtensible Markup Language), extremely suitable for parameter information encoding (Lst. 1). Syntax correctness of each file is guaranteed through the use of XML Schema Grammars (XSD). MOtoNMS provides user-friendly MATLAB graphical interfaces that allow the user to handily configure the toolbox execution and automatically create the XML files, ensuring their syntax correctness (Fig. 15).

Listing 1: An example of an *elaboration.xml* file generated with the graphical user interface.

```

1 <?xml version="1.0" encoding="utf-8"?>
  <elaboration>
    <FolderName>.\InputData\UNIPDsubject\2014-06-09</FolderName>
    <Trials>Walking1 Walking2 FastWalking1 FastWalking2 Running1
      Running2</Trials>
    <Filtering>
6     <Trial>
      <Name>Walking</Name>
      <Fcut>
11        <Markers>8</Markers>
        <Forces>8</Forces>
        <CenterOfPressure>7</CenterOfPressure>
      </Fcut>
    </Trial>
    <Trial>
16     <Name>FastWalking</Name>
      <Fcut>
        <Markers>10</Markers>
        <Forces>10</Forces>
        <CenterOfPressure>7</CenterOfPressure>
      </Fcut>
21     </Trial>
      . . . .
    </Filtering>
    <WindowSelectionProcedure>
      <StanceOnFPfromC3D>
26     <Leg>Right</Leg>
      <LabelForHeelStrike>Foot Strike</LabelForHeelStrike>
      <LabelForToeOff>Foot Off</LabelForToeOff>
      <Offset>20</Offset>
      </StanceOnFPfromC3D>
31 </WindowSelectionProcedure>

```

```

36  <Markers>C7 RA LA L5 RPSIS LPSIS RASIS LASIS RGT LGT RLE ...
    </Markers>
    <EMGMaxTrials>Running1 Running2 MVCadd MVCtibant MVCper
      MVCtfl ...</EMGMaxTrials>
    <EMGsSelection>
      <EMGSet>UNIPD-CEINMS</EMGSet>
      <EMGs>
      <EMG>
        <OutputLabel>addmag_r</OutputLabel>
        <C3DLabel>Right Adductor Longus</C3DLabel>
      </EMG>
41    ...
      </EMGs>
    </EMGsSelection>
    <EMGOffset>0.2</EMGOffset>
    <OutputFileFormats>
46    <MarkerTrajectories>.trc</MarkerTrajectories>
      <GRF>.mot</GRF>
      <EMG>.mot</EMG>
    </OutputFileFormats>
  </elaboration>

```

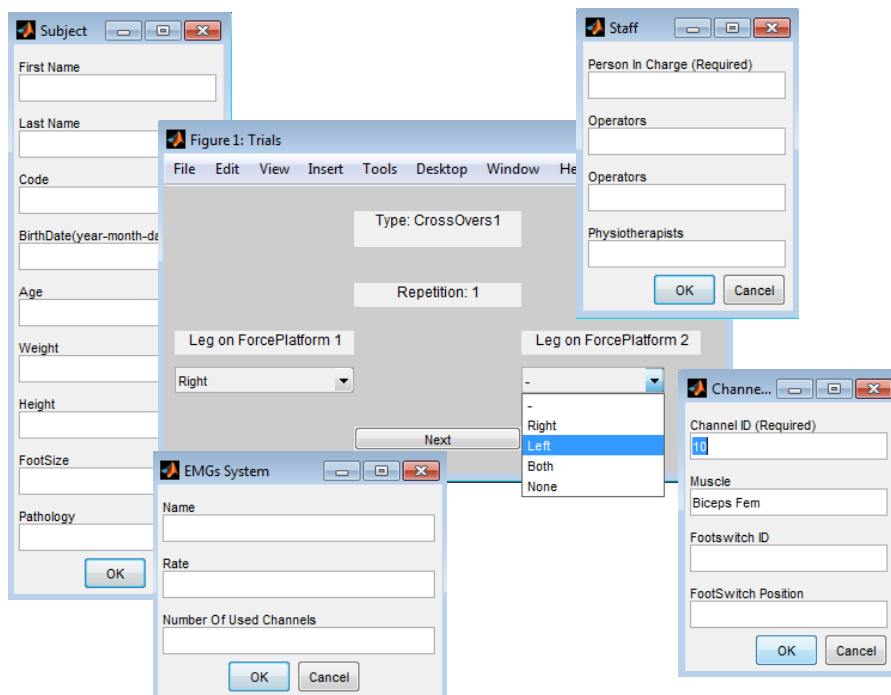


Figure 15: **MOTO NMS GUI**. Examples of user-friendly graphical MATLAB interfaces available in MOTO NMS for the configuration of the toolbox procedures (acquisition, elaboration, static configuration files).

3.4 RESULTS

Data from four institutions were processed using MOtoNMS. The four gait laboratories are characterized by different instrumentations and setups (Tables 3 and 4): (1) three motion capture systems: BTS, Vicon, and Qualysis; (2) three types of FPs, requiring different computation for plates moments and CoP (Table 2); (3) four different setup for the global reference system, and FP positions and orientations along the walkway, resulting in different rotations from each FP reference system to the global one; (4) different configurations of analog channels; and (5) marker and EMG protocols dependent on each laboratory routine analysis.

Experimental data were collected from four healthy subjects, one for each institution, who gave their informed consent. MOtoNMS was used to elaborate the collected movement trials and produce the following outputs: (1) .trc and .mot files for OpenSim (Fig. 16), (2) joint centers for hip, knee, and ankle and, depending on data availability, also wrist, elbow, and shoulder (Fig. 17), (3) normalized EMG linear envelopes (Fig. 18), and (4) plots of processed data (Fig. 19).

Tests aimed at proving the correctness of execution on different combinations of configuration options, i.e., the definition of the analysis window, the cut off frequencies for filtering, number and combination of trials to be elaborated and different sets of trials for the computation of the maximum EMG peak.

To illustrate MOtoNMS capabilities, a selection of the collected trials and examples of obtained results with the corresponding configuration files are available online and can be freely downloaded (Mantoan and Reggiani, 2014a). Three elaborations for the dynamic trials and one for the static acquisitions are included for each data set. Resulting .trc and .mot files can be directly loaded in OpenSim and used to visualize the processed data. The full MATLAB source code of MOtoNMS with the User Manual (Mantoan and Reggiani, 2014b) is also included to allow reproducibility of results and additional testing.

Results show that, despite the differences in instruments, configurations, and protocols (Table 3 and 4), MOtoNMS succeeded in processing data in a consistent and repeatable way, based on the parameters selected in the user-defined configuration files.

3.5 DISCUSSION

MOtoNMS enables processing motion data collected with different instruments and procedures, and generates inputs for neuromusculoskeletal modeling software. Marker trajectories, GRFs, and joint centers are processed and saved using OpenSim file formats (Delp et al., 2007), while normalized EMG linear envelopes are exported by de-

Table 3: Characteristics of the laboratories testing MOtoNMS. Four institutions are involved: Department of Information Engineering, University of Padova, Italy (UNIPD), Department of Neurorehabilitation Engineering, Georg August University in Göttingen, Germany (UMG), Centre of Musculoskeletal Research, Griffith University, Gold Coast, Australia (GU), and School of Sport Science, Exercise and Health, University of Western Australia, Perth, Australia (UWA).

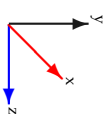
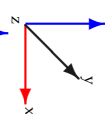
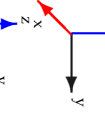
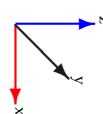
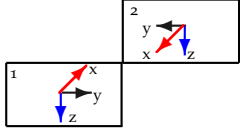
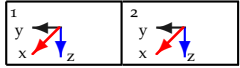
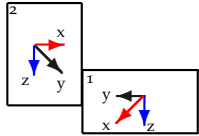
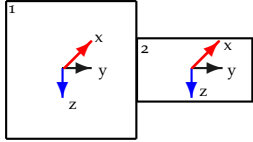
Institution	Acquisition Device (Hardware/Software)	Global Reference System	Kinematic Sampling Rate(Hz)	Markers Protocol	EMG Device	Analog Rate (Hz)	Analog Channels: Output Data
UNIPD	BTS Smart E BTS Smart Capture		60	modified version of IORgait (Del Din et al., 2011)	BTS Pocket EMG	1020	1-6: FP1; 7-12: FP2; 13-17: EMG
UMG	Qualysis Qualysis Track Manager (QTM)		240	modified version of Dorn et al. (2012)	-	720	1-6: FP1; 8-13: FP2
GU	Vicon Vicon Nexus		200	10 Points Cluster (Cereatti et al., 2006)	Aurion Zero Wire	1000	1-6: FP1; 7-12: FP2; 29-44: EMG; 13-28, 45-52: Biodex
UWA	Vicon Vicon Nexus		250	UWA full-body (Dempsey et al., 2007)	Noraxon 2400T G2	2000	1-6: FP1; 7-12: FP2; 13-28: EMG

Table 4: **Force platforms characteristics of the laboratories testing MOtoNMS.** Different FP types require different procedures for plate moments and CoP computation. Force platform of type 3 is not available in the laboratories, but it is implemented in the toolbox and it has been tested by another institution.

Institution	Num	Brand and Model	Type	Sizes(mm)	Position along the walkway
UNIPD	2	Bertec 4060-08-1000	1	400x600 400x600	
UMG	2	Bertec 4060-07-1000	4	400x600 400x600	
GU	2	Kistler 9287B	2	900x600 800x600	
UWA	2	AMTI BP12001200 Kistler 9281C	2	1200x1200 400x600	

fault to the OpenSim motion file format (.mot), compatible also with CEINMS (Lloyd et al., 2014).

MOtoNMS has been designed to be flexible and highly configurable, to satisfy the requests of different research groups without the need of accessing and modifying the code. Indeed, processing properties (i.e., selected trials, cut-off frequencies, data analysis window, markers list, joint centers of interest, ...) can be selected directly from user-friendly graphical interfaces and stored, together with the laboratory arrangements, in configuration files. In addition, processed data, along with the configuration and processing log files, are automatically organized in output directories with a uniquely defined structure. This becomes an essential feature for information retrieval and when results are shared among different research teams, especially if large amount of data are involved. Finally, MOtoNMS has been developed in MATLAB for its large diffusion in biomechanics research, and works on the most diffused operating systems (Windows, Linux, and Mac OS X).

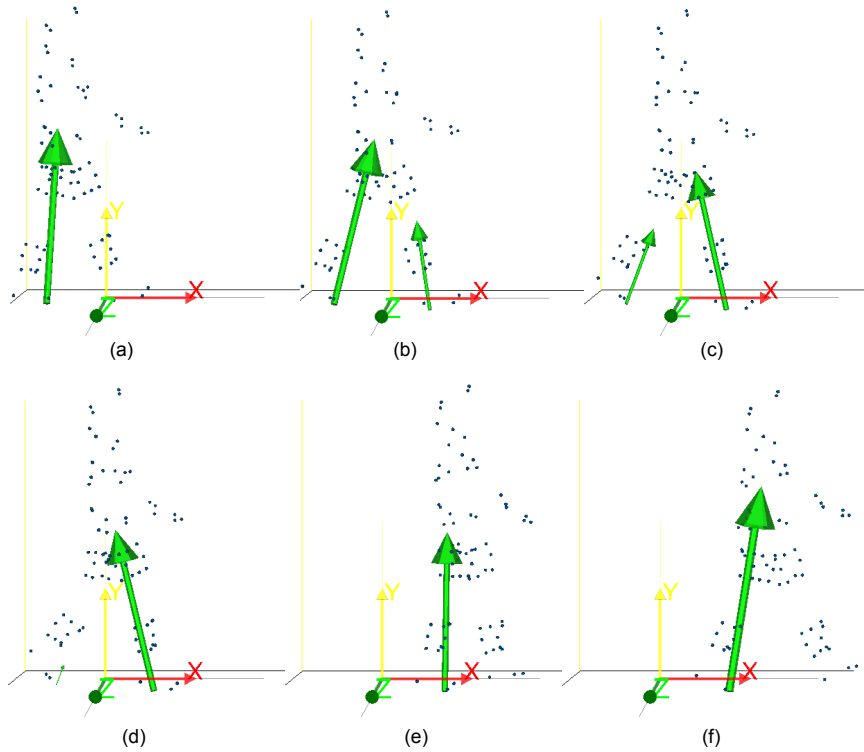


Figure 16: **Gait cycle in OpenSim.** Example of .trc and .mot files generated using MOtoNMS and loaded in OpenSim. The sequence (a-f) reproduces a gait cycle on the laboratory force platforms.

Currently available alternatives to MOtoNMS do not provide complete solutions that generalize across laboratories. Lee S. and Son J. proposed a toolbox that converts motion data in OpenSim inputs (Lee and Son, 2012), however it is limited to VICON systems only. Other MATLAB functions with a broader applicability are available on the SimTK.org website (Dunne, 2013; Seth, 2008; Lichtwark et al., 2013). While they implement several tasks, they are not connected in a well-structured instrument able to fully process data in a single procedure. The users are required to go through a sequence of MATLAB functions and often to adapt the code to their own laboratory configuration and experimental protocols. Tim Dorn provides a complete tool with the C3D Extraction Toolbox (Dorn, 2011). However, support and testing of different laboratory setup is limited to specific instrumentation types (i.e., assumption of AMTI force plates). Finally, none of these solutions provide a tool to process the recorded data supplying filtering blocks, several methods for the analysis windows selection, computation of joint centers, EMG linear envelopes and maximum EMG peaks from selected trials for normalization.

Results showed that MOtoNMS could instead be used to process data from laboratories of four institutions (Table 3) with three different motion capture systems (i.e., Vicon, BTS, Qualisys), EMG units (Noraxon, BTS, and Zerowire), as well as GRF data generated by four

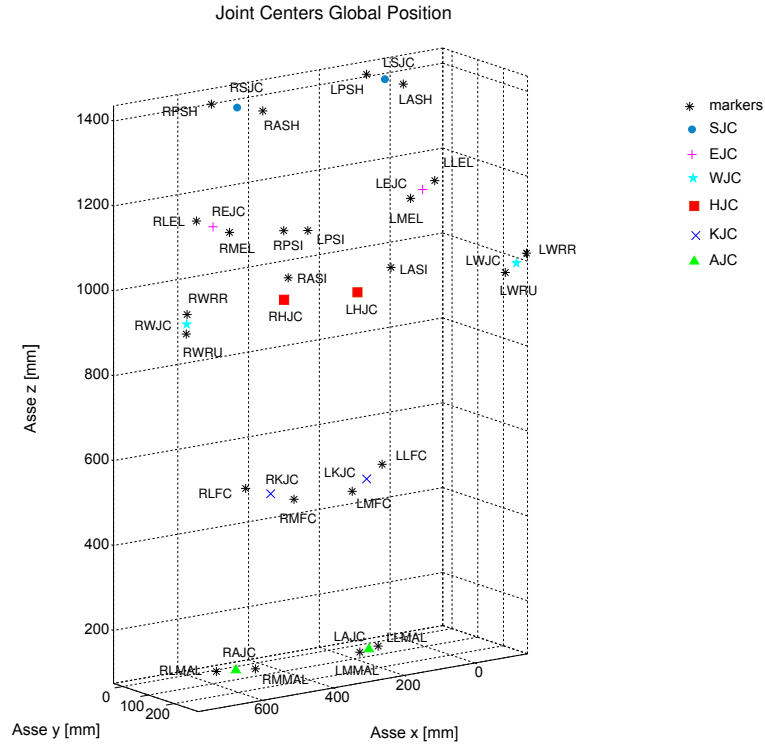


Figure 17: **Joint Centers.** A 3D view of hip (HJC), knee (KJC), ankle (AJC), elbow (EJC), shoulder (SJC) and wrist (WJC) joint centers and markers used for their computation.

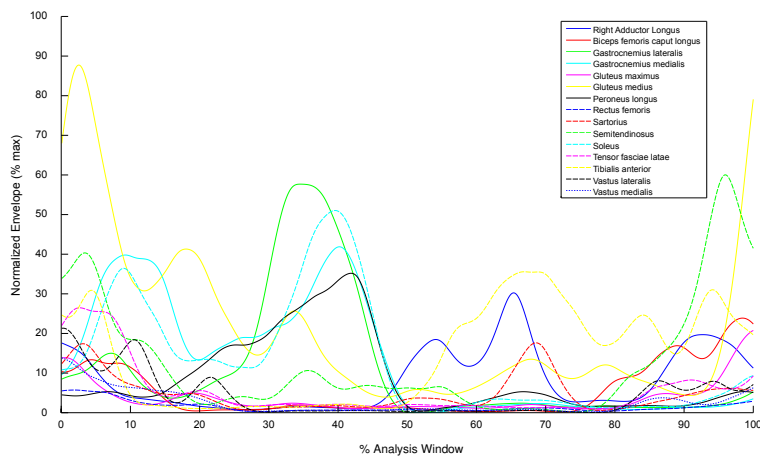


Figure 18: **Normalized EMG linear envelopes.** Normalized EMG linear envelopes versus the percentage of the analysis window selected for the elaboration. All muscles of a single acquisition are grouped together to provide a global picture of the output of the EMG processing step.

different force plate types (i. e., types 1 to 4 by Bertec, AMTI, and

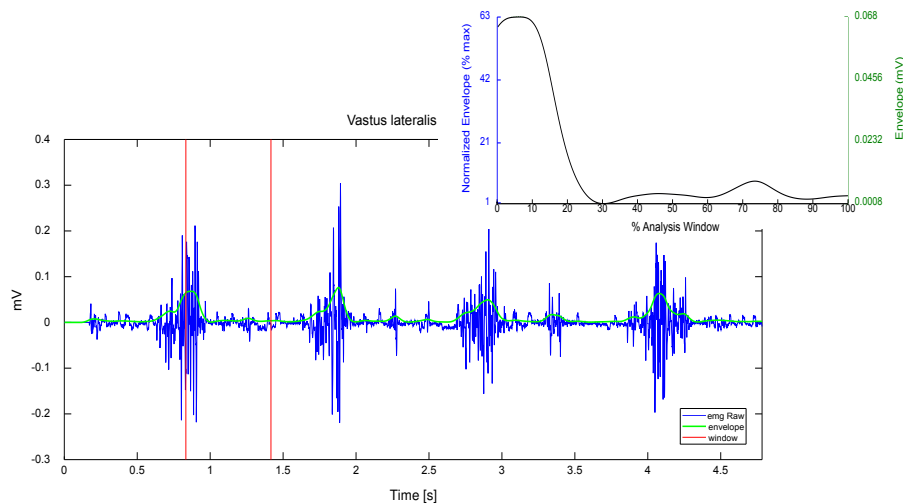


Figure 19: **Example of output EMG plots.** The main plot shows raw EMG (blue) for an overall trial, together with the computed envelope (green) and the analysis window (red). An example of plot of an envelope within the analysis window is reported in the smaller picture. Two measurement scales are visible in the graph: the normalized one (blue, on the left), and the voltage from the acquisition device (green, on the right).

Krisler, Table 4). This makes MOTO-NMS the first toolbox that allows users to easily configure the processing of motion data from laboratories with different instruments, software, protocols, and methodologies, and export data processed for musculoskeletal applications. MOTO-NMS currently supports OpenSim and CEINMS file formats. Nevertheless, its design facilitates the generation of output files compatible with other musculoskeletal applications.

3.6 MOTO-NMS AND THE OPEN-SOURCE APPROACH

Open-source musculoskeletal software, such as OpenSim (Delp et al., 2007), NMS Physiome (Testi et al., 2012), OpenMaf (Viceconti et al., 2007), are commonly used within the community. They have been developed to facilitate the process of modeling and simulating musculoskeletal systems and to share models, algorithms, simulations, that can be improved by any users. Other software in the field have been recently proposed, still supporting an open-source approach (Barre and Armand, 2014). Several authors recognized in the lack of user-friendly and efficient software one of the main limitations for the diffusion of NMS modeling techniques (Erdemir et al., 2007; Reinbolt et al., 2011), and stressed the importance of sharing models, simulations tools, results, for validation and verification purposes (Hicks et al., 2015). Following this trend, we also strongly believe in the importance of sharing materials and tools that can contribute to advancements in the research field. These can only be achieved if researchers

start to share the instruments they use to get the results, not only making public their conclusions. We thus embraced an open-source policy, making our work freely available, supporting it with documentation constantly updated, allowing others to test, reproduce and extend the tool capabilities (Table 5).

We created a dedicated OpenSim project page at the SimTK.org website (Mantoan and Reggiani, 2014a) to officially release the tool on the 9th May 2014, under GNU GPL License (The Free Software Foundation, 2013). The choice of the GPL License was carefully evaluated and concurs in giving emphasis to the open source approach. It indeed ensures that any application exploiting MOtoNMS or other derivatives and future extensions of the software will be distributed under the terms and conditions of the GLP License, and thus be also equally free and open-source.

Latest versions of the toolbox are constantly uploaded on the created project page at the SimTK.org website (Mantoan and Reggiani, 2014a), together with updates in the user manual (Mantoan and Reggiani, 2014b). We also provide a set of testing data as a sample to help MOtoNMS newbies in gaining confidence with the tool and in testing it (Table 5). The package includes: (i) a selection of collected data from the four institutions involved in the study; (ii) examples of setup files for laboratory and experimental configurations; (iii) a few examples of configuration files for MOtoNMS execution; (iv) processed data resulting from the execution of MOtoNMS on the input data according to the parameters defined in configuration files, to allow reproduction and comparison of results (Section 3.4).

At present, MOtoNMS is listed in the online OpenSim Documentation among the tools made available by members of the OpenSim community to prepare experimental data for their use within the OpenSim software (Links, Table 5).

The source code is managed in a public GIT repository (<https://github.com/RehabEngGroup/MOtoNMS>), where the master branch is normally kept in a stable version with only the tagged release versions that are made available on the project home page. The user manual was initially available as a public document, and now it is even hosted on GitHub Pages (Mantoan and Reggiani, 2014b). The GitHub repository of the project was introduced to provide an easy way for anyone to do an update to the latest version of the tool, but mostly for developers, to trace changes in the development of the software and to encourage contributions to extend MOtoNMS capabilities from other users.

3.7 CONCLUSIONS AND FUTURE WORKS

This chapter presented MOtoNMS, a toolbox freely available to the community, that has been developed to provide a complete, flexible

Project name	Matlab MOTion data elaboration Toolbox for NeuroMusculoSkeletal applications (MOtoNMS)
Project home page	https://simtk.org/home/motonms/
Available materials	Source Code User Manual Test Data
License	GNU General Public License v3
Repository	public GIT repository https://github.com/RehabEngGroup/MOtoNMS
Documentation	http://rehabenggroup.github.io/MOtoNMS [User Manual]
Links	http://simtk-confluence.stanford.edu:8080/display/OpenSim/Tools+for+Preparing+Motion+Data
Programming language	MATLAB
Operating system(s)	Platform independent
Other requirements	Biomechanical Toolkit (BTK, https://code.google.com/p/b-tk/) or C3Dserver (http://www.c3dserver.com/)
Releases	v. 1.0 (February 17, 2014, initial release) v. 2.0 (May 9, 2014, first online release) v. 2.1 (September 8, 2014)

Table 5: Overview on the open-source MOtoNMS project.

and user friendly tool to automatically process experimental motion data from different laboratories in a transparent and repeatable way, for their subsequent use in neuromusculoskeletal software.

The toolbox description and results showed that MOtoNMS succeeds in generalizing data processing methods across laboratories, while meantime simplifying and speeding up the processing workflow. MOtoNMS, indeed, implements commonly required processing steps, and its generic architecture simplifies the integration of new user-defined processing components. Moreover, users can easily setup their own laboratory and processing procedures, without constraints in instruments, software, protocols, and methodologies, and without change in the MATLAB code. In addition, the software improves data organization, providing a clear structure of input data and automatically generating output directories, thus simplifying the processing and management of large datasets. Finally, storing to file the configuration choices allows to fully reproduce the processing steps and results.

MOtoNMS is an ongoing software with a dynamic cycle of development, aimed at extending its features. Additional methods for joint center computation, e.g. based on functional movements, may be included in a near future. Customizable algorithms for a better control in the computation of EMG maximum and average could also be introduced. We are also planning to distribute a database of configuration files for the most popular acquisition protocols (Davis et al., 1991; Kadaba et al., 1990; Cappozzo et al., 1995).

MOtoNMS can be useful to the research community, reducing the gap between experimental movement data and neuromusculoskeletal simulation software, and uniforming data processing methods across laboratories. Moreover, its support to several devices, a complete implementation of the processing procedures, its simple extensibility, the available user interfaces, and its free availability, can boost the translation of neuromusculoskeletal methods in daily and clinical practice.

THE NMS MODEL CALIBRATION: EMG NORMALIZATION

4.1 INTRODUCTION

The fundamental advantage of an EMG-driven NMS approach is that it exploits EMG signals from an individual to assess how muscle activate in response to the neural drive, and how the forces they generate are partitioned to produce the given movement. However, prior to use the model in open-loop as a predictive system, it must be calibrated to account for the actual behavior of the neuromusculoskeletal system of the subject, which is unique and cannot be generalized (Lloyd and Buchanan, 1996; Buchanan et al., 2004; Fregly, 2009).

At this stage of modeling, calibration is referred to the process of determining the set of parameters that defines the muscle force generating properties for each muscle-tendon unit of an individual. Parameters in the NMS model can be divided into two groups. The first set defines the musculotendon unit's activation dynamics (Section 2.2.1), which characterize the transformation of muscle excitation to muscle activation. The second parameter group defines the musculotendon contraction dynamics (Section 2.2.2), which transform the muscle activation and musculotendon kinematics into force.

Several strategies have been proposed to set these model parameters (Fregly, 2009; Pandy and Andriacchi, 2010; Chèze et al., 2012; Menegaldo and Oliveira, 2012; Hicks et al., 2015). As described more in detail in Section 2.2.4, the EMG-driven NMS model under investigation starts from a set of uncalibrated parameters and exploits an optimization algorithm, such as simulating annealing, to alter the values of parameters so that the moments estimated for a set of calibration trials, closely track the corresponding joint moments derived from inverse dynamics calculations (Lloyd and Buchanan, 1996; Lloyd and Besier, 2003; Buchanan et al., 2004; Sartori et al., 2012a). The result of the calibration is a subject-specific neuromusculoskeletal model.

There are numerous evidence that values assigned to the parameters in a model have a large influence on the accuracy of model predictions (Pandy and Andriacchi, 2010; De Groote et al., 2010; Chèze et al., 2012; Hicks et al., 2015). Calibration of the NMS model is indeed crucial to obtain accurate subject-specific estimates of muscle forces and joint moments on novel set of data.

In this work, we examined one of the possible source of error in the estimation of these parameters during the calibration process. The final set of model parameters is highly dependent on the control vari-

able used in the minimization process (i.e. joint moments estimated using an inverse dynamic approach) as widely argued in Lloyd and Besier (2003), but also on the input used to drive the model. If the prediction is based on input with some kind of errors, parameters will be refined to account also for this inaccuracy in the input data. As introduced in Section 2.4.4, basic model input are the musculotendon lengths and moment arms, which are related to the musculoskeletal geometry definition, and the EMG signals.

A branch of research in this field is focusing on the creation of accurate and personalized musculoskeletal models (Blemker et al., 2007; Scheys et al., 2008; Fregly et al., 2012; Valente et al., 2014). This would lead to more representative estimations of muscle tendon lengths and muscle moment arms for individuals.

EMG signals have also a great impact on the adjustment of model parameters. Koo and Mak (2005), in testing validity and accuracy of their NMS model of the elbow, concluded that the estimate of muscle activation from recorded EMG signals appeared to be the major source of uncertainty within the EMG-driven model. Chèze et al. (2012), in their review about the state of the art of models and methods to predict muscle forces, summarized the advantages and the main limitations of EMG-driven methods. Among the latter, they evidenced the influence of electrodes positioning and tissue conductivity, which are known to drastically affect the amplitude of the signal (De Luca, 1997), the influence of EMG processing on the model computations (Staudenmann et al., 2007; Disselhorst-Klug et al., 2009; Oliveira and Menegaldo, 2012), and the inability to access EMG data from deeply located muscles. A review on methodological aspects of surface EMG recordings for force estimation has been recently proposed (Staudenmann et al., 2010), while guidelines for processing raw EMG signals for neuromusculoskeletal applications have been reported in the literature (Lloyd and Besier, 2003; Buchanan et al., 2004), and are described in Sections 2.2.1 and 2.4.3. Therein, the most critical step is identified in the normalization of EMG amplitudes, due to difficulties in obtaining true maximum EMG values. Since his first works on the NMS model, even Professor D. Lloyd recognized in the stochastic nature of the EMG signal and the recordings of maximum EMGs, two sources of error (Lloyd and Buchanan, 1996). More recently, several other authors pointed out the difficulties in the estimation of the EMG normalization factor, and the consequences in the achievable accuracy of model predictions (Koo and Mak, 2005; Oliveira and Menegaldo, 2012). This aspect represents therefore a critical problem and cannot be neglected.

EMG normalization

EMG normalization is usually performed to allow comparison among different subjects, muscles, studies and testing sessions. However, nu-



Figure 20: An example of isokinetic dynamometer (Biodex System 4 Pro).

merous methods have been proposed due to a lack of agreement on the more appropriate (Burden, 2010; Burden et al., 2003; Knutson et al., 1994; Burden and Bartlett, 1999; Bolgla and Uhl, 2007). Maximal voluntary isometric contraction (MVC) appears to be the most common normalization method used (Burden, 2010; Norcross et al., 2010). It is the same suggested by Buchanan et al. (2004) and adopted by most authors when recurring to single-DOF NMS models for muscle force estimation (Koo et al., 2002; Lloyd and Besier, 2003; Koo and Mak, 2005; Doorenbosch et al., 2005; Besier et al., 2009; Winby et al., 2009a; Shao et al., 2009; Oliveira and Menegaldo, 2012). It is a common practice to obtain measurements of muscle strength capabilities using external dynamometers (e.g. Biodex, Fig. 20), load cells or training machines, against which subjects exert maximal voluntary contractions of muscles in static (isometric) tests (Kroemer and Marras, 1980; Konrad, 2005; Doorenbosch et al., 2005; Koo and Mak, 2005; Burnett et al., 2007; Menegaldo et al., 2014).

EMG normalization in EMG-driven NMS modeling

In the field of EMG-driven NMS, the previously described approach is particularly suitable for single-DOF models, and their applications for example to the knee joint (Lloyd and Buchanan, 2001; Lloyd and Besier, 2003; Lloyd et al., 2005) or to the elbow (Koo and Mak, 2005). Focusing on lower extremities, consider for example the hip joint: the execution of tasks involving the recruitment of hip muscles is usually not feasible with this kind of testing machine, and other methodologies have to be exploited (Bolgla and Uhl, 2007).

Lloyd and Besier (2003), when applying for the first time their single-DOF model to the knee joint to predict the knee moment across a wide set of tasks, normalized the processed EMG data from each muscle dividing by the single maximum value obtained from all that muscle's corresponding MVC trials. However, they noticed that muscle inhibition can occur during MVC trials, leading to a muscle activation in the model above 1. Calibration dataset, instead, is usually different to that use to compute the maximum EMG peak. In this study, it included a passive knee flexion-extension (FE) on a Biodex isokinetic dynamometer, running, crossover and sidestepping tasks,

and maximal isokinetic concentric knee FE at 120° on a Biodex dynamometer. The authors stressed the importance of using a variety of tasks to encompass a wide range of contractile conditions. During the calibration process, model parameters were altered to achieve the closest estimation of FE knee moment to that computed for the chosen calibration dataset using an inverse dynamic approach, after normalization of the corresponding input EMG signals against the peak EMG values from MVC trials. From a methodological point of view, subsequent applications originated from this work of Professor D. Lloyd, mainly differ for the joints and tasks examined, for the data set used to calibrate the model, and for the method used to estimate the maximum EMG value by which normalize the EMG linear envelopes (Table 6).

For instance, Besier et al. (2009), to predict muscle forces during walking and running, used three calibration trials, including walking, running and a static squat, and normalized the EMG signals to the maximum value for each muscle obtained during MVC trials of the knee extensors, knee flexors and ankle plantar flexors. Differently to previous single-DOF studies, the MVC were performed with the aid of a tester, who oppose manual resistance to the movement.

Winby et al. (2009a) applied an EMG-driven model to healthy human gait, using the predicted muscle forces to estimate knee joint contact loads and the relative contribution of the muscles. In this work, linear envelopes for each muscle were normalized against their maximum value obtained combining maximal isometric and isokinetic contractions with dynamic tasks such as calf raises, walking and running. The calibration data set included instead five trials: two normal walking, two fast walking and a running trial.

Moving to more clinical applications related to neurological disorders, Shao et al. (2009) applied their EMG-driven model to estimate muscle forces and the ankle joint moment during stance for four patients following stroke. At our knowledge, they were the first to calibrate an EMG-driven NMS model for the lower limbs on a single walking trial only. They collected MVC to normalized the EMG data, but in the paper it is not described how they did.

EMG normalization in multi-DOF EMG-driven NMS modeling

There are only two applications of a multi-DOF model in the literature: Sartori et al. (2012a) and Barrett et al. (2007). The first one focused on demonstrating that the multi-DOF model solutions provide a more accurate prediction of the actual muscle behavior than it is possible with single-DOF models. The calibration dataset in this case included two repetitions of the following motor tasks: walking, running, sidestepping, and crossover cutting maneuvers. The dataset used to validate the model included ten repeated novel trials for each of the four considered motor tasks. Moreover, EMG data were normal-

ized with respect to the peak processed EMG values obtained from the entire set of recorded trials, that is, no MVC, but only dynamic conditions, were considered.

The work of Barrett et al. (2007) is the most divergent. He used kinematic and EMG data from Winter (2009), and the calibration process minimised the sum of squares error between simulated and measured angular kinematics of the hip, knee and ankle joints. Interestingly, the filtered EMG data for 11 muscles from Winter (2009) were normalized to the maximum values obtained during the gait cycle.

Multi-DOF model means that muscles are constrained to produce forces that satisfy moments about multiple DOFs (Section 2.2). The augmented level of complexity is accounted within the calibration process, and thus it may have an impact on the calibration strategy. Conducting MVC with an external dynamometer allows to perform a set of tasks often limited to a single DOF. Therefore, coming to multi-DOF applications, the acquisition protocol should be extended to include exercises with or without manual resistance, able to recruit all the muscles of interest. However, to date, there are no studies proposing and validating such a protocol.

Alternatively, Sartori et al. (2012a) exploit multiple motor tasks such as running, crossover and sidestepping both to calibrate the model and to compute the maximum EMG values. The authors justified the choice of the four motor tasks for the calibration dataset as they allow to generate high moments about the four considered DOFs, and because they are supposed to guarantee different contraction dynamics. No considerations were made, instead, on the effects of adopting the same strategy for the EMG normalization. Nevertheless, the problem with this solution is that it cannot be performed by aged or impaired people, and thus it is not replicable in the clinical practice.

On the contrary, feasibility of Barrett et al. (2007) approach for EMG normalization would be interesting in a clinical context, where patient may be not able to perform MVC contractions or may suffer fatigue due to the longer acquisition protocol. However, it needs to be further investigated. Differently from Sartori et al. (2012a), Barrett et al. (2007) reported in the paper the optimal values of model parameters resulting from calibration. Compared to those from previous single-DOF applications, they appear to be very close to their physiological bounds (Table 7, from Barrett et al. (2007)). This might suggest an overfitting, and deserves further testing and analysis. Moreover, in the same article, considerations about muscle forces were not proposed.

Chapter Overview

We believe that results of the calibration process must be critically evaluated prior to trust the model predictions, in accordance with Fregly (2009); Menegaldo and Oliveira (2012); Hicks et al. (2015), and

that moving to multi-DOF applications, the impact of the methodology used to calibrate the model has not been yet examined.

Few sensitivity analysis can be found in the literature for single-DOF models. Koo and Mak (2005) ascertained the feasibility of their model through a parametric analysis, revealing a high sensitivity of results to the EMG normalization factor. In the same year, Doorenbosch et al. (2005) tested the applicability of submaximal voluntary contractions to calibrate a simple EMG to force model of the knee for clinical applications. Lastly, Oliveira and Menegaldo (2012) addressed limitations due to an unreliable normalization from MVC. At present, there are no equivalent studies for a multi-DOF model.

In this chapter, it is shown how different EMG normalization techniques can lead to different results for a multi-DOF EMG-driven NMS model. We demonstrate that looking at the matching between external and predicted joint moments is not sufficient to validate the model, as the prediction of muscle forces may be significantly different with a comparable level of agreement in joint moments estimation.

A direct validation of muscle forces is not possible since they can not be measured, thus we propose a methodological approach to assess the validity of results obtained both in the calibration process and in the subsequent open-loop execution.

With the aim of bringing EMG-driven NMS models to clinical practice, where isokinetic dynamometers are seldom available and the degree of impairment of subjects limited the dynamic tasks that can be selected for the calibration data set, we decided to evaluate the impact of using an approach similar to that found in Barrett et al. (2007) on model results. In this context, the calibration dataset was restricted to walking trials, while two methodologies for EMG normalization based on the maximum EMG value were compared: the one suggested by Barrett et al. (2007), named WTN normalization (Walking Trials Normalization) to indicate that the peak EMG value for each muscle is obtained from all the collected walking trials, and the MVCTN normalization (MVC Trials Normalization), where the maximum EMG value is extracted from MVC. For collecting MVC trials, in the first study we designed a protocol based on manual testing, since a isokinetic dynamometer was not available. From a general perspective, combining exercises with and without a isokinetic dynamometer to satisfy the requirements of a multi-DOF model, may be more time-consuming and thus less convenient for the patients. We obtained higher levels of muscle activation when the normalization factors were derived from walking trials, which then resulted in remarkable differences in muscle forces estimation.

To assess the results, we looked at the muscle-tendon parameters values after calibration, and considered the muscle contributions to each net joint moment. We found that changing the method for EMG nor-

malization has a strong impact on calibration parameters. In the WTN case, muscle parameters are mostly comparable to those obtained by Barrett et al. (2007), while the MVCTN approach leads to parameters values less close to the physiological bounds.

As a consequence of these findings, we designed a second study aiming to generalize and standardize the procedure for conducting MVC tests for lower limbs, so that it can be performed in any context without the need of expensive devices or an expert manual tester. We propose a minimal protocol of simple adoption by different laboratories, characterized by equipment limited to common and inexpensive tools and by a minimum number of tasks in order to reduce execution time and patients' discomfort. A case study is presented comparing results accomplished using the new protocol for EMG normalization and those derived from a WTN approach. Results confirmed those obtained in the first study, pointing out the fundamental relevance of the EMG normalization strategy, and that the proposed minimal protocol is able to reproduce results achieved with the aid of an expert manual tester.

The remainder of this chapter is organized as follow: firstly, the objectives of the two parts are briefly summarized. Then, the two studies are presented in sequence, each of them with its own methods, results and discussion sections. Finally, a general conclusion on the overall work ends the chapter.

4.2 AIMS

4.2.1 *Aim of the First Study*

This study aims at determining the applicability and reliability of the WTN method, as a method for normalizing gait EMGs, by evaluating its impact on the multi-DOF EMG-driven NMS model calibration and open-loop predictions.

4.2.2 *Aim of the Second Study*

This second study aims at consolidating results from the previous work, replicating the analysis on another subject, thus enlarging the dataset.

In addition, this investigation aims at defining a standard *minimal* protocol for conducting maximum voluntary contraction tests for lower limb muscles that answers the following requirements:

- be operator-independent;
- be replicable in any laboratory without the need of expensive devices;

Table 6: Comparison of some EMG-driven NMS models derived from Lloyd and Besier (2003).

DOF	Validation Dataset	Calibration Dataset	Trials for peak EMG Computation
Lloyd and Besier (2003)	KneeFE 30 tasks with Biodex dynamometer or within gait lab	passive KneeFE (Biodex); straight run; sidestep; maximal isokinetic concentric KneeFE at 120°(Biodex); crossover cut;	MVC manual MVC for knee extensors, knee flexors and ankle plantar flexors
Besier et al. (2009)	KneeFE 2 x walking, running	1 x walking, running, static squat	manual MVC for knee extensors, knee flexors and ankle plantar flexors
Shao et al. (2009)	AnkleFE 3 walking	1 walking	MVC
Barrett et al. (2007)	HipFE, KneeFE, AnkleFE walking from Winter (2009)	walking from Winter (2009)	walking from Winter (2009)
Sartori et al. (2012a)	HipFE, KneeFE, AnkleFE 10 x walking, running, sidestepping, crossover	2 x walking, running, sidestepping, crossover	the entire set of recorded trials

Table 7: Initial values for maximum isometric force (F_0) and muscle parameters obtained from model calibration in Barrett et al. (2007). The force scaling factor (FSF) was allowed to vary between 0.50 and 1.50, while the shape factor (A) and the recursive filtering coefficients (C_1 and C_2) were defined according to model's constraints ($-3 < A < 0$, and $|C_1| < 1$, $|C_2| < 1$, Lloyd and Besier (2003), Section 2.2.1). The parameters were calibrated for each muscle (source: Barrett et al. (2007)).

Muscle	F_0 (N)	FSF	A	C_1	C_2
m. semimembranosus	1030	0.50	-0.01	-0.998	-0.998
m. semitendinosus	328	0.50	-0.01	0.979	0.979
m. biceps femoris (long)	717	0.50	-0.01	-0.998	-0.998
m. biceps femoris (short)	402	0.60	-3.00	0.985	0.985
m. gluteus maximum (sup)	382	1.50	-3.00	-0.949	-0.949
m. gluteus maximum (mid)	546	1.50	-3.00	-0.954	-0.954
m. gluteus maximum (inf)	368	1.50	-2.58	-0.959	-0.959
m. iliacus	1500	1.50	-3.00	0.984	0.984
m. rectus femoris	779	0.50	-0.01	-0.989	-0.989
m. vastus medialis	1294	0.50	-0.01	-0.966	-0.967
m. vastus intermedius	1356	0.50	-0.01	-0.967	-0.967
m. vastus lateralis	1871	0.50	-0.01	-0.966	-0.966
m. gastrocnemius (med)	2372	0.50	-2.46	-0.998	-0.998
m. gastrocnemius (lat)	488	0.50	-0.01	0.954	0.954
m. soleus	2839	0.50	-0.01	0.989	0.989
m. tibialis anterior	603	0.69	-2.12	0.995	0.995

- be possibly performed by aged and pathological patients who can walk.

With the more general intent to foster the adoption of neuromusculoskeletal modeling techniques by multiple laboratories and research groups, it is indeed important that such protocol be easily performed routinely. The name *minimal* recalls that particular attention is given to keeping the number of tasks to execute to a minimum, and to only adopt common, inexpensive equipment.

4.3 FIRST STUDY

As described in 2.4, the workflow included: i) collecting human movement data using motion capture technology, ii) processing and preparing experimental data for their use in musculoskeletal software iii) musculoskeletal modeling and simulation of the recorded human movement, iv) calibrating and executing the EMG-driven NMS model.

4.3.1 Data Collection

Experimental movement data were collected and processed to enable the EMG-driven model calibration and subsequent execution.

4.3.1.1 Subject and Experimental Setup

One healthy male subject (age: 60, height: 182cm, mass: 92Kg) was enrolled for this investigation and gave his informed consent before participating in the experiment.

Retro-reflective markers were placed on the whole body of the subject (modified version of Leardini et al. (2007), as in Del Din et al. (2011)), and three-dimensional marker trajectories measured at 60 Hz using a BTS 6-camera motion capture system. Ground reaction forces and electromyographic signals were simultaneously recorded at 1020 Hz from a force plate (FP4060-10, Bertec Corporation, Columbus, OH) and 16-channel EMG system (Pocket EMG, BTS Spa). Surface EMG electrodes were placed on fifteen muscles: gluteus maximus (GLUTMAX), gluteus medius (GLUTMED), tensor fasciae latae (TFL), adductor longus (ADDLONG), sartorius (SAR), medial hamstrings (SEMITEN), lateral hamstrings (BIFEMLH), rectus femoris (RECFEM), vastus medialis (VASMED), vastus lateralis (VASLAT), peroneus longus (PERLONG), gastrocnemius medialis (GASMED), gastrocnemius lateralis (GASLAT), soleus (SOL) and tibialis anterior (TIBANT). EMG data were taken separately from both legs. For this investigation, we chose at random to consider the left side.

Motion data collected from the subject included a static pose, at least ten walking trials at a self-selected pace, and MVCs for normalization of EMG data and comparison with Barrett et al. (2007) ap-

proach. The following section briefly described the protocol adopted in this study to conduct the MVC tests of the selected lower limb muscles.

4.3.1.2 *Manual MVC Protocol*

In absence of instrumentation for the recording of MVCs (e.g., a Biodex isokinetic dynamometer, Fig. 20), and considering limitations due to mobility impairments of a pathological population (i.e., running, crossover, sidestepping as used in the literature were not eligible), a protocol for MVC trials has been designed for this study based on recommendations from the literature (Kendall et al., 1993; Konrad, 2005; Palastanga and Soames, 2011). A set of 6 feasible exercises were identified to recruit and allow for an effective maximum innervation of the following muscles: TFL, ADDLONG, SEMITEN, BIFEMLH, RECFEM, VASMED, VASLAT, PERLONG, GASMED, GASLAT, SOL and TIBANT. Despite the MVC tests has to be performed for each investigated muscle separately (Konrad, 2005), we grouped some muscles within the same task to reduce the acquisition time. A simple and common exercise for all quadriceps muscles (RECFEM, VASMED and VASLAT) is a single leg knee extension from a sitting position, with the knee flexes at 90° (Fig. 21, left). Similarly, a knee flexion at 90° from a standing position involves both the hamstrings (Fig. 21, right). A single test have been included also for the GASMED, the GASLAT and the SOL. It consisted in a plantar flexion of the ankle from a standing position, with the body weight of an external operator applied to both the shoulders of the subject (Fig. 22, left). ADDLONG and TFL were instead tested separately starting from standing position and keeping the knee fully extended. The subject performed respectively a hip adduction (Fig. 22, right) and a hip abduction against a resistance. An operator was called to oppose manual resistance to the subject's leg movement in all the tasks described, except for the MVC tests planned for the TIBANT, and for the PERLONG. In the first case, the subject was asked to perform an ankle dorsiflexion from a standing position, forcing muscle contraction. For the PERLONG, the subject in a standing position, lifted and everted the foot under test, so that the face of the foot faced laterally. The positions described for each task were maintained for 10-15 seconds.

4.3.2 *Processing Workflow*

4.3.2.1 *Data preparation*

Motion data were exported into a standard C3D format (Motion Lab Systems, 2014), and processed for their subsequent use in musculoskeletal simulation software using MOtoNMS software (Chapter 3). Marker trajectories and force plate data were low-pass filtered using



Figure 21: MVC trial for the quadriceps muscles (RECFEM, VASMED and VASLAT) on the left, and MVC trial for the hamstrings muscle group (SEMITEN, BIFEMLH) on the right.



Figure 22: MVC trial for the posterior leg muscles (GASMED, GASLAT and SOL) on the left, and MVC trial for the ADDLONG on the right.

a zero-lag fourth-order Butterworth filter with a cut-off frequency of 6Hz. The portion of data corresponding to the left stance phase striking the force plate (from when the left heel contacts the force plate until the left toe leaves the ground) was selected and transformed to be consistent with the OpenSim global coordinate system.

Raw EMG data were processed by a band-pass filtering (30-300Hz), then full wave rectifying and low-pass filtering (6Hz) using a Butterworth filter, according to Lloyd and Besier (2003). The processed signal is the *linear envelope*, which needs to be normalized against the maximum value from all EMG linear envelopes available. Two different strategies for EMG amplitude normalization were applied in order to pursue the objective of the investigation, and are described in the next subsection.

EMG NORMALIZATION

Firstly, the obtained EMG linear envelopes were normalized with respect to the time: the left stance phase (100 % stance) striking the force plate was selected, synchronously with marker trajectories and ground reaction forces. However, an anticipatory time offset equals to 0.1 seconds was added before the heel contact to allow CEINMS software (Section 2.3) to account for the electromechanical delay (Mantoan and Reggiani, 2014b).

Coming to amplitude normalization of gait EMGs, two different methods were applied: the WTN and the MVCTN. In the first case, the peak amplitude of each EMG linear envelope was computed from the 10 walking trials. The MVCTN method consists instead in calculating the maximum EMG value from the MVC measured during the tasks previously described (4.3.1.2).

All processed EMGs from gait trials were divided by the peak EMG for the corresponding muscle, resulting in a normalized linear envelope in the range between 0 and 1 for each muscle.

Two different dynamic elaborations were run with MOtoNMS software for the maximum EMG value computation and envelope amplitude normalization with the two approaches (Chapter 3, Mantoan and Reggiani (2014b)).

For both methods, the mean EMG normalized envelope with the corresponding standard deviation was then obtained for each muscle from the 10 EMG profiles during the walking trials.

4.3.2.2 *Musculoskeletal modeling and simulation*

The freely available musculoskeletal modeling software OpenSim (Delp et al., 2007) was used to scale a generic musculoskeletal model (Delp et al. (1990)) to the subject to match his anthropometry based on the experimentally measured marker positions from the static pose. The Gait2392 model was chosen among the few available musculoskeletal

models with the trunk and on the basis of the number and the type of MTU modeled. The Gait2392 model is indeed characterized by 92 musculotendon actuators to represent 76 muscles in the lower extremities and torso (OpenSim, 2013). Using a full-body model helps in improving the inertial properties and inverse dynamics calculations within the simulation.

During the scaling process, virtual markers were created and placed on the musculoskeletal model based on the position of the experimental markers. After the anthropometric scaling, the OpenSim IK, ID and MA tools were run exploiting the OpenSimProcessingScripts toolbox (Mantoan and Reggiani, 2014c), to obtain respectively joint angles, joint moments and estimates of musculotendon lengths and moment arms as a function of joint angles and time.

4.3.2.3 *EMG-driven NMS model calculations*

The CEINMS software was used to implement the EMG-driven NMS model calculations (Section 2.3, Lloyd et al. (2014)). The MTUs considered within the model are reported in Table 1, while the mapping of experimental EMG signals to the individual MTU is represented in Fig. 23.

A modification was necessary with respect to the original configuration presented by Sartori et al. (2012a) (Fig. 4), to account for the absence of the experimental EMG signal from the gracilis muscle. This muscle was excluded conceiving the EMG protocol due to the difficulties in an accurate identification of sensor location, for its thin and flattened shape, and in avoiding artifacts related to electrodes movements during walking. For the NMS model computations, it was therefore associated to the adductor muscle group.

Besides that, we introduced an additional variation to the mapping proposed by Sartori et al. (2012a), but not related to the experimental setup. We found questionable and not completely justified the assumption of modeling the vastus intermedius muscle as the mean between the vastus lateralis and medialis. We preferred instead to account for the close anatomic relationship of this muscle with the vastus medialis (Palastanga and Soames, 2011), and therefore modeled it with the experimental EMG signal from that muscle only (Fig 23).

These changes were made possible by the flexibility of CEINMS software, that allows users to easily configure their own allocation of experimental EMG signals to the MTUs considered in the NMS model.

From the dynamic gait trails, two distinct datasets were created: one for the calibration of the EMG-driven NMS model, and one for its execution. The calibration dataset included five walking trials chosen at random. The remaining five trials were used to execute the calibrated model in open loop. Two distinct calibrations of the NMS model were run: one using as input the EMG linear envelope normal-

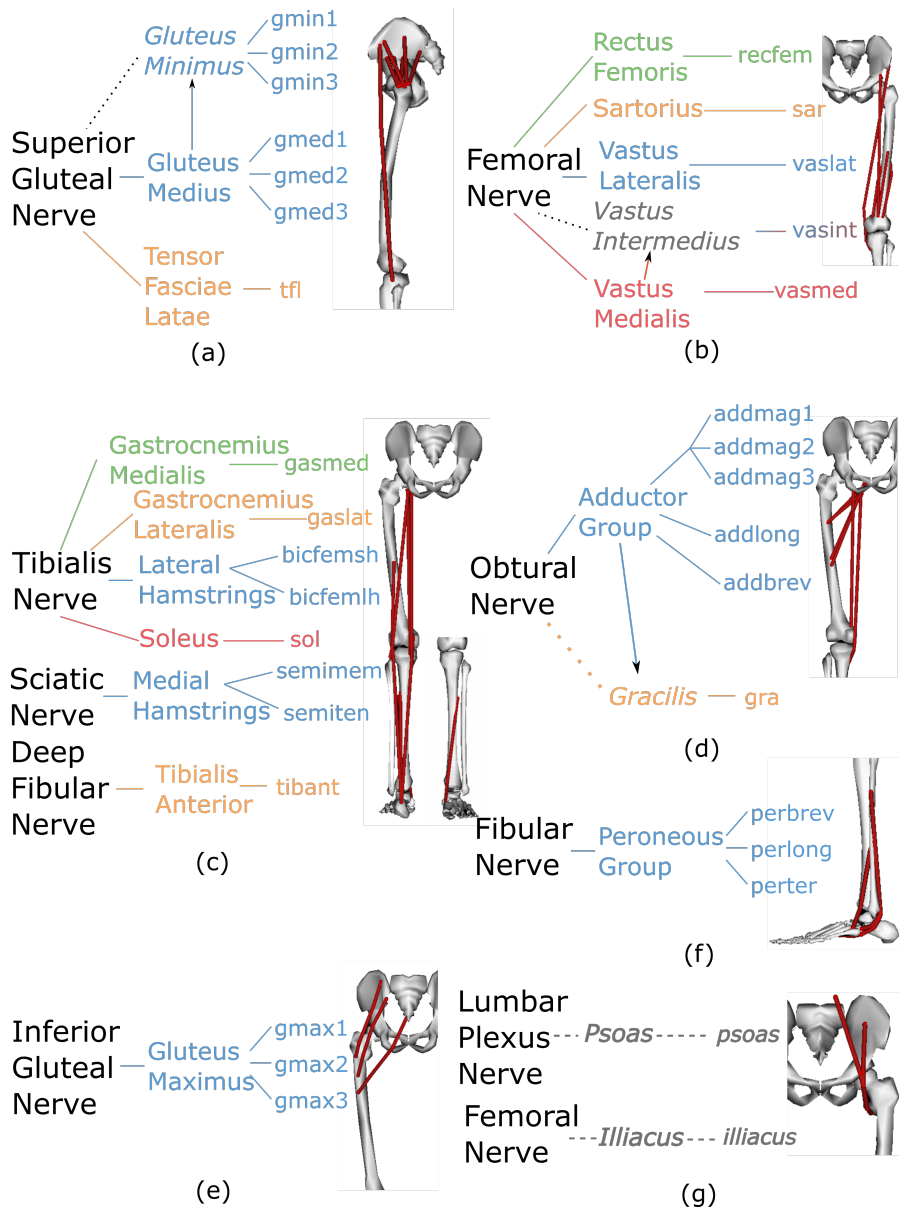


Figure 23: Mapping of the experimental EMG signals to individual musculotendon units used in this study (adapted from Sartori et al. (2012a), Section 2.2.1).

ized with WTN method (WTN calibration), and one inputting EMG obtained with MVCTN method (MVCTN calibration).

CEINMS software allows the user to set even the range where each model parameter can vary during the optimization process. Differently from the original model description (Section 2.2.1, Lloyd and Besier (2003)), the values of C_1 and C_2 were constrained to be both negative, as some problems with the damped response of the filter have occurred when the coefficients had different signs or were very close to zero. Tendon slack lengths and optimal fiber lengths were allowed to change within $\pm 5\%$ of their initial values coming from the scaled musculoskeletal model (Lloyd and Buchanan, 1996). Strength coefficients were calibrated dividing muscles into 11 groups as described in Sartori et al. (2012a): the same parameter value was assigned to muscles belonging to the same group. During calibration, they were varied between 0.5 and 3.5. Different values have been used in the literature for the EMD (Lloyd and Besier, 2003; Barrett et al., 2007), known to range from 10 msec to 100 msec (Buchanan et al., 2004), and sometimes it has been calibrated (Besier et al., 2009). We decided to fix it to 15 msec. Finally, the tendon was modeled as elastic.

The same configuration of parameter constraints were use for the two calibrations. The parameter sets obtained with the two calibrations were compared against the physiological range set in the configuration files of the calibration process (Section 2.3).

Three degrees of freedom were considered: the flexion-extension of the hip (HipFE), knee (KneeFE) and ankle (AnkleFE) joints.

The multi-DOF EMG-driven NMS model was then executed twice on the 5 walking trials not included in the calibration dataset: once exploiting the subject parameters set resulting from WTN calibration (WTN execution), the second with results from the MVCTN calibration (MVCTN execution).

4.3.3 *Data Analysis Procedure*

Results of the NMS model obtained exploiting the two different calibrations were average on the five repetitions, and then compared. The analysis included comparison of the following quantities for the two cases:

- peak EMG value for each collected EMG signal;
- mean normalized envelope for each collected EMG signal;
- predicted with the NMS model versus inverse dynamics joint moments about HipFE, KneeFE and AnkleFE;
- calibrated muscle-tendon parameters;
- mean muscle forces from the considered MTUs;

- single muscle contribution to the three FE joint moments;
- flexors and extensors contributions to the three FE joint moments.

Similarity between joint moments predicted with the NMS model and obtained from inverse dynamics was evaluated for both model executions computing the squared Pearson product moment correlation R^2 and the percentage mean absolute error (%MAE). The MAE was first obtained as follows:

$$MAE = \frac{1}{N} \sum_{i=1}^N |\hat{M}_{X,i} - M_{X,i}| \quad (13)$$

where X is the DOF of interest, \hat{M}_X the corresponding external joint moment from inverse dynamics and N refers to the number of point in the curves. Then, the percentage MAE was calculated by dividing Eq. 13 with respect to the range of variation spanned by the external joint moments \hat{M} , (i.e. $\max(\hat{M}_X) - \min(\hat{M}_X)$).

Muscle contribution to a joint moment was computed as the product of the force generated by that muscle and the corresponding moment arm (Eq. 14). The distribution of flexors and extensors muscle forces to produce each net FE moment was calculated firstly, dividing muscles in the two groups of flexors and extensors for that joint (Table 8), and then summing the corresponding muscle forces (Eq. 15, 16).

Joint	Flexors Muscles	Extensors Muscles
Hip	addlong addbrev gmed1 gmin1 gra recfem tfl illiacus psoas sar	addmag1 addmag2 ad- dmag3 bicfemlh gmax1 gmax2 gmax3 gmed3 gmin3 semimem semiten
Knee	bicfemsh bicfemlh gra gaslat gasmed sar semimem semiten	recfem vasint vaslat vasmed
Ankle	perter tibant	gaslat gasmed perbrev per- long sol

Table 8: Flexors and Extensors muscles for the hip, knee and ankle joint accounted in the multi-DOF EMG-driven NMS model, based on OpenSim Gait2392 musculoskeletal model (OpenSim, 2013).

$$M_{\text{muscle}} = F_{\text{muscle}} \times \text{ma}_{\text{muscle}} \quad (14)$$

Consequently, for the flexors muscles:

$$M_{flex} = \sum_{f=1}^{n_{flex}} F_f \times ma_f \quad (15)$$

where n_{flex} is the total number of flexors muscles for the considered joint, and f identifies a single flexor muscle. Similarly, for the extensors muscles:

$$M_{ext} = \sum_{e=1}^{n_{ext}} F_e \times ma_e \quad (16)$$

where n_{ext} is the total number of extensors muscles for the considered joint, and e identifies a single extensor muscle.

4.3.4 Results

4.3.4.1 EMG Analysis

Muscle	Peak EMG	
	MVCTN[V]	WTN[V](% MVC)
ADDLONG	0.1088	0.0591 (54%)
BICFEMLH	0.2459	0.0783(32%)
GASLAT	0.0993	0.0652 (66%)
GASMED	0.1510	0.1223 (81%)
GLUTMAX	0.0569	0.0232 (41%)
GLUTMED	0.0908	0.0638 (70%)
PERLONG	0.2869	0.2869 (100%)
RECFEM	0.1558	0.0245 (16%)
SAR	0.1242	0.0101 (8%)
SEMITEN	0.2008	0.0418 (21%)
SOL	0.0849	0.0615 (72%)
TFL	0.1142	0.0459 (40%)
TIBANT	0.2292	0.2138 (93%)
VASMED	0.3530	0.0994 (28%)
VASLAT	0.1419	0.0418 (30%)

Table 9: Maximum EMG activation levels obtained from MVC (MVCTN) and Walking (WTN) trials.

Table 9 shows maximum EMG amplitudes obtained considering in one case the MVC tests (MVCTN), and secondly the gait trials (WTN). Seven out of 15 muscles went above the 50% of the MVC during the

walking tasks. These were: ADDLONG, GASLAT, GASMED, GLUTMED, PERLONG, SOL,TIBANT. The same peak EMG was reached by the PERLONG, while a very similar value was obtained for the TIBANT (93% MVC) in the two cases.

These peak EMG resulted in mean normalized envelopes that are partly shown in Fig. 24 - 29. Some examples of muscles with a remarkable difference among the two methods are reported first (Fig. 24 - 27), followed by others with no (Fig. 27a) or less discrepancy (Fig. 27b,29).

An overall view on the effects of the two normalization strategies on the resulting mean muscles activation level is given by Fig. 30. It shows in the same graphs, the mean normalized envelope for all recorded muscles during stance, obtained with the MVCTN (Fig. 29a) and the WTN (Fig 29b) method. Depending on the normalization approach, muscles are assumed to reach significantly different activation levels during the same task (i. e., gait). We hypothesized this has the potential to impact the NMS modeling process and outcomes.

4.3.4.2 Predicted Torque

The multi-DOF NMS model predicted hip, knee and ankle FE moments close to those calculated from inverse dynamics in both cases (Fig. 31, 32). The two normalization strategies led to comparable results in terms of R^2 and %MAE in joint moments estimation for the three DOFs (Table 10). A reduction of the standard deviation occurred when using the MVCTN method, especially in the prediction of hip and knee FE moments (Fig. 31, 32). The estimated HipFE joint moment resulted smaller than the associated external moment (from inverse dynamics computations) during the hip-flexing phase of stance (i. e., 70%-100%), in line with results from Sartori et al. (2012a). As argued by the authors, this is due to the absence of EMG data from deeply located muscles, such as the iliacus and psoas. Those are hip-flexors and the EMG-dependent active forces they are able to generate could not be predicted by the model.

In the same stance phase, the predicted KneeFE moment showed a time delay with respect to the corresponding external moment from inverse dynamics, but this occurred similarly in the two cases.

Calibration	Hip FE		Knee FE		Ankle FE	
	R^2	%MAE	R^2	%MAE	R^2	%MAE
WTN	0.825	9.536	0.871	8.177	0.941	6.239
MVCTN	0.839	9.387	0.907	7.807	0.945	6.085

Table 10: Comparison between external and predicted joint moments using two different calibration strategies for 5 walking trials.

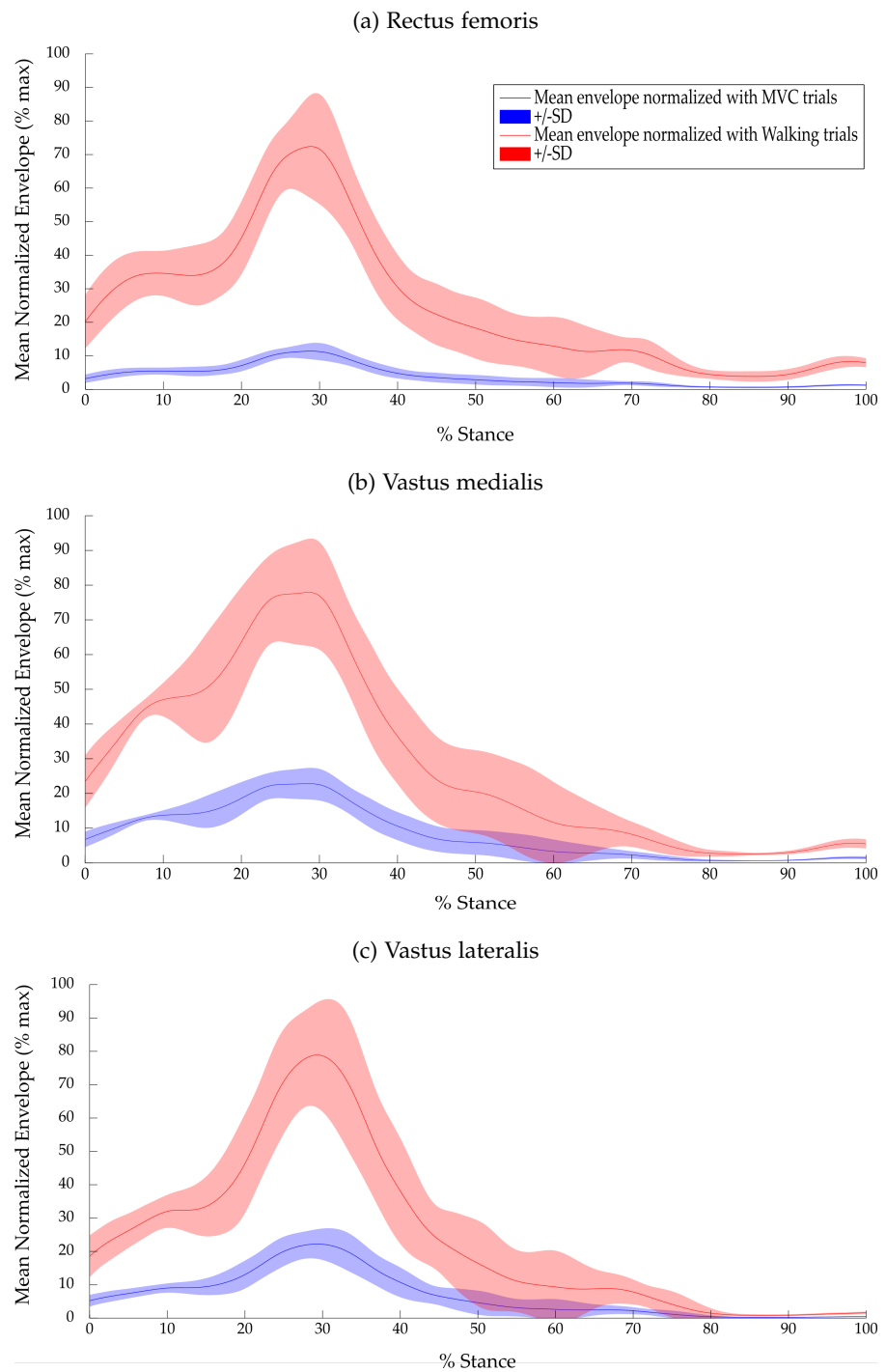


Figure 24: Mean Normalized Envelopes for the quadriceps muscle group.

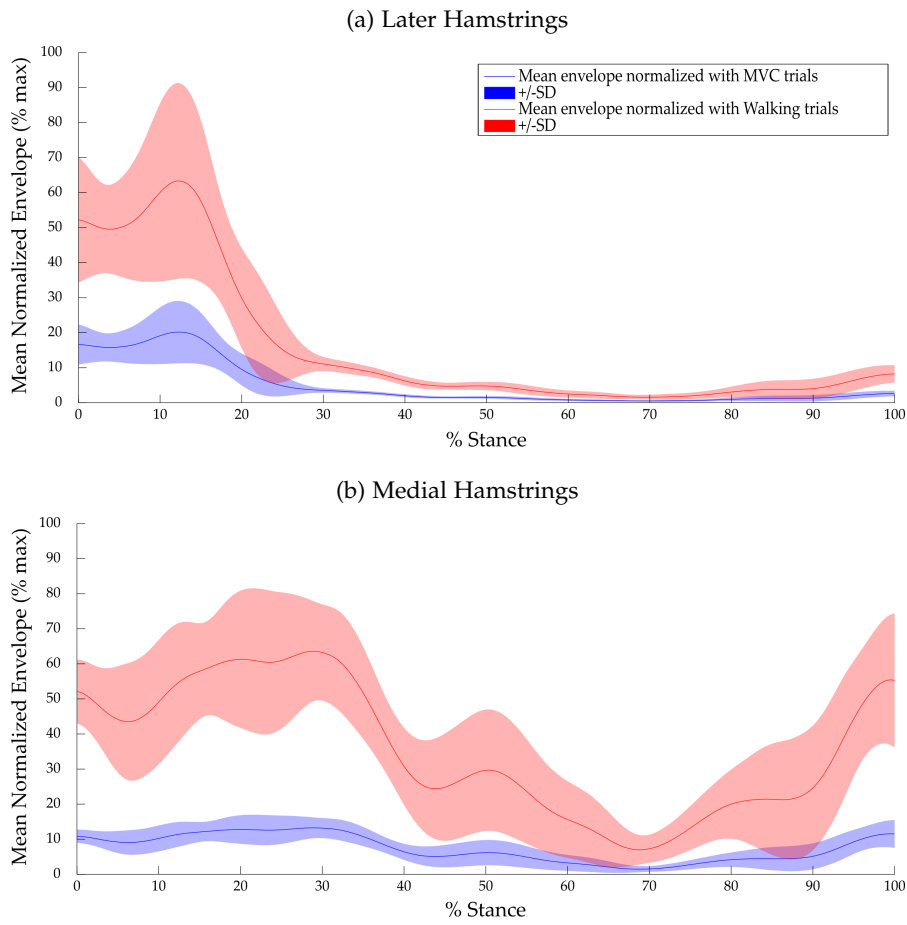


Figure 25: Mean Normalized Envelope for the Hamstrings muscles group.

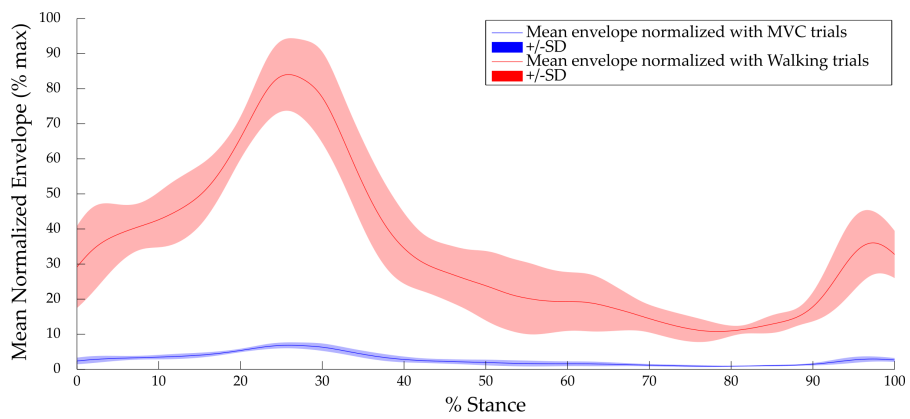


Figure 26: Mean Normalized Envelope for the Sartorius muscle.

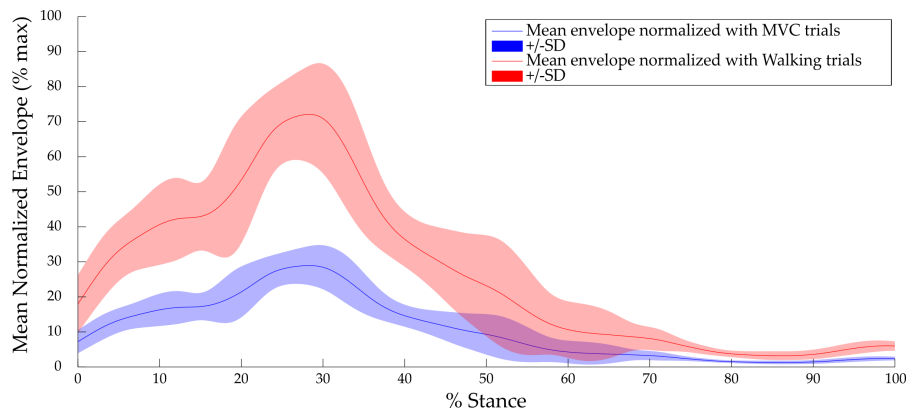
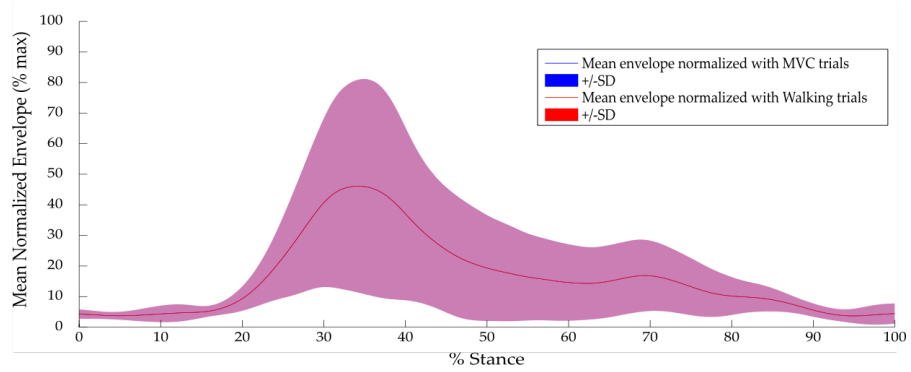


Figure 27: Mean Normalized Envelope for the Tensor Fasciae Latae muscle.

(a) Peroneus Longus



(b) Tibialis Anterior

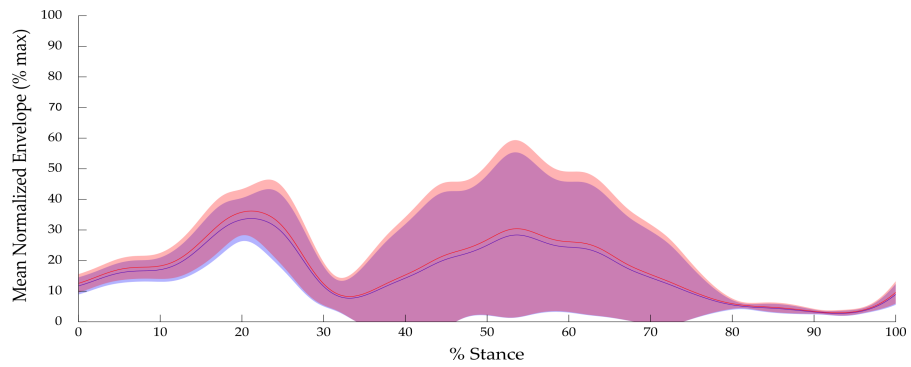


Figure 28: Mean Normalized Envelope for the (a) Peroneus Longus and the (b) Tibialis Anterior muscles.

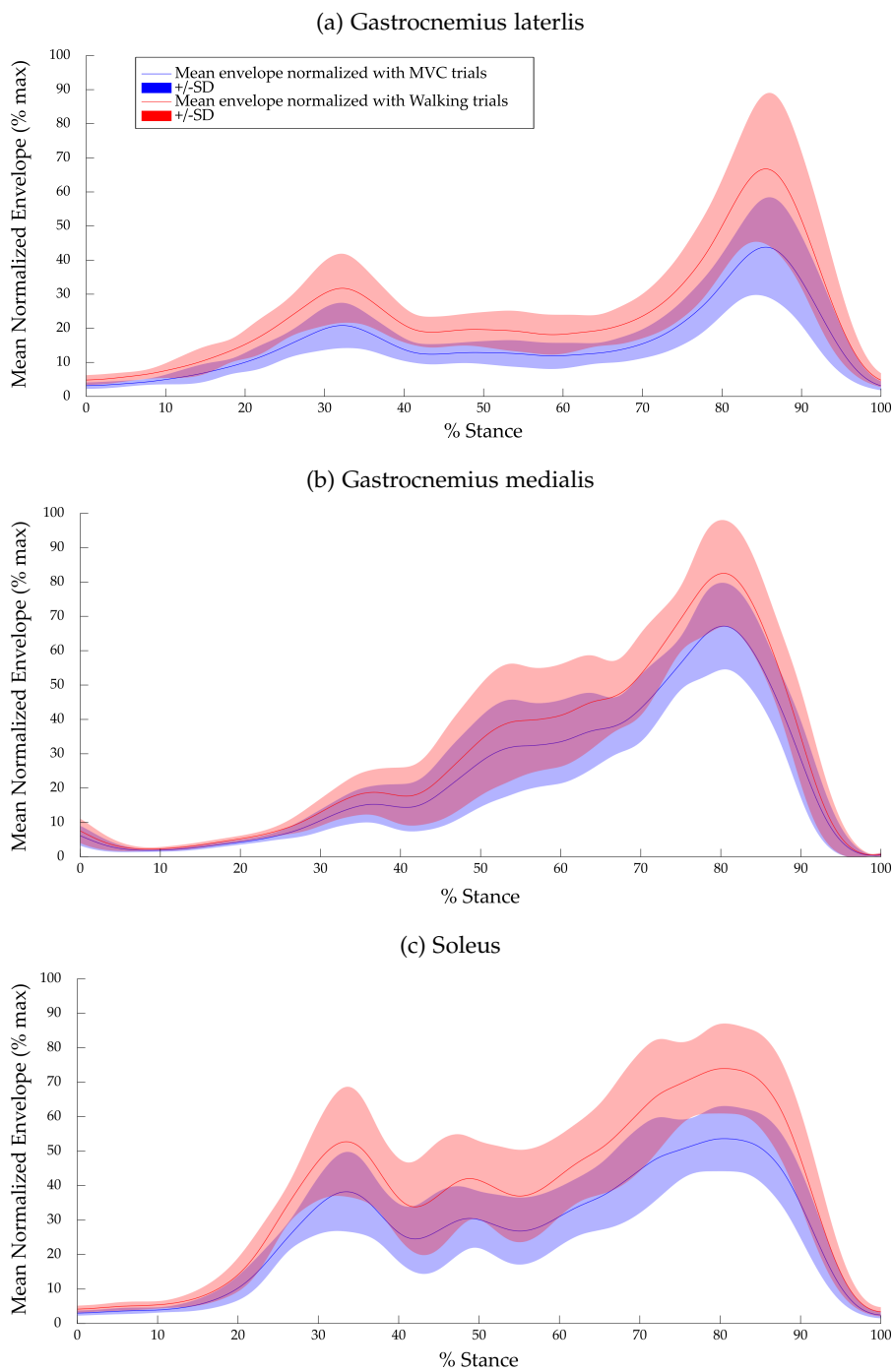


Figure 29: Mean Normalized Envelope for the posterior leg muscles.

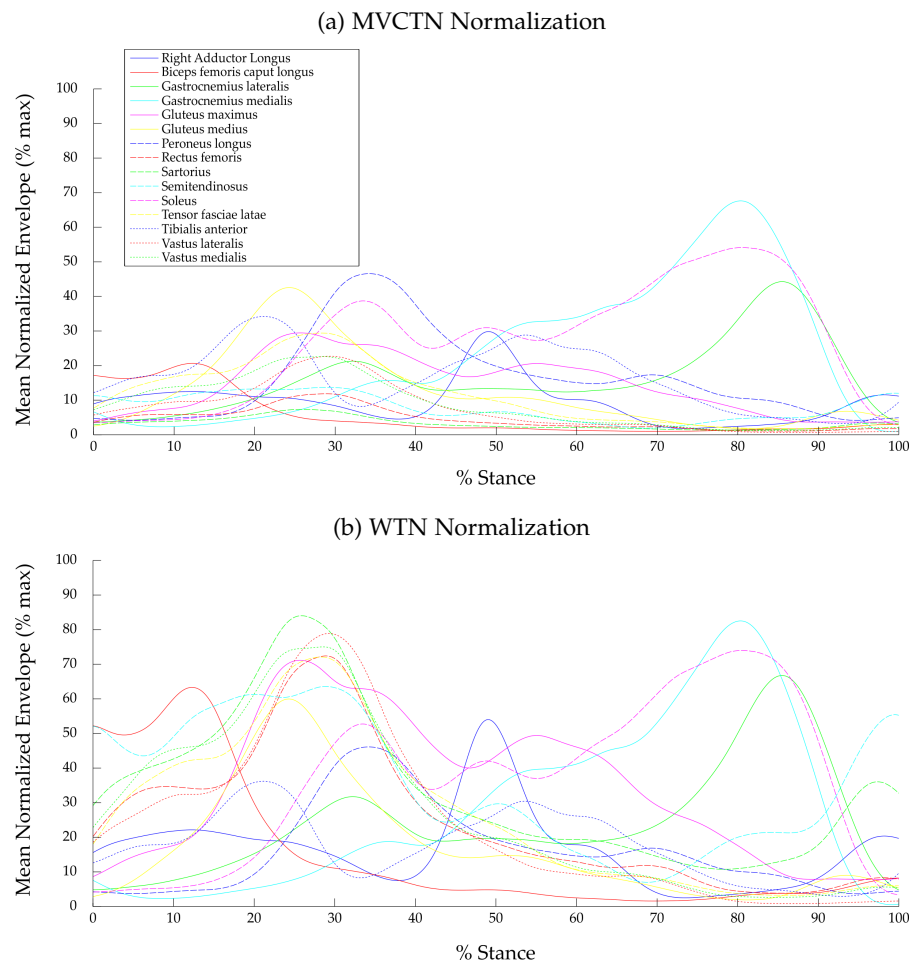


Figure 30: Mean Normalized Envelope from all muscles obtained with (a) MVCTN and (b) WTN normalization of input EMG signals.

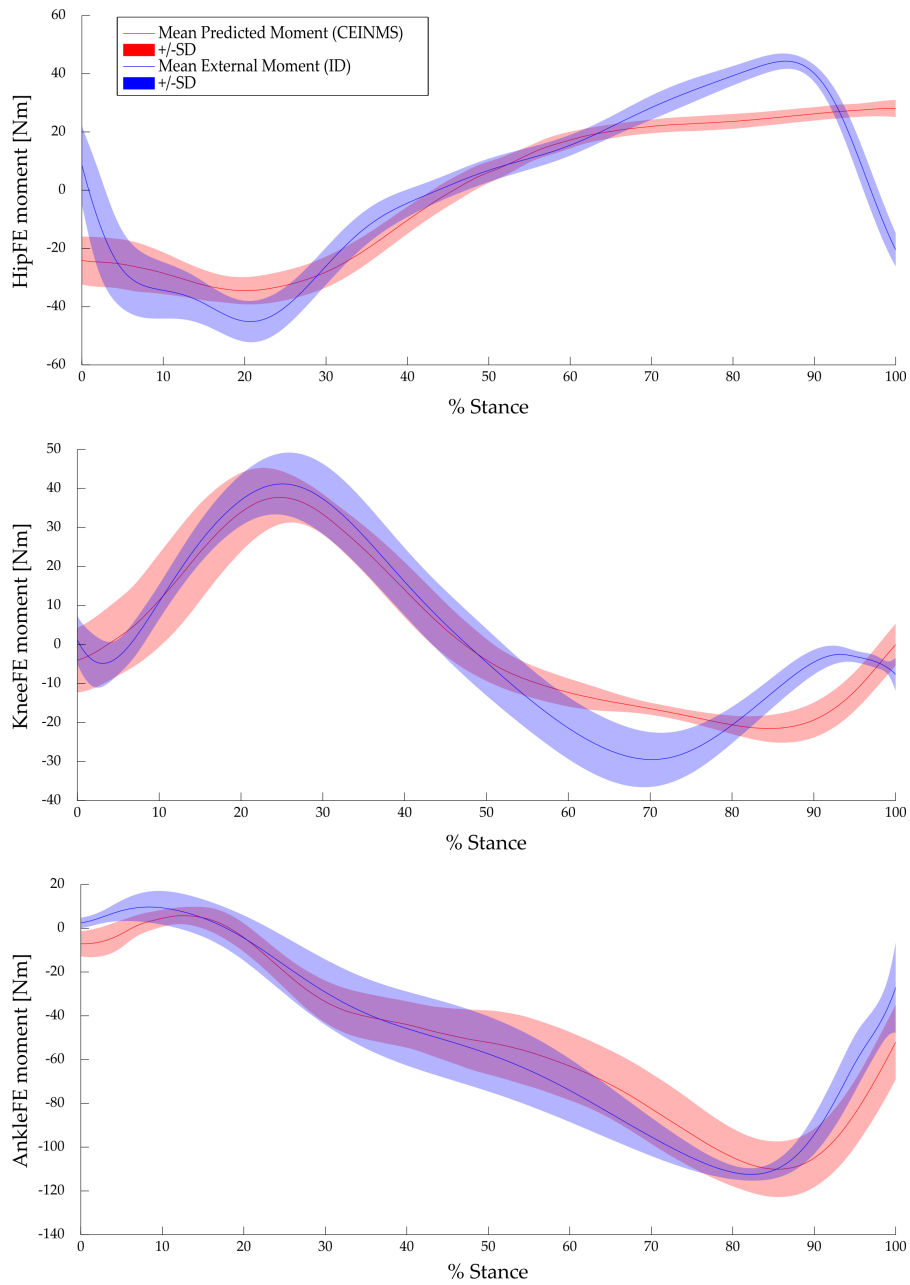


Figure 31: Joint Moments obtained normalizing input EMGs with the MVCTN method.

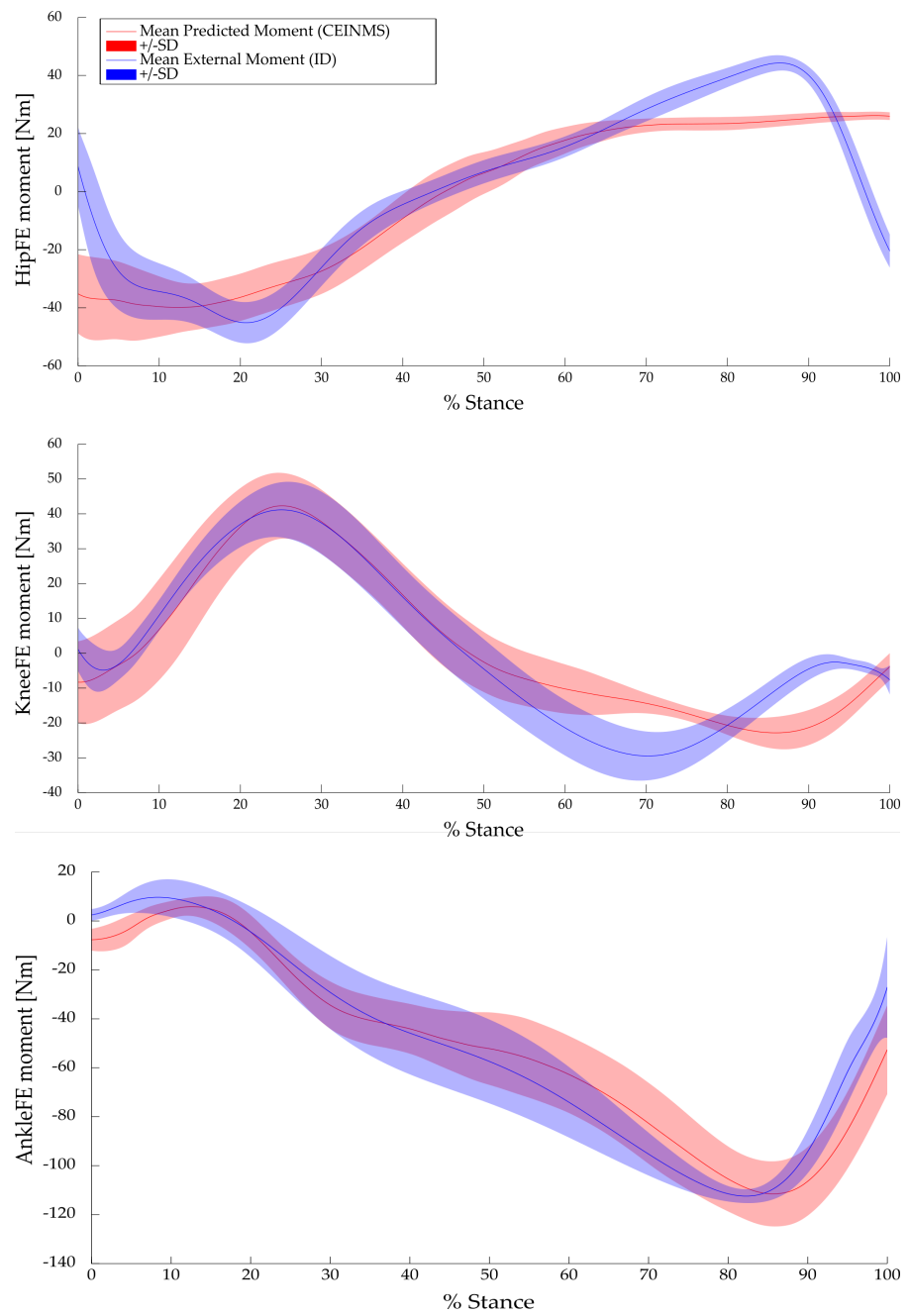


Figure 32: Joint Moments obtained normalizing input EMGs with the WTN method.

4.3.4.3 Calibrated Muscle Parameters

Muscle parameters following the two calibrations (i. e., using as input the EMG normalized with the WTN and MVCTN methods) are summarized in Tables 11 and 12. Parameters are global in that a unique value is assigned to all muscles. These are the recursive filter coefficients and the shape factor (Table 11), associated to the Muscle Activation model (Section 2.2.1). Using the WTN calibration, the shape factor A and C_1 were equal to the upper bound of their range defined on the basis of model's constraints. The MVCTN calibration led to a more physiological value for C_1 , while significant improvements could not be inferred for A , and C_2 assumed similar values in the two cases.

Global Parameters	WTN	MVCTN	Range
C_1	-0.050	-0.343	[-0.950,-0.050]
C_2	-0.872	-0.851	[-0.950,-0.050]
A	-0.001	-0.004	[-2.999,-0.001]

Table 11: Global parameters obtained after model calibration using as input EMG linear envelopes normalized with the peak EMG from walking trials (WTN) and from the MVC tests (MVCTN).

Table 12 shows strength coefficients for the eleven muscle groups defined as in Sartori et al. (2012a) according to their functional action. Using as model input EMG normalized with the WTN method, 8 groups (corresponding to 28 MTUs out of the overall 34 considered) reached the imposed inferior bound as a result of the optimization process. The MVCTN calibration moved the strength coefficients of 4 of these groups (equivalent to 13 MTUs) within the range.

4.3.4.4 Mean Muscles Forces

Muscle forces during stance were computed for the 34 MTUs included in the multi-DOF EMG-driven NMS model (Section 2.2.1). The normalized linear envelopes of the recorded EMG signals are associated to the MTU according to the mapping shown in Fig. 23 and based on Sartori et al. (2012a). For instance, computation of muscle forces for the peroneous group, which includes 3 MTUs (perbrev, perlong and perter) is related to the single normalized linear envelope derived from the experimental EMG signal of the PERLONG muscle. Thus, for each experimental EMG signal, the effects of the normalization strategy can be seen in the muscle forces of all the associated MTUs. Examples are muscle forces estimated for perbrev, perlong and perter MTUs, which were very similar comparing results from the two normalization approaches (Fig. 33). This is a consequence of

Muscle Groups	Strenght Coefficient	
	WTN calibration	MVCTN calibration
addlong addbrev ad- dmag1 addmag2 ad- dmag3	0.5	0.5
bicfemlh semimem semiten sar	0.5	0.5
bicfemsh	0.5	2.771
gaslat gasmed	0.774	0.948
gmax1 gmax2 gmax3	0.5	2.183
gmed1 gmed2 gmed3 gmin1 gmin2 gmin3	0.5	2.183
gra recfem tfl	0.726	1.759
illiacus psoas	3.5	3.5
perbrev perlong perter tibant	3.5	3.5
sol	0.908	1.141
vasint vaslat vasmed	0.5	1.4

Table 12: Strenght coefficients following the two calibrations for each defined muscle group (Sartori et al., 2012a). The range of variation was set to [0.5,3.5].

the detected peak EMG, which was the same despite the different method used for its computation (Table 9).

Marked differences in the evaluation of the maximum EMG amplitude value for input signals normalization resulted in substantial differences in muscle forces estimation (Fig 34, 35). The only exception was represented by those muscles with a peak EMG greater than the 60% of the corresponding MVC during the gait trials (Fig. 33, 36).

4.3.4.5 *Muscle Contributions to the Net Joint Moments*

Differences in the distribution of muscle forces imply different contributions from each muscle to the net joint moments. An example from a single trial is shown for the three DOFs in Fig. 37 - 39. Main variations were for the *recfem* and its antagonist, the hamstrings group, including *bicfemlh*, *semiten* and *semimem* MTUs, that affected both the hip and knee joints. Less marked were differences in muscle contributions from ankle dorsi and plantar flexors at the ankle joint (Fig. 39).

4.3.4.6 *Flexors and Extensors Contributions to the Net Joint Moments*

The mean contributions of flexors and extensors muscles to the three net joint moments resulting from a MVCTN and WTN execution of the model were compared (Fig. 40 - 42). Results revealed a substantial difference in the two cases for the hip and knee joints (Fig. 40, 41). On the contrary, muscle contributions to the ankle moment were very similar (Fig. 42).

4.3.5 *Discussion*

The purpose of this study was to evaluate the applicability and reliability of the WTN method as a method for normalizing gait EMGs, and to assess its impact on the NMS model outcomes. We designed a protocol to acquire MVC for a multi-DOF application involving 15 lower limb muscles, based on manual resistance and literature indications. The computation of the peak EMG from the associated MVC was considered the reference method for the EMG normalization (MVCTN method). We hypothesized that the overall higher muscle activation level resulting from the WTN normalization with respect to the MVCTN method, would lead to meaningful differences in muscle forces estimation, despite agreement in the predictions of joint moments.

Our results confirm this hypothesis, suggesting that the WTN method can be unreliable when exploited for the normalization of EMG signals in the application of multi-DOF EMG-driven NMS models. For nine out of the total fifteen muscles (*ADDLONG*, *BICFEMLH*, *GLUTMAX*, *RECFEM*, *SAR*, *SEMITEN*, *TFL*, *VASMED*, *VASLAT*), the maximum ac-

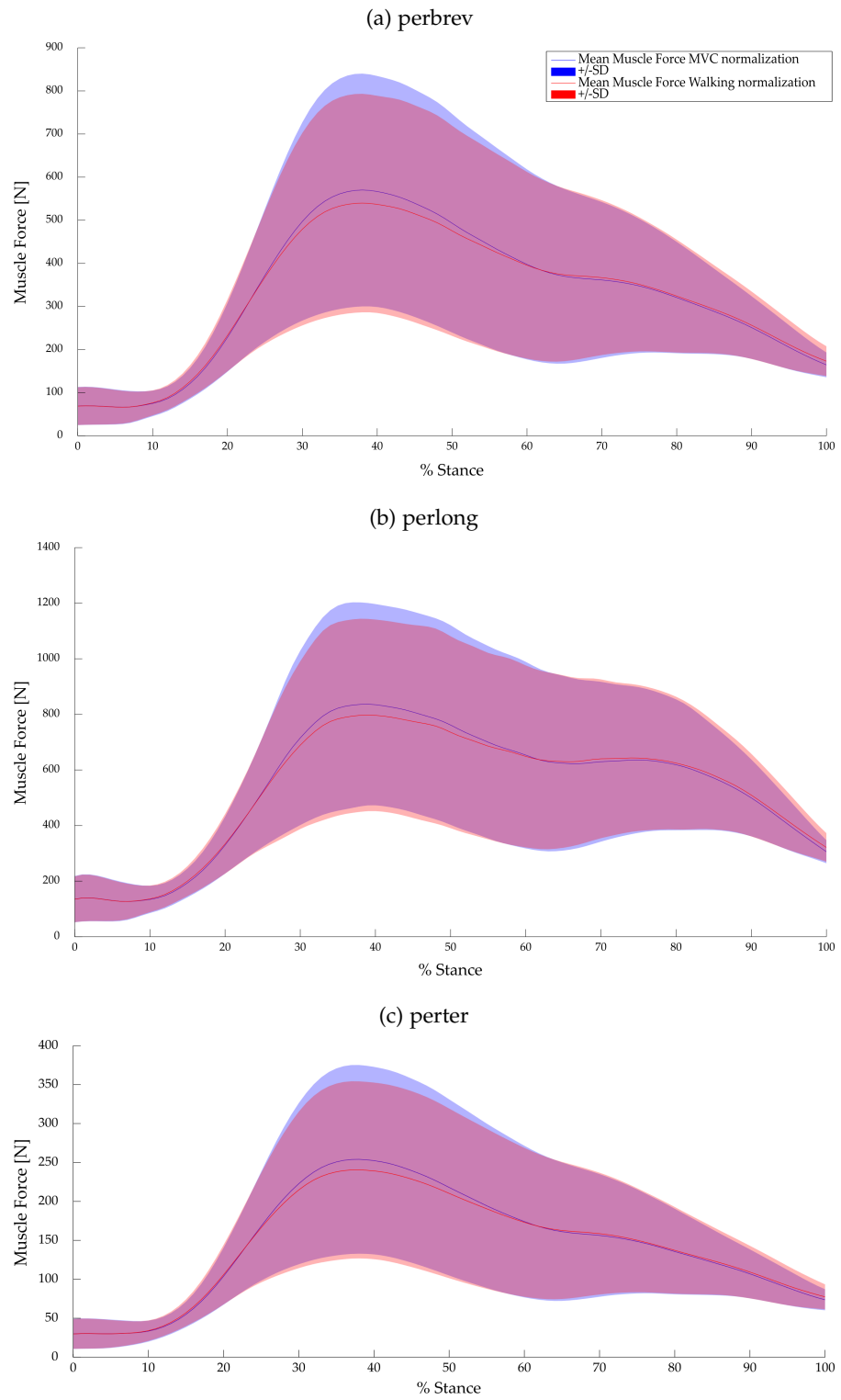


Figure 33: Comparison of Mean Muscle Forces estimated with CEINMS using MVC (blue) and walking (red) trials for normalization of input EMG signals.

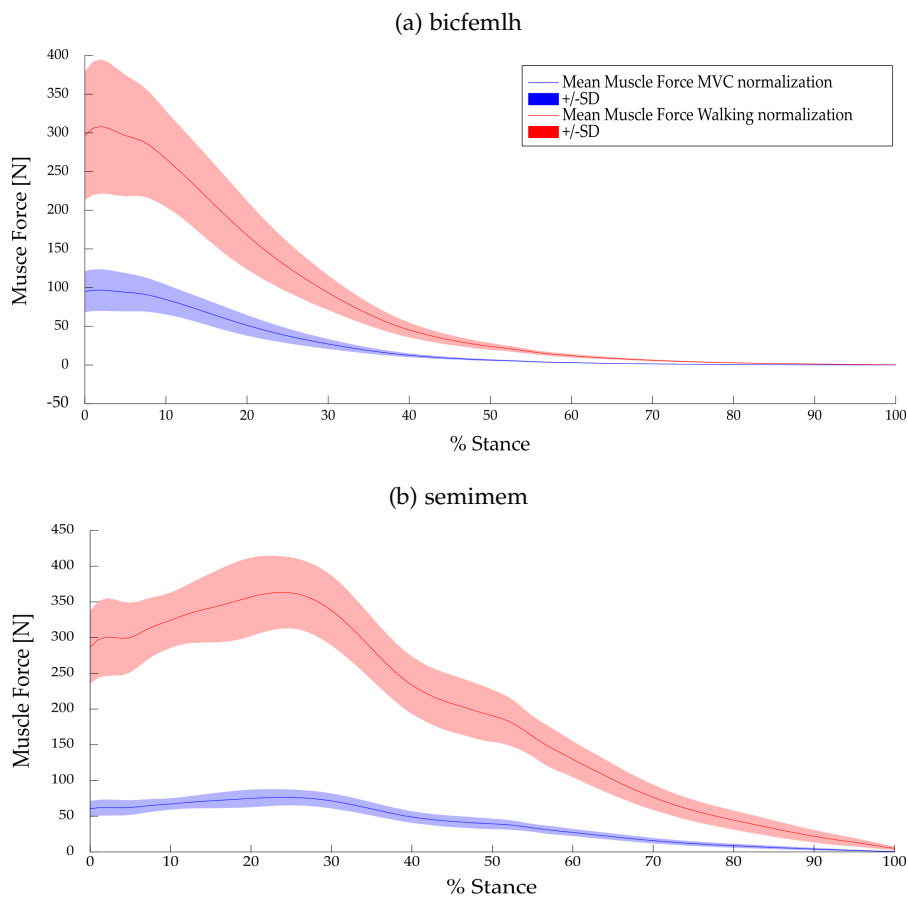


Figure 34: Comparison of Mean Muscle Forces estimated with CEINMS using MVC (blue) and walking (red) trials for normalization of input EMG signals.

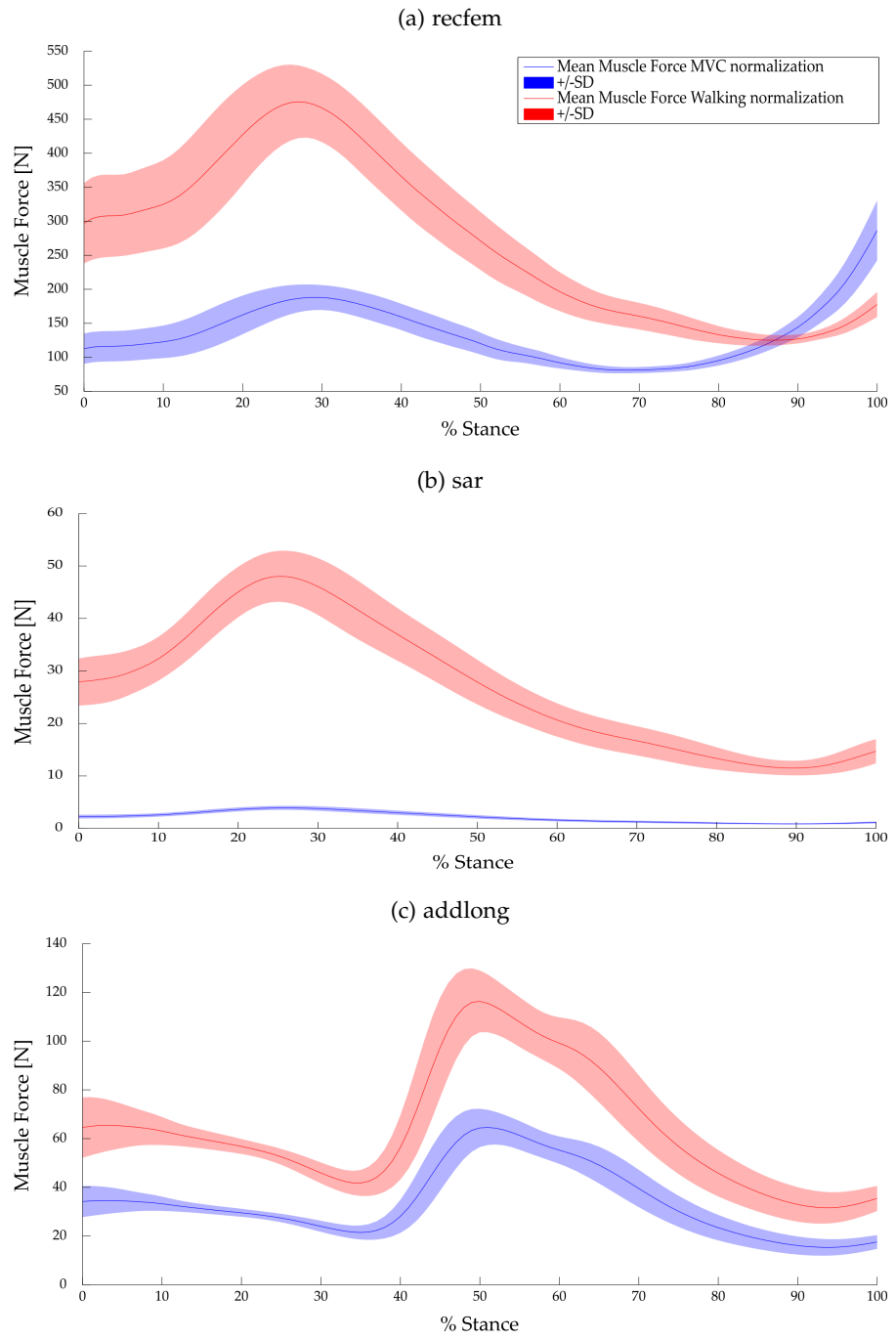


Figure 35: Comparison of Mean Muscle Forces estimated with CEINMS using MVC (blue) and walking (red) trials for normalization of input EMG signals.

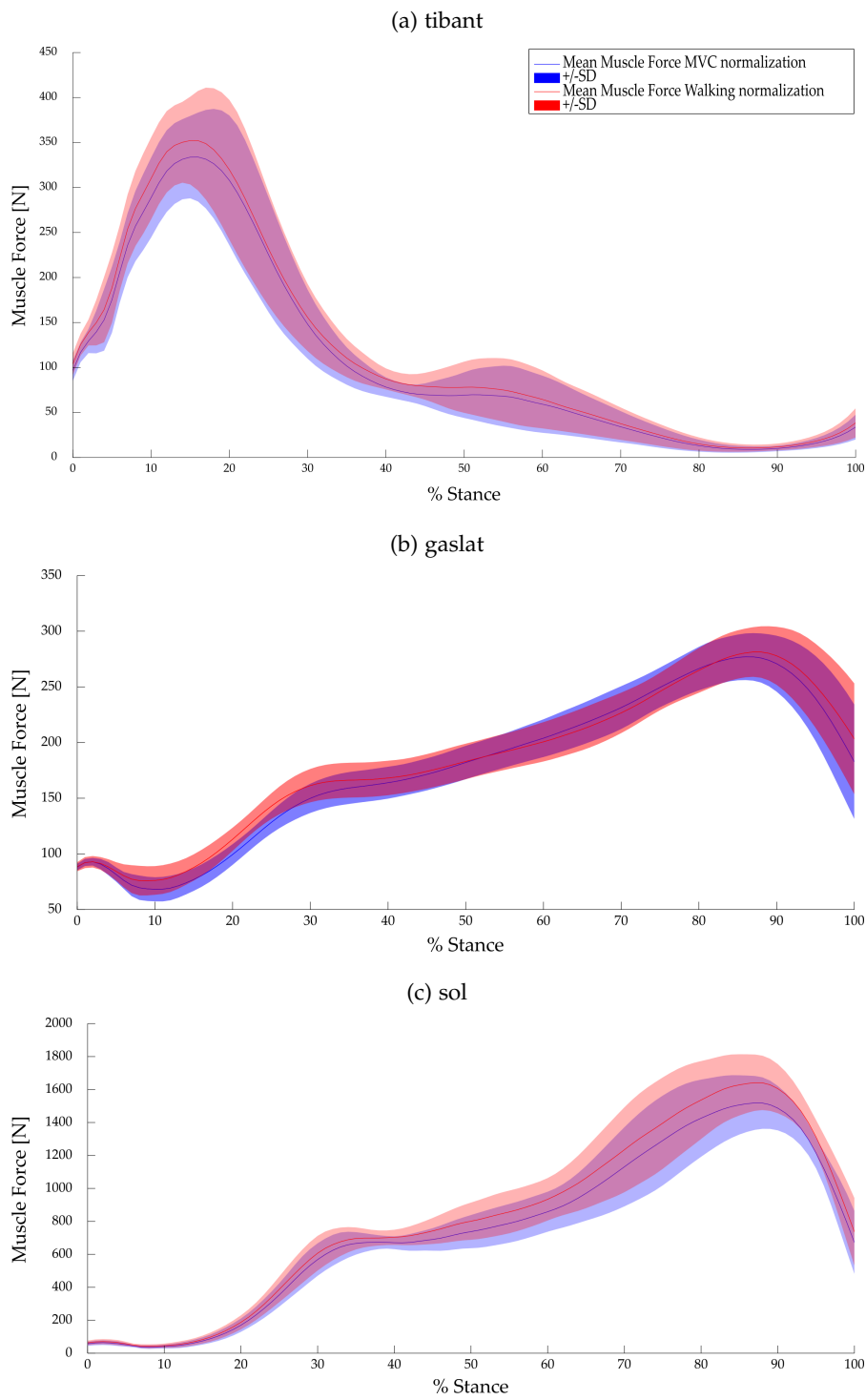


Figure 36: Comparison of Mean Muscle Forces estimated with CEINMS using MVC (blue) and walking (red) trials for normalization of input EMG signals.

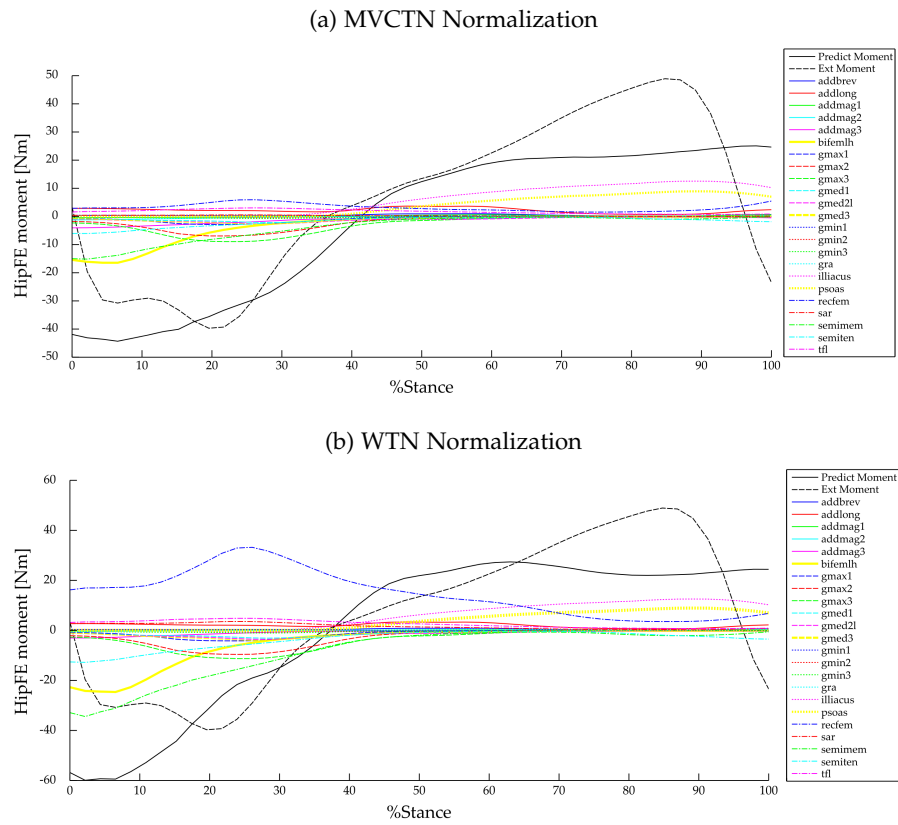


Figure 37: Example of Muscle Contributions to the net HipFE moment during a gait trial obtained with (a) MVCTN and (b) WTN normalization of input EMG signals.

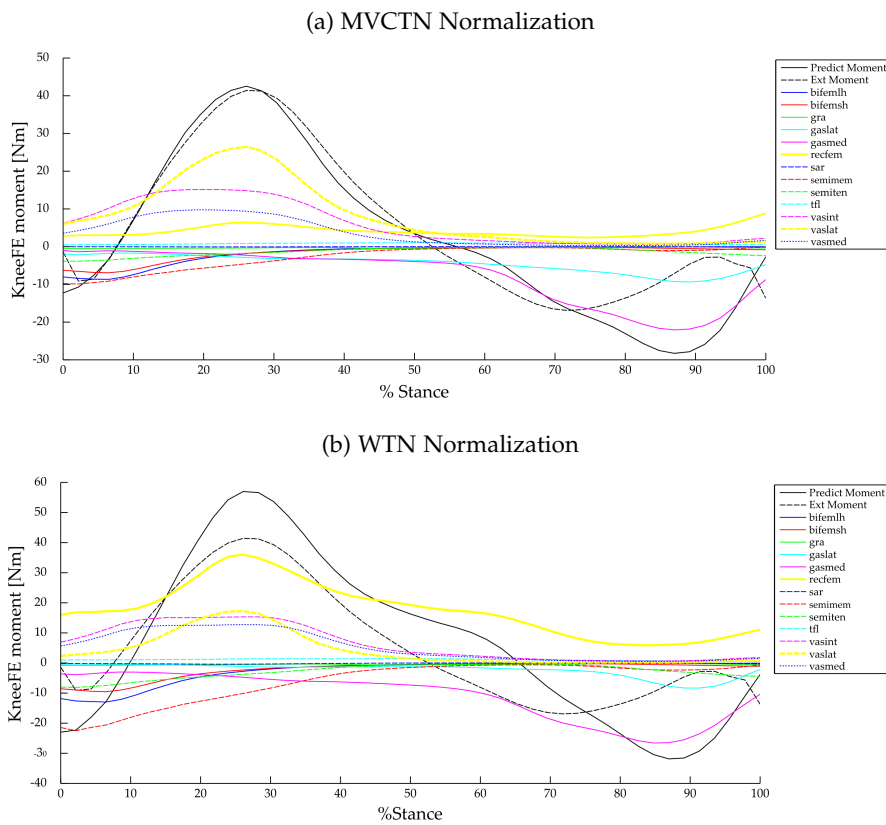


Figure 38: Example of Muscle Contributions to the net KneeFE moment during a gait trial obtained with (a) MVCTN and (b) WTN normalization of input EMG signals.

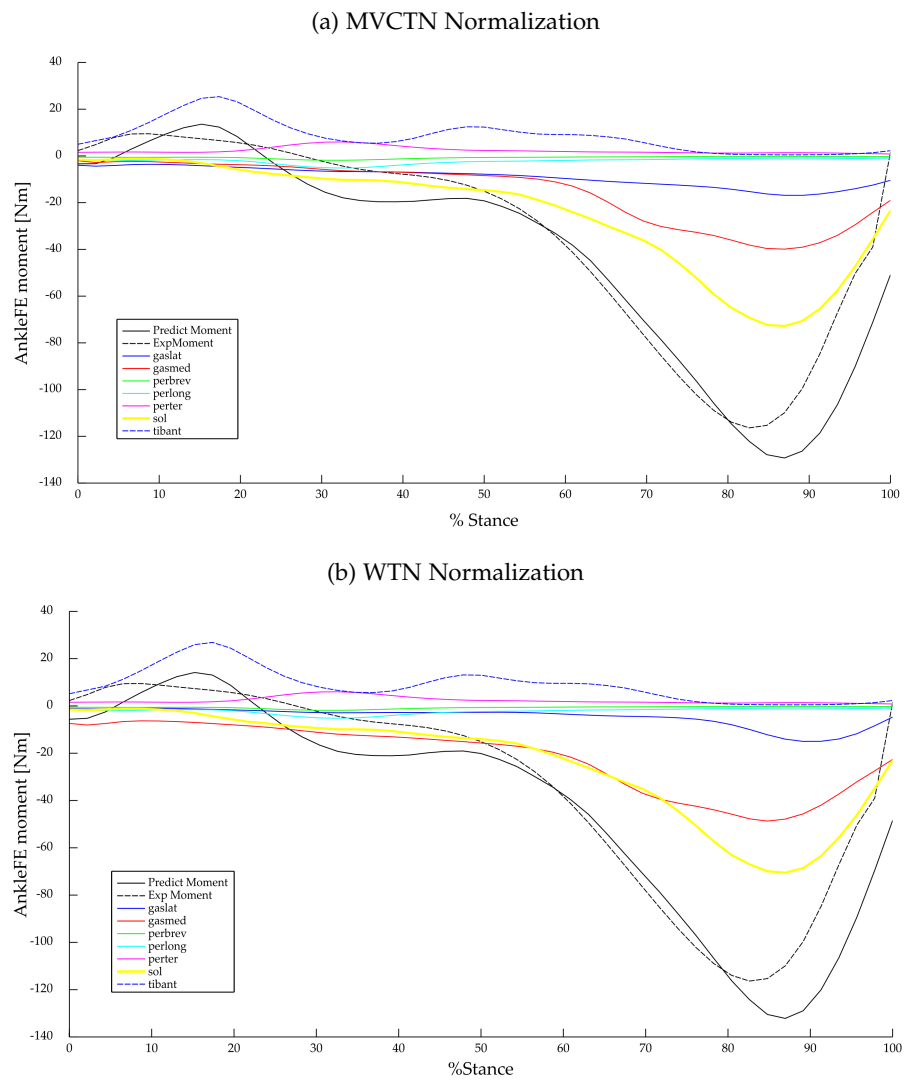


Figure 39: Example of Muscle Contributions to the net AnkleFE moment during a gait trial obtained with (a) MVCTN and (b) WTN normalization of input EMG signals.

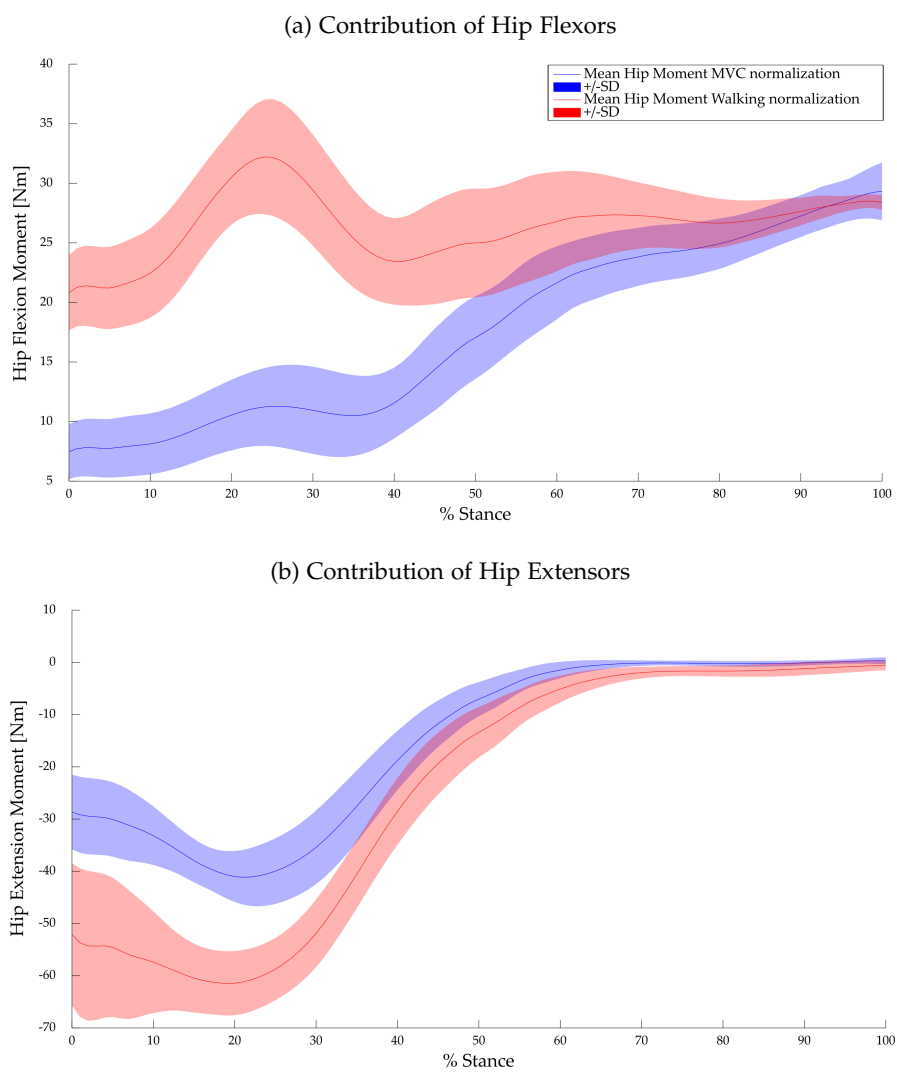


Figure 40: Mean Muscle Contributions of (a) hip flexors and (b) hip extensors to the net HipFE moment.

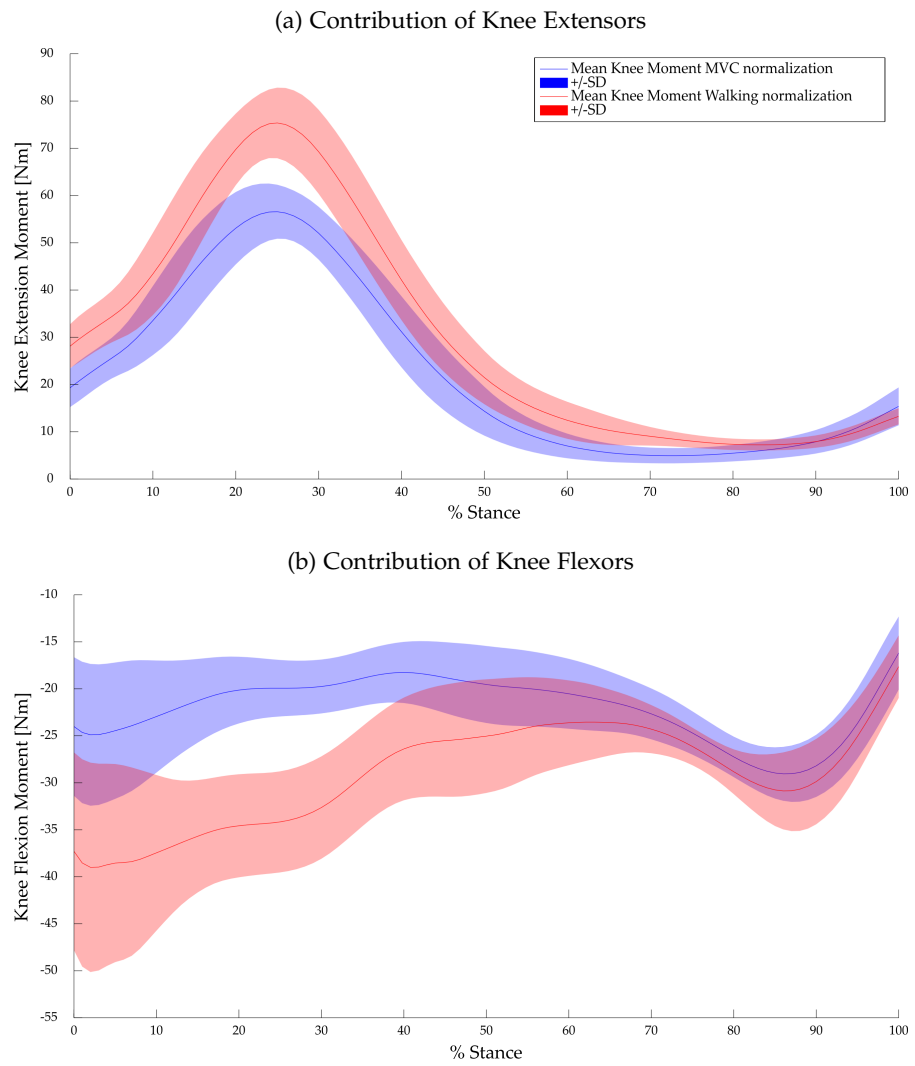


Figure 41: Mean Muscle Contributions of (a) knee extensors and (b) knee flexors to the net KneeFE moment.

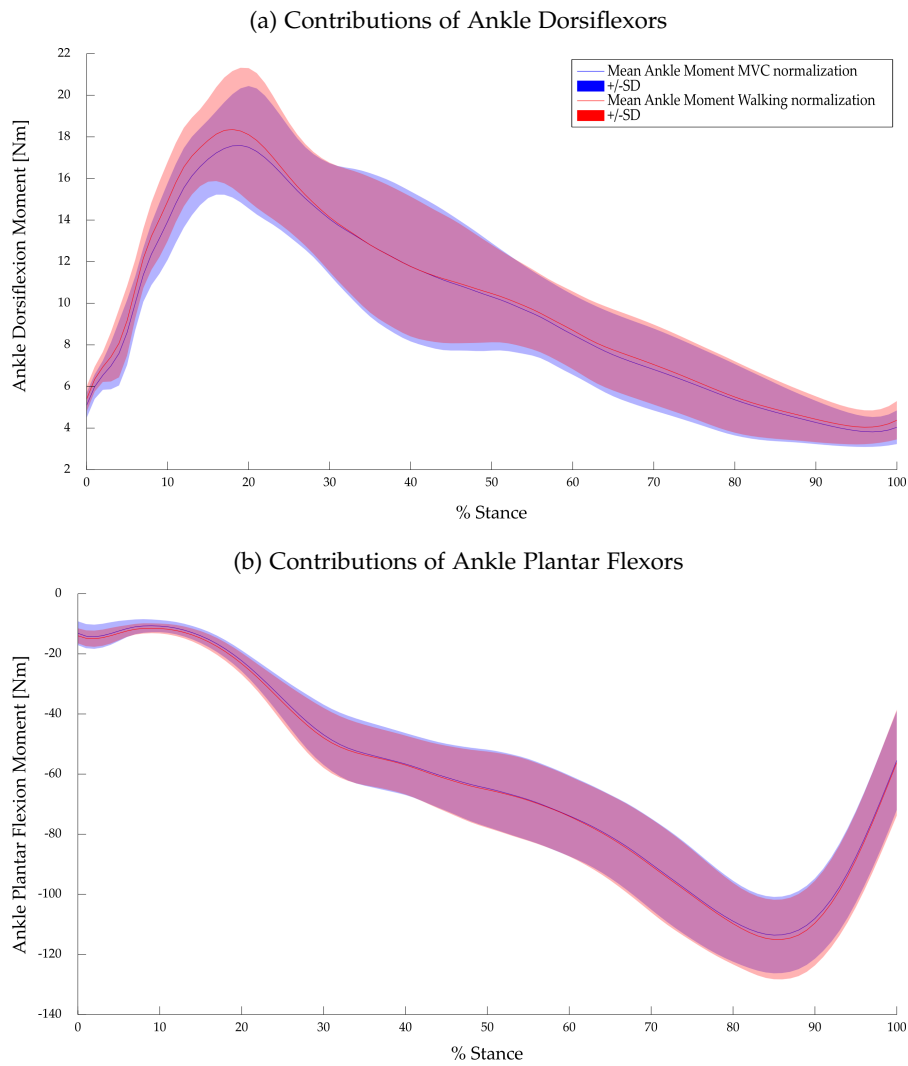


Figure 42: Mean Muscle Contributions of (a) ankle dorsiflexors and (b) ankle plantar flexors to the AnkleFE moment.

tivation level reached during the walking trials was found to be less than the 60% of the corresponding MVC. The major differences in muscle forces and muscle contributions to the net joint moments were obtained for these muscles. It is worth to note that the SAR is the muscle with the greatest gap between the two methods (peak EMG at the 8% MVC during walking trials), despite no MVC test was designated for it. With its small physiological cross-sectional area compared to the quadriceps, hamstrings and gastrocnemius muscles, the SAR does not contribute as much to the KneeFE moment during walking. Moreover, it is involved in several movements, such as hip and knee flexion, and hip external rotation and abduction, thus a plausible maximum value can be found in MVC tests planned for other muscles. However, this occurred for this subject, but it may not be true in general and needs to be further investigated.

The same peak EMG was reached instead with the two methods by the PERLONG, similarly to the TIBANT, that achieved a maximum EMG amplitude equal to the 93% MVC. Muscle forces estimated for these two muscles reflected this result, being very close comparing the two normalization approaches. However, this is clearly a consequence of an ineffective MVC: the PERLONG and TIBANT muscles were indeed the only muscles for which the related MVC was performed without manual resistance. Even the maximum activation level of the GLUTMED and the posterior leg muscle group, comprised between the 65% and 85% of the MVC, is likely related to unreliable MVC tests. The exercise for the MVC of the abductors group was conducted against a resistance, but probably it was not enough or properly distributed to involve the recruitment of the GLUTMED muscle (70% MVC against the 40% of the TFL muscle). The posterior leg muscles group is known to have an important role in human walking (Zajac et al., 2003; Anderson and Pandy, 2003; Arsenault et al., 1986). However, its high activation level may be partly due to an unreliable MVC test. In absence of training machines or weights as usually recommended (Konrad, 2005), performing an effective MVC for GASLAT, GASMED and SOL may be an hard task. We exploited the body weight of the manual tester, but this method can be questionable as it can lead to uncertain results. Therefore, improvements in the definition of a protocol for MVC testing are needed to evaluate the actual impact of the WTN approach on multi-DOF EMG-driven NMS model calculations.

From this investigation, we can nevertheless notice a marked variation in the standard deviation among the two strategies. This may appear obvious when referring to the mean normalized envelopes, as the maximum EMG value detected in the two cases influences the range of variation considered. However, the same result occurred for the hip and knee FE moments, the estimated muscle forces and the subsequent muscle contributions to joint moments.

Moreover, this study revealed two important findings. Firstly, the meaningful discrepancy in the assessment of muscle forces between the two methods exploited for EMG signals normalization occurred despite comparable results were instead obtained in joint moments estimation. The EMG-driven NMS model indeed predicted flexion-extension moments at the hip, knee and ankle joints close to those calculated from inverse dynamics with a similar accuracy in the two cases (MVCTN: hip $R^2=0.839$, knee $R^2=0.907$, ankle $R^2=0.945$; WTN: hip $R^2=0.825$, knee $R^2=0.871$, ankle $R^2=0.941$). The multi-DOF NMS model under investigation was previously validated in comparison with single-DOF models (Sartori et al., 2012a), but sensitivity studies about the influence of input accuracy and calibrated muscle tendon parameters on muscle forces estimation have not been made yet. These results confirmed previous studies saying that errors in input data significantly affect model predictions (Koo and Mak, 2005; Oliveira and Menegaldo, 2012) and demonstrated that validation of EMG-driven NMS models can not be based on joint moments prediction only, when muscle forces are of main interest.

Secondly, variations in the calibration of model parameters were obtained with the two methods. With the WTN calibration, two of the three global parameters, the shape factor A and C_1 , were equal to the upper bound of their range defined according to the model's construction, while the strength coefficients of eight groups among the eleven defined (corresponding to 28 MTUs out of the overall 34 considered) reached the imposed inferior bound as a result of the optimization process. This outcome is in contrast with calibrated parameters reported in previous single-DOF applications of this NMS model (Lloyd and Besier, 2003), while it confirms values obtained by Barrett et al. (2007) using the same normalization approach (Table 7). We think that moving from single-DOF to multi-DOF applications significantly increase the number of parameters within the model, exacerbating the risk of incurring in phenomena of overfitting. In this scenario, parameters reaching the limits of their acceptable range may represent a first indication of a non physiological behavior of the model.

Using as input EMG normalized with the MVCTN method moved C_1 and the strength coefficients of four groups (equivalent to thirteen MTU) within their imposed range, suggesting a more representative behavior.

We can argue that the WTN calibration can lead to unreliable model results, and that it must be used with caution. Physiological correctness of muscle tendon parameters can be considered as an aid in inferring about validity of muscle forces. Nevertheless, this first study involved one subject only and further investigations are needed for a generalization of these findings.

4.4 SECOND STUDY

This second study aims at consolidating results from the previous work, focusing the attention on the limitations arose about the protocol defined for the MVC tests.

As described in 2.4, the workflow included: i) collecting human movement data using motion capture technology, ii) processing and preparing experimental data for their use in musculoskeletal software iii) musculoskeletal modeling and simulation of the recorded human movement, iv) calibrating and executing the EMG-driven NMS model.

4.4.1 Data Collection

Experimental movement data were collected and processed to enable the EMG-driven model calibration and subsequent execution.

4.4.1.1 Subject and Experimental Setup

One healthy female subject (age: 28, height: 169cm, mass: 58Kg) was enrolled for this investigation and gave his informed consent before participating in the experiment.

The same laboratory instrumentation and setups, acquisition procedure and protocols of the previous study were adopted for this data collection (4.3.1.1). The only exception is represented by the protocol to conduct the MVC tests of the selected lower limb muscles, which is described in the next section.

4.4.1.2 Minimal MVC Protocol

Within this study, we attempt at proposing a standard *minimal* protocol for MVC testing of lower limb muscles. *Minimal* protocol means that particular attention has been given to keeping the number of tasks to execute to a minimum, and to only adopt common, inexpensive equipment. A padded ankle strap and a steel cable (or chain) are all that is needed to perform the tasks that will be described in the following sections. A dynamometer (Fig. 43) in series with the steel cable is also useful to verify that the subject is maintaining the maximum contraction. One end of the dynamometer is fixed to the wall or floor, while the other end is connected via the steel cable to the segment located distal to the muscle tested.

The testing positions for each task and muscle groups are described in the following paragraphs. The subject maintained each of them for 10-15 seconds.

ADDUCTORES



Figure 43: The dynamometer and the steel cable used for conducting the MVC tests.

MOTION: hip adduction from standing position.

Starting from standing position, keeping the knee fully extended and the ankle at 90° , move the leg towards the contralateral side. The cord opposes this movement as its fixed attachment point is on the same side as the leg under test (Fig. 44a).

TENSOR FASCIAE LATAE, GLUTEUS MEDIUS

MOTION: hip abduction from standing position.

Tensor Fasciae Latae and Gluteus Medius are two abductors of the hip. A common practice to test hip abduction assumes the subject on a side-lying position (Bolgia and Uhl (2007)). However, often instrumentation does not allow the subject to lie down. Moreover, Konrad (2005) reports that some subjects show higher EMGs performing hip abduction in standing position. The proposed task, therefore, starts from a standing position. Keeping the knee fully extended and the ankle at 90° , move the leg outwards (Fig. 44b). The cord opposes this movement as its fixed attachment point is on the opposite side than the leg under test.

GLUTEUS MAXIMUS

MOTION: hip extension from a standing position.

Keeping the knee fully extended and the ankle at 90° , the leg is moved backwards (Fig. 44c). The hip should be extended at least 20° before reaching and holding the maximum contraction position. The fixed attachment point of the cord that provides resistance is in front of the subject.

SARTORIUS

MOTION: lifting the leg with the knee bent from a sitting position.

The sartorius muscle flexes the hip and knee, rotates the hip externally and abducts the hip. Due to its biarticular nature and its function in different movements, manual testing is usually preferred even when more sophisticated and expensive instruments (e.g., Biodex) are available. Fig. 44d show a proposal for a testing exercise. From a sitting position with the knee and ankle both at 90° , flex and rotate the hip externally while adducting the knee. The cable must be regulated so that the foot doesn't reach the opposite knee during the movement.

BICEPS FEMORIS, SEMITENDINOSUS, SEMIMEMBRANOSUS

MOTION: knee flexion at 90 degrees

The subject is in standing position, leaning on a fixed support to ensure stability. The knee is flexed against the resistance of the cord (Fig. 44e). The length of the cord should be regulated so that the knee angle is kept at about 90° during the maximum contraction. The fixed attachment point of the cord is in front of the subject, at knee height.

RECTUS FEMORIS, VASTUS LATERALIS, VASTUS MEDIALIS

MOTION: knee extension.

The quadriceps femoris muscles are tested together as a functional group. With the subject sitting with the trunk approximately perpendicular to the floor, the knee is extended (Fig. 44g), keeping the ankle at 90° . The length of the cord should be regulated so that the knee angle is kept at about 45° during the maximum contraction. The fixed attachment point of the cord is to the back of the subject.

MEDIAL GASTROCNEMIUS, LATERAL GASTROCNEMIUS, SOLEUS

MOTION: unilateral plantar flexion of the ankle.

From a sitting position, on the ground or on an examination table, perform a plantar flexion of the ankle (Fig. 44h). The ankle strap is placed around the midfoot, and the fixed attachment point of the cord is to the back of the subject. The length of the cord should be regulated so that the maximum plantar flexion angle of the ankle is not reached.

PERONEUS LONGUS

MOTION: eversion of the foot.

The subject is in standing position, leaning on a fixed support to ensure stability. The foot under test is slightly lifted and everted, so that the sole of the foot faces laterally (Fig. 44f). The ankle strap is placed around the midfoot, and the fixed attachment point of the cord is on the ipsilateral side, close to the ground.

TIBIALIS ANTERIOR

MOTION: unilateral dorsiflexion of the ankle.

From a sitting position, on the ground or on an examination table, perform a dorsiflexion of the ankle (Fig. 44i). The ankle strap is placed around the midfoot, and the fixed attachment point of the cord is in front of the subject. The length of the cord should be regulated so that the maximum dorsiflexion angle of the ankle is not reached.

4.4.2 *Processing Workflow*

Data acquired for this second study were processed likewise the whole procedure presented in Section 4.3.2.

4.4.3 *Data Analysis Procedure*

The NMS EMG-driven model output obtained in this second case were analyzed and compared according to the approach described in Section 4.3.3.

4.4.4 *Results*

4.4.4.1 *EMG Analysis*

Table 13 shows maximum EMG amplitudes obtained considering in one case the MVC tests (MVCTN), and secondly the gait trials (WTN). With respect to the previous study, a significant reduction in the activation level of the PERLONG and the TIBANT muscles was achieved during the walking trials, respectively from the 100% to 12%MVC and from the 93% to 19%MVC. Conversely, the MVC task designed for the posterior leg muscles did not bring to a decrease in the maximum EMG amplitude: it was indeed uniformly distributed among the 78% (SOL) and the 82% MVC (GASLAT). None of other muscles reached a peak EMG above the 60%MVC during the gait trials, while only the SEMITEN muscle went above the 50%MVC.

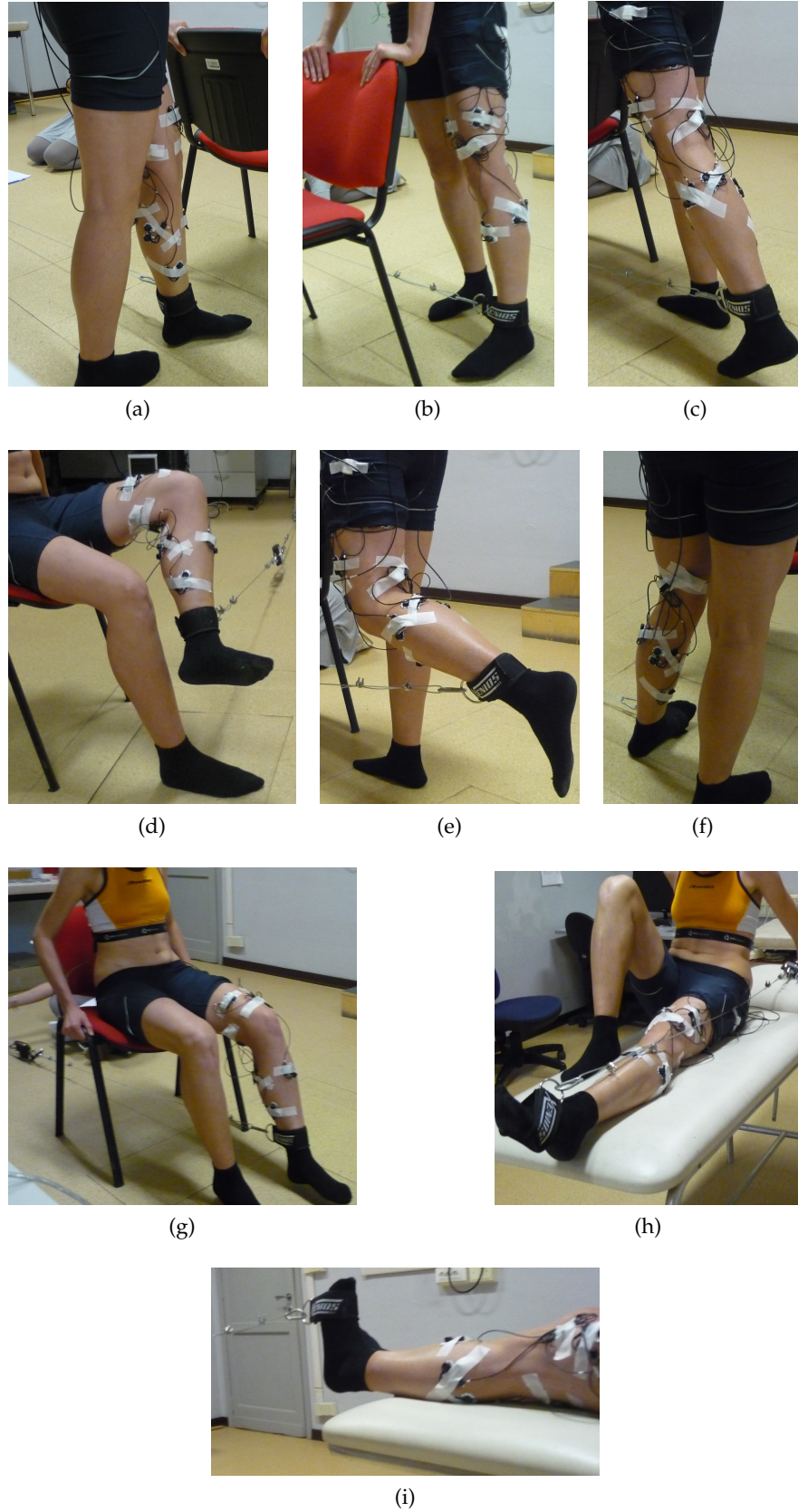


Figure 44: *Minimal MVC Protocol*: proposal of MVC test exercises for the (a) adductores muscles, (b) abductors muscle group, (c) gluteus maximus, (d) sartorius, (e) hamstrings, (f) peroneus longus, (g) quadriceps muscle group, (h) posterior leg muscles, and the (i) tibialis anterior muscle.

Muscle	Peak EMG	
	MVCTN[V]	WTN[V](% MVC)
ADDLONG	0.2898	0.0322 (11%)
BIFEMLH	0.3665	0.1209 (33%)
GASLAT	0.1478	0.1215 (82%)
GASMED	0.1491	0.1193 (80%)
GLUTMAX	0.0729	0.0303 (42%)
GLUTMED	0.3931	0.0770 (20%)
PERLONG	0.3574	0.0430 (12%)
RECFEM	0.2114	0.0231 (11%)
SAR	0.1806	0.0081 (5%)
SEMITEN	0.1369	0.0776 (57%)
SOL	0.1646	0.1277 (78%)
TFL	0.1621	0.0230 (14%)
TIBANT	0.3640	0.0700 (19%)
VASMED	0.1824	0.0423 (24%)
VASLAT	0.2239	0.0164 (7%)

Table 13: Maximum EMG activation levels obtained from MVC (MVCTN) and Walking (WTN) trials.

Calibration	Hip FE		Knee FE		Ankle FE	
	R ²	%MAE	R ²	%MAE	R ²	%MAE
WTN	0.792	17.403	0.848	19.218	0.962	8.271
MVCTN	0.813	12.617	0.866	10.443	0.940	9.329

Table 14

These peak EMG values resulted in mean normalized envelopes that are partly shown in Fig. 45 - 50.

An overall view on the effects of the two normalization strategies on the resulting mean muscles activation level is given by Fig. 51. It shows in the same graphs, the mean normalized envelope for all recorded muscles during stance, obtained with the MVCTN (Fig. 50a) and the WTN (Fig. 50b) method. Again, depending on the normalization approach, muscles showed significantly different activation levels during the same task (i. e., gait). The discrepancies are more marked during the initial and the final phase of stance. Starting from these evidences, we investigated how these results impact the NMS modeling process and outcomes.

4.4.4.2 Predicted Torque

The predicted hip, knee and ankle FE moments resembled those calculated from inverse dynamics in both cases (Fig. 52, 53). Using the WTN normalization, the estimated knee extension moment is slightly smaller than the corresponding resulting from a MVCTN normalization of input EMG signals. However, and importantly, the two normalization strategies led to comparable results in terms of R² and %MAE in joint moments estimation for the three DOFs (Table 14). Additional considerations regarding the accuracy of model predictions for the HipFE and KneeFE joint moments in the single case agreed with those observed in the first study and are reported in Section 4.3.4.2.

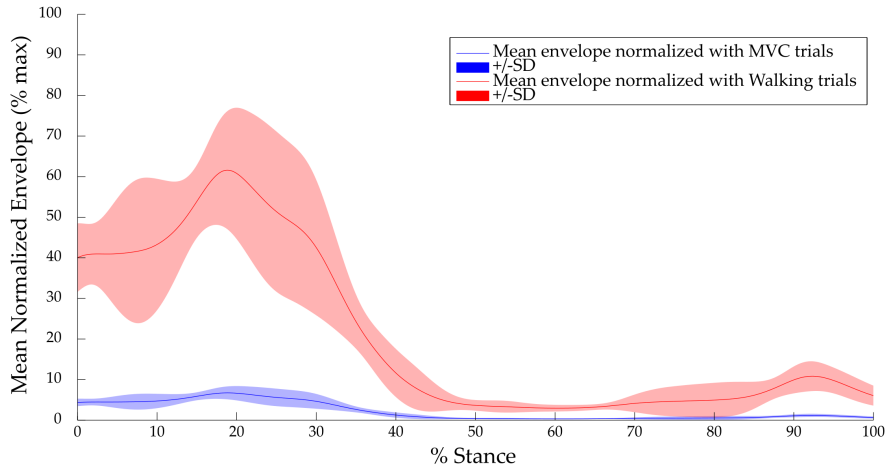
4.4.4.3 Calibrated Muscle Parameters

Global parameters, (i. e., the recursive filter coefficients, C₁ and C₂, and the shape factor A), that assume the same value for all the MTUs, are shown in Table 15. The shape factor A and C₂ were found to be equal or very close to the imposed limits of their ranges when using the WTN calibration. Differently, with the MVCTN approach, their values moved inside the associated range with an relevant margin.

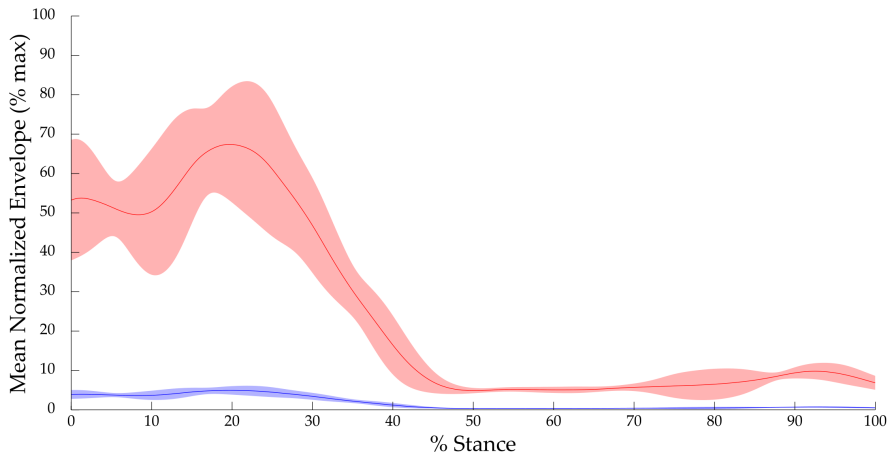
4.4.4.4 Mean Muscles Forces

Results confirmed those obtained from the previous investigation. Marked differences in the evaluation of the maximum EMG ampli-

(a) Rectus femoris



(b) Vastus medialis



(c) Vastus lateralis

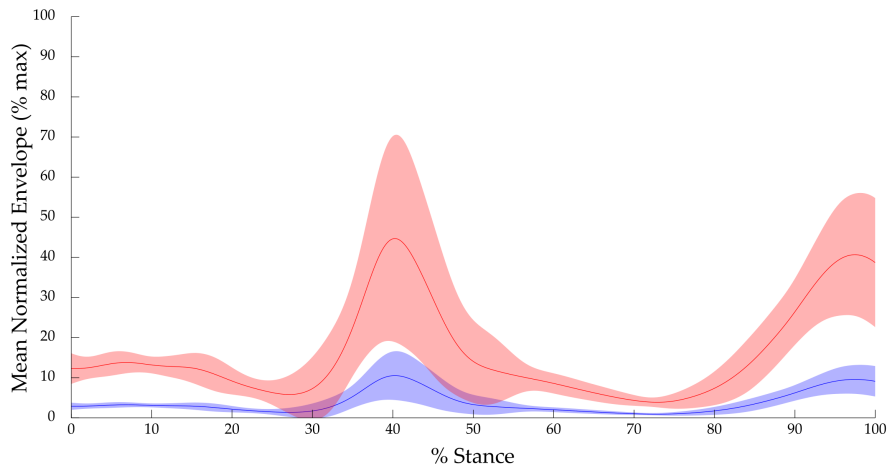
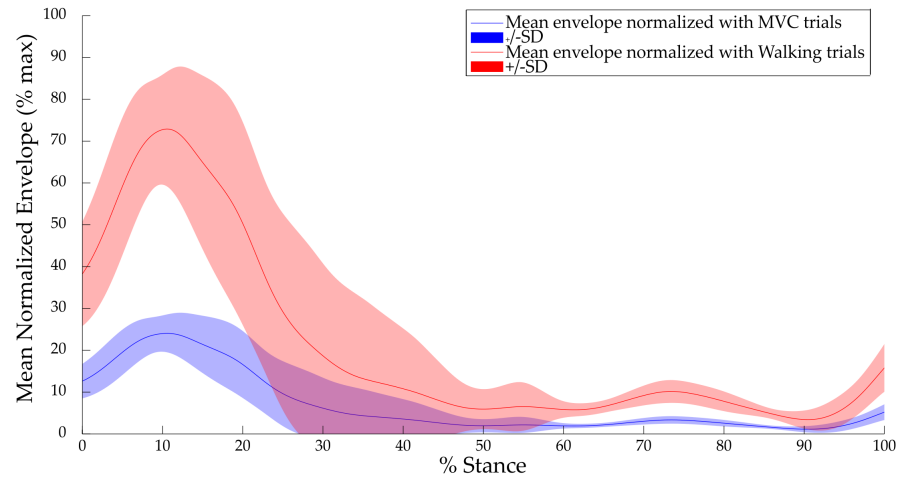


Figure 45: Mean Normalized Envelopes for the quadriceps muscle group.

(a) Later Hamstrings



(b) Medial Hamstrings

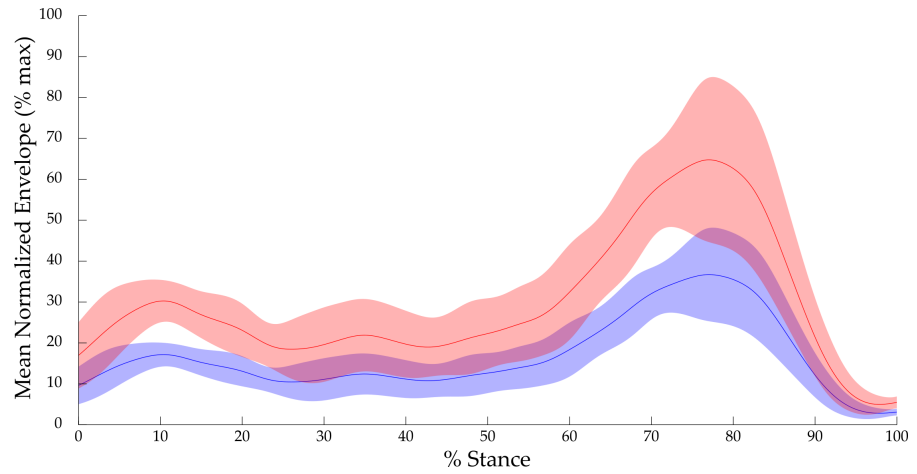


Figure 46: Mean Normalized Envelope for the Hamstrings muscle group.

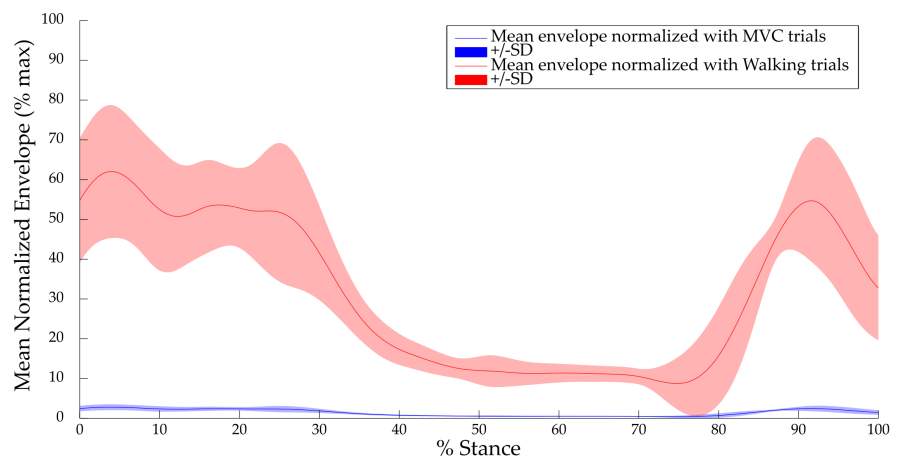


Figure 47: Mean Normalized Envelope for the Sartorius muscle.

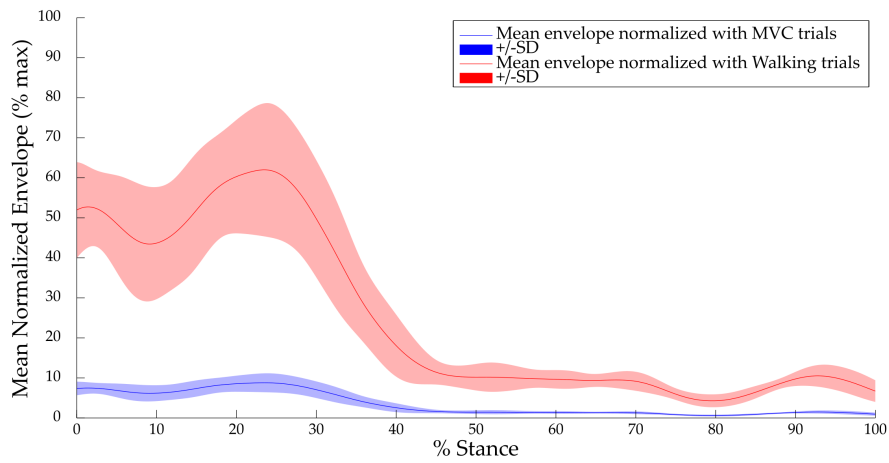
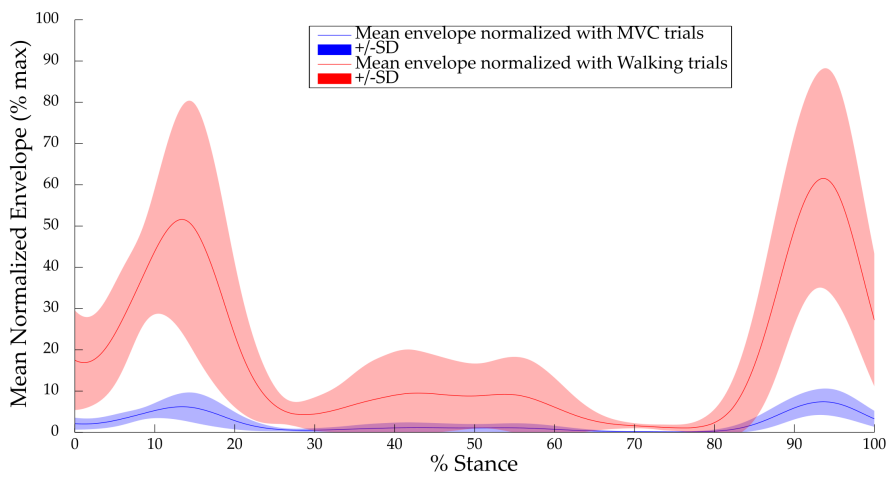


Figure 48: Mean Normalized Envelope for the Tensor Fasciae Latae muscle,

(a) Peroneus Longus



(b) Tibialis Anterior

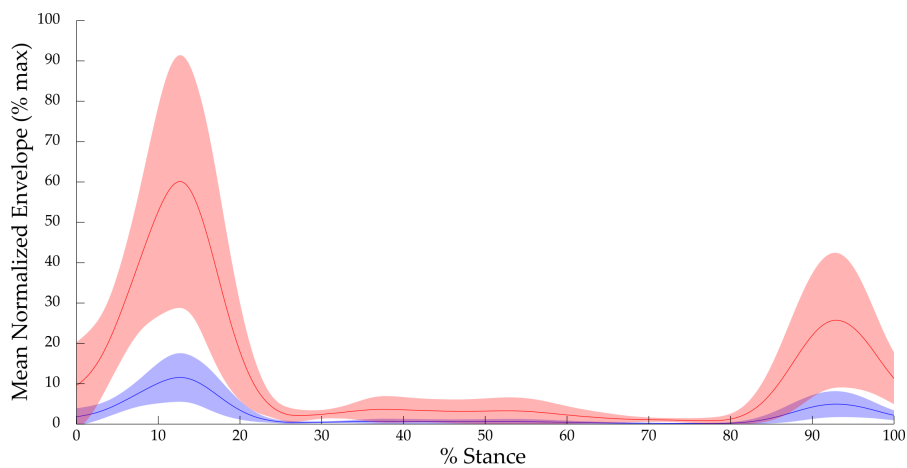
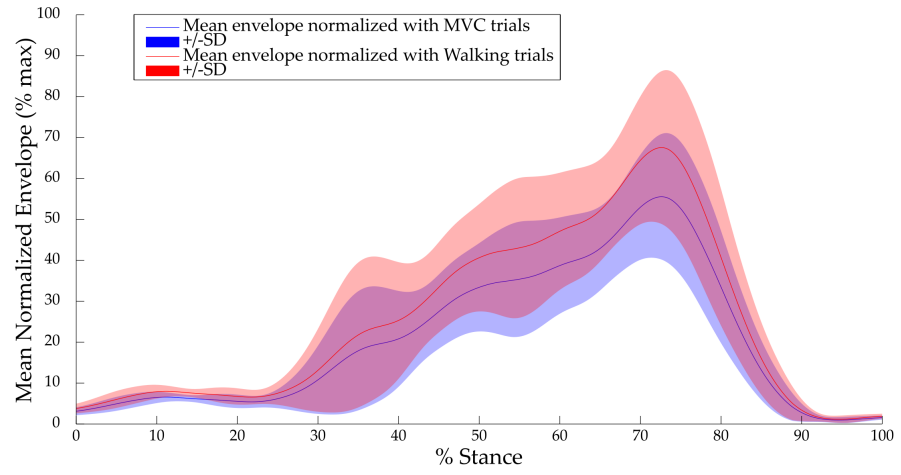
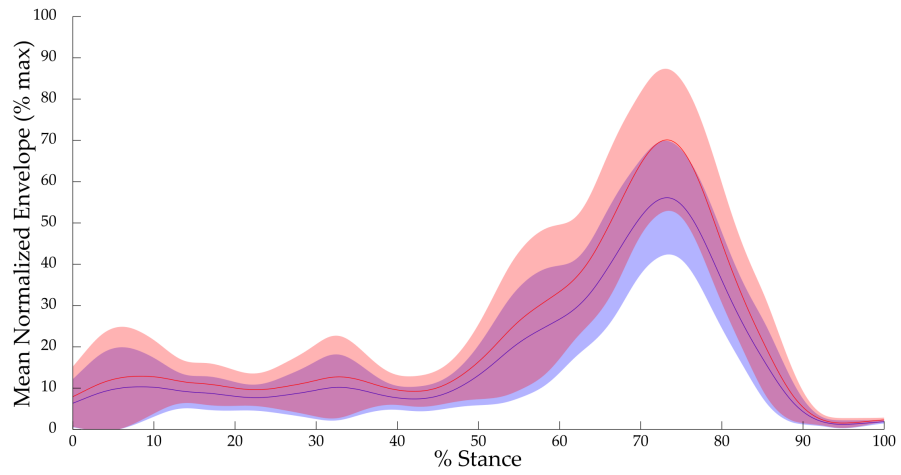


Figure 49: Mean Normalized Envelope for the (a) Peroneus Longus and the (b) Tibialis Anterior muscles.

(a) Gastrocnemius lateralis



(b) Gastrocnemius medialis



(c) Soleus

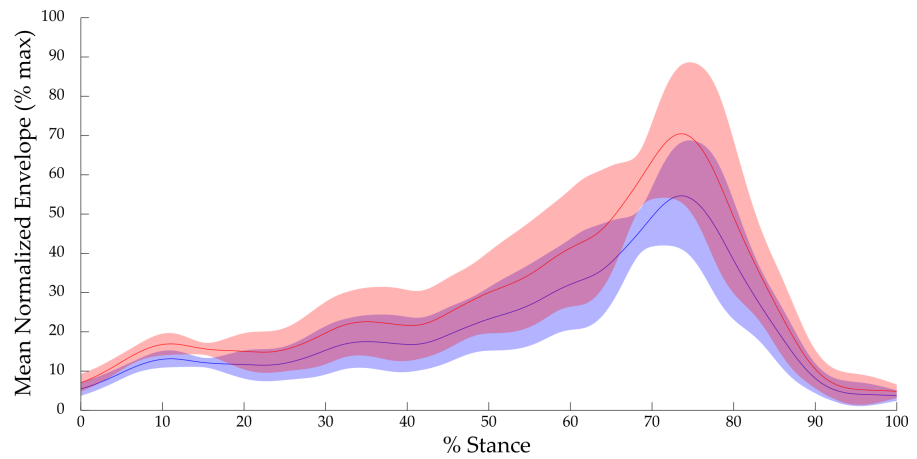


Figure 50: Mean Normalized Envelope for the posterior leg muscles.

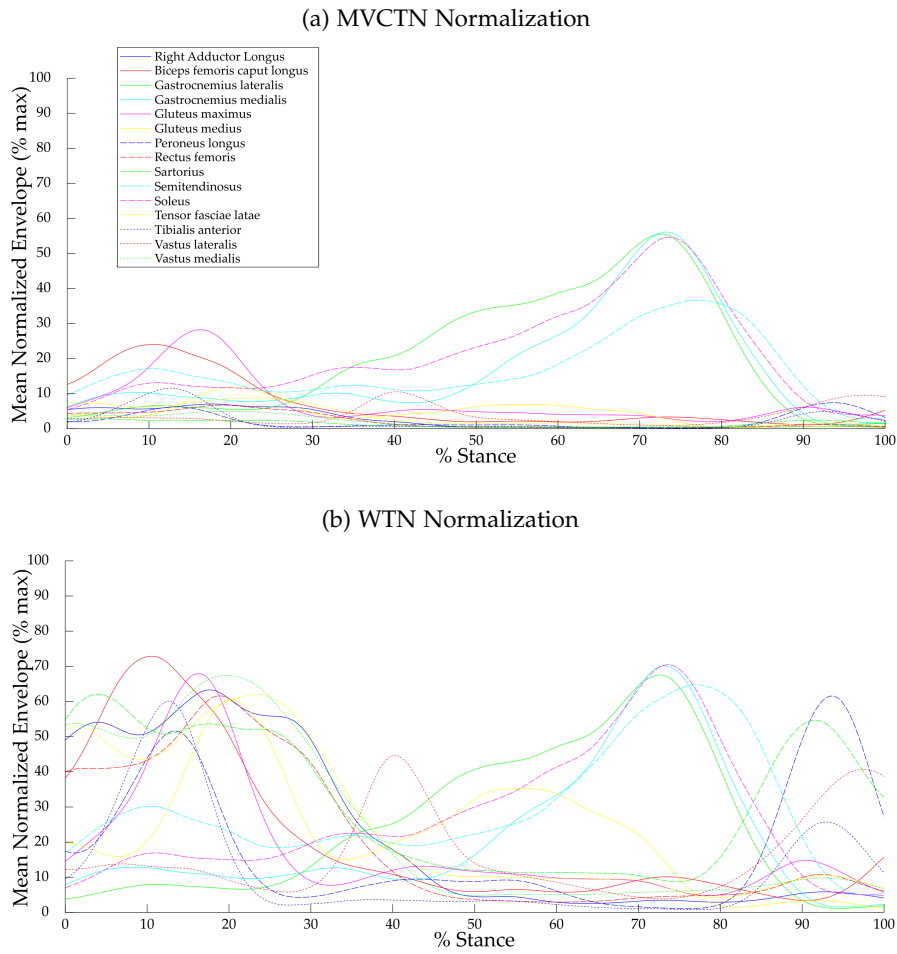


Figure 51: Mean Normalized Envelope from all muscles obtained with (a) MVCTN and (b) WTN normalization of input EMG signals.

Global Parameters	WTN calibration	MVCTN calibration	Range
C_1	-0.924	-0.833	[-0.950,-0.050]
C_2	-0.069	-0.815	[-0.950,-0.050]
A	-0.001	-0.199	[-2.999,-0.001]

Table 15: Global parameters obtained after model calibration using as input EMG linear envelopes normalized with the peak EMG from walking trials (WTN) and from the MVC tests (MVCTN).

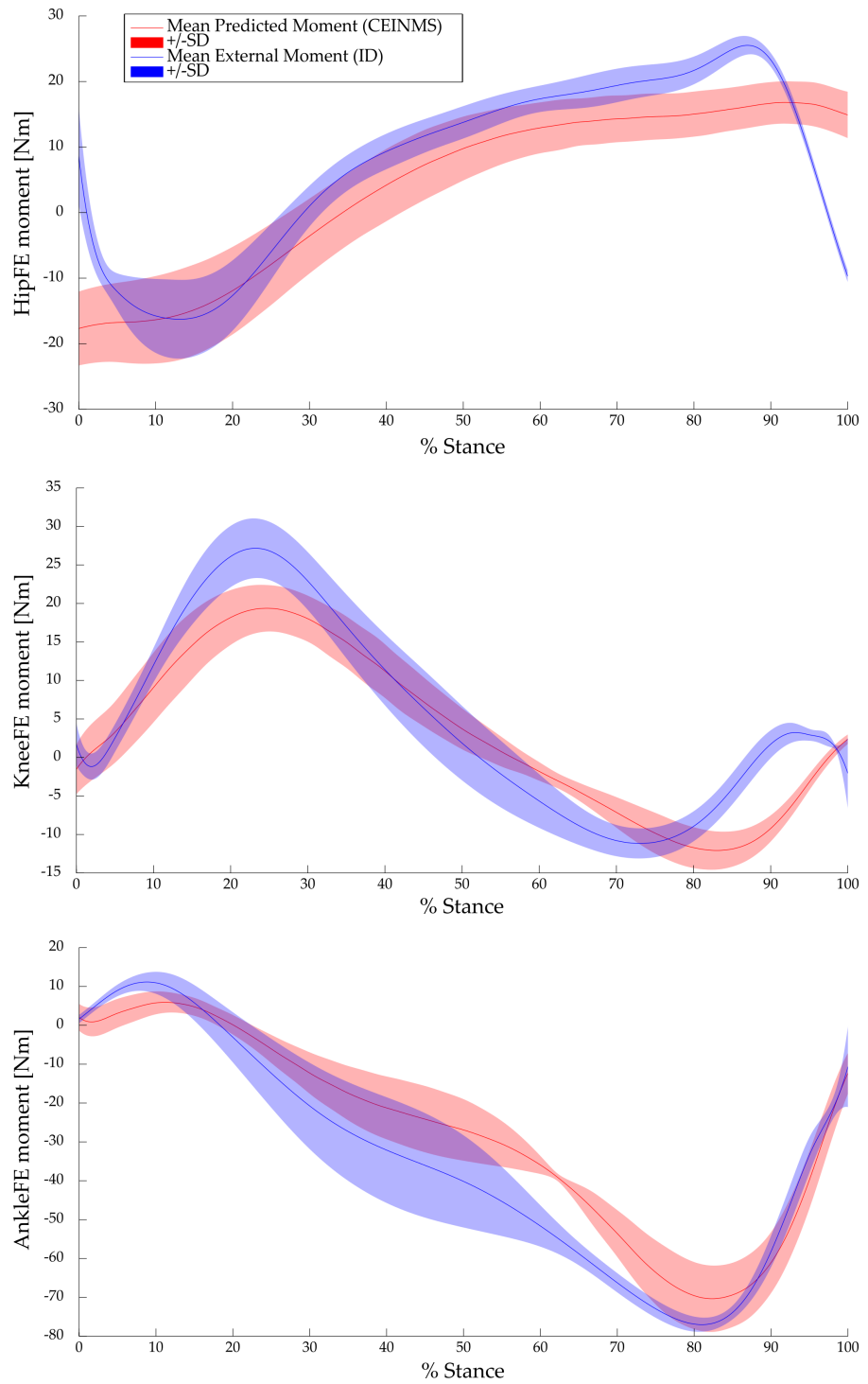


Figure 52: Joint Moments obtained normalizing input EMGs with the MVCTN method.

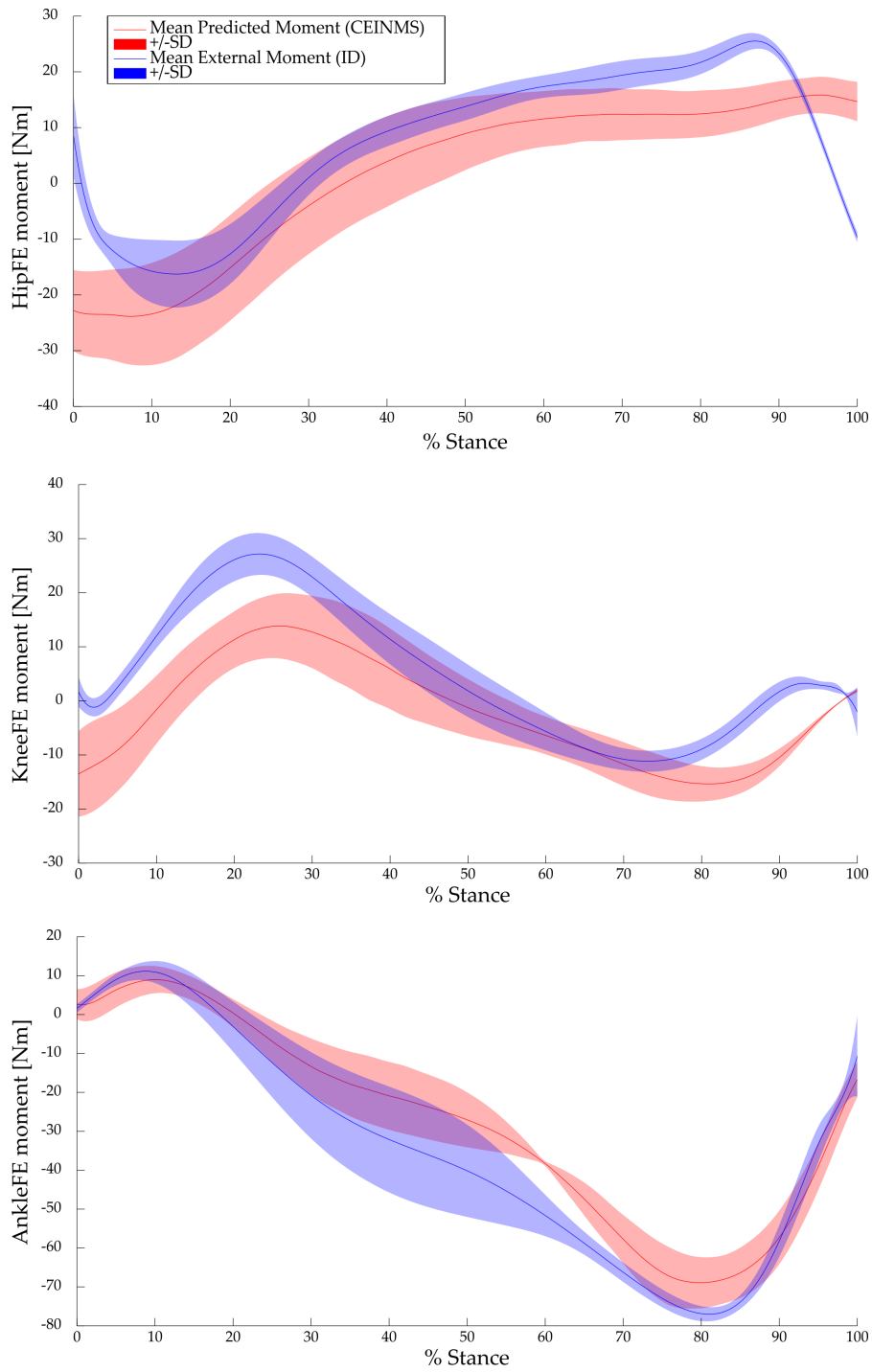


Figure 53: Joint Moments obtained normalizing input EMGs with the WTN method.

tude values led to substantial differences in muscle forces estimation (Fig. 54 - 56, 57a). Improvements in the MVC protocol were effective for the *PERLONG* and *TIBANT* muscles. Differently from the first study, a significant gap in the estimation of the peak EMG was indeed obtained with the *WTN* and *MVCTN* normalization strategies. This achievement affected the computation of the associated muscle forces, since a remarkable difference is evident in this case (Fig. 54, 57a).

The same result, instead, was not accomplished for the posterior leg muscles, as anticipated by the corresponding peak EMG values (Table 13). The task proposed within the *Minimal* MVC protocol for this muscle group did not bring to meaningful differences in the estimation of muscle forces. as a consequence of the two normalization strategies (Fig. 57b, 57c).

Lastly, the standard deviation was reduced for almost all muscles exploiting the *MVCTN* method, with the only exceptions of the posterior leg muscles and the *TIBANT* muscle.

4.4.4.5 *Muscle Contribution to the Net Joint Moments*

Differences in the distribution of muscle forces imply different contributions from each muscle to the net joint moments. An example from a single trial is shown for the three DOFs respectively in Fig. 58 - 60. Similarly to the first study, the two normalization approaches impacted mostly in the quadriceps and hamstrings contribution to the hip and knee moments. Nevertheless, in this case, the discrepancies among results from the two methods were more stressed if compared to those from the previous work. Clear examples were the behaviors of the *recfem* and *bicfemlh* shown in Fig. 58 and 59. Differences in muscle contributions from ankle dorsi and plantar flexors at the ankle joint were instead less marked (Fig. 60), as for the previous study.

4.4.4.6 *Flexors and Extensors Contribution to the Net Joint Moments*

The mean contributions of flexors and extensors muscles to the three net joint moments resulting from a *MVCTN* and *WTN* execution of the model were compared (Fig. 61 - 63). Results revealed a substantial difference in the two cases for the hip and knee joints (Fig. 61, 62). This discrepancy appeared to be greater than in the first study, especially for the knee joint. Moreover, as occurred for muscle forces, the *MVCTN* method allowed for a reduction in the standard deviation. A meaningful gap among the two normalization strategies was found also in the estimation of ankle dorsiflexors contribution to the ankle moment, while a slight variation resulted for the ankle plantar flexors. This was not the case for the ankle joint in the previous study.

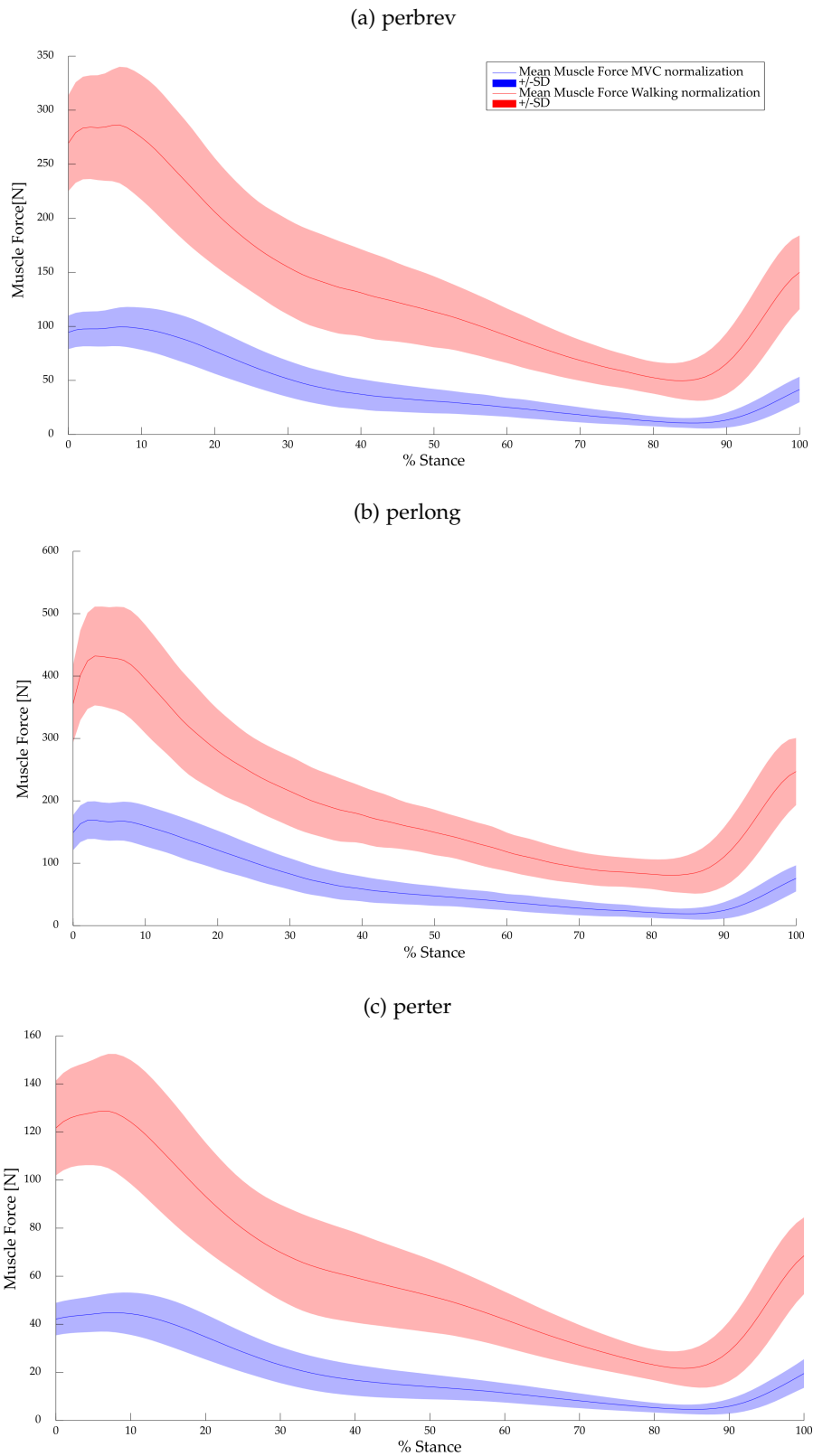


Figure 54: Comparison of Mean Muscle Forces estimated with CEINMS using MVC (blue) and walking (red) trials for normalization of input EMG signals.

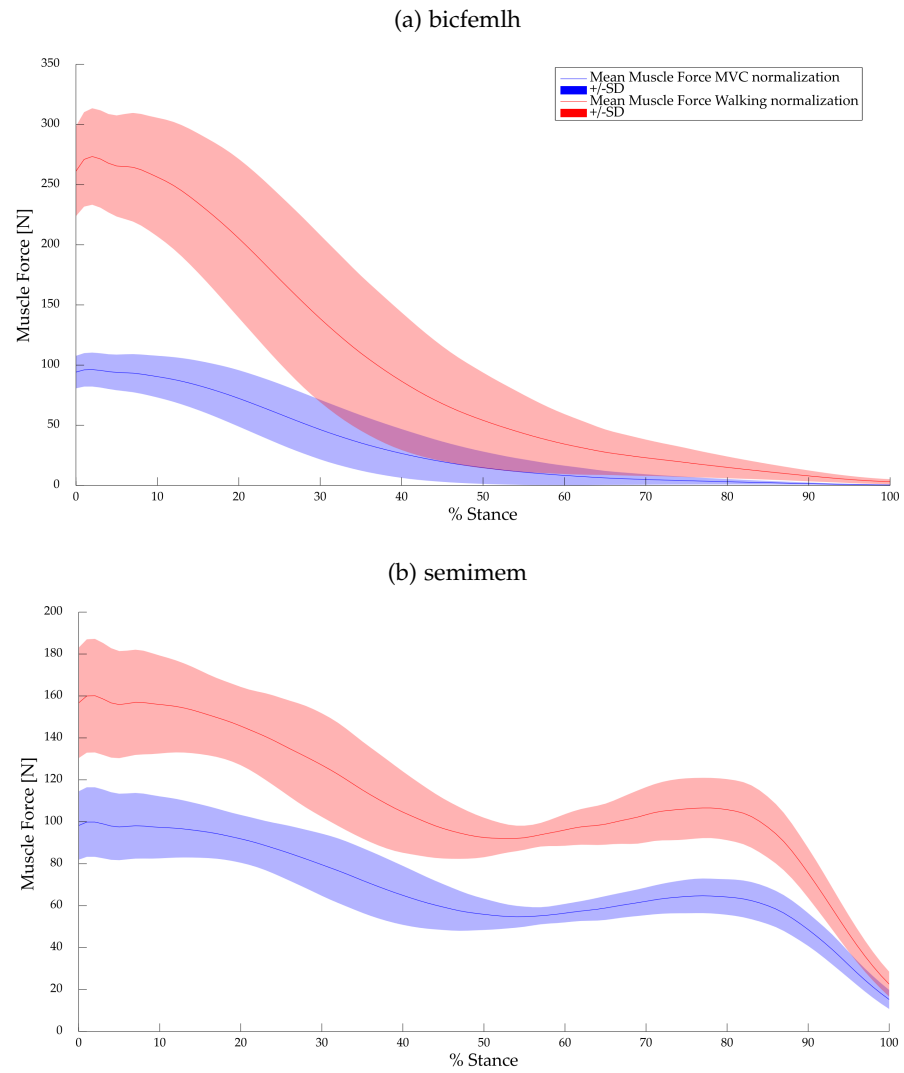


Figure 55: Comparison of Mean Muscle Forces estimated with CEINMS using MVC (blue) and walking (red) trials for normalization of input EMG signals.

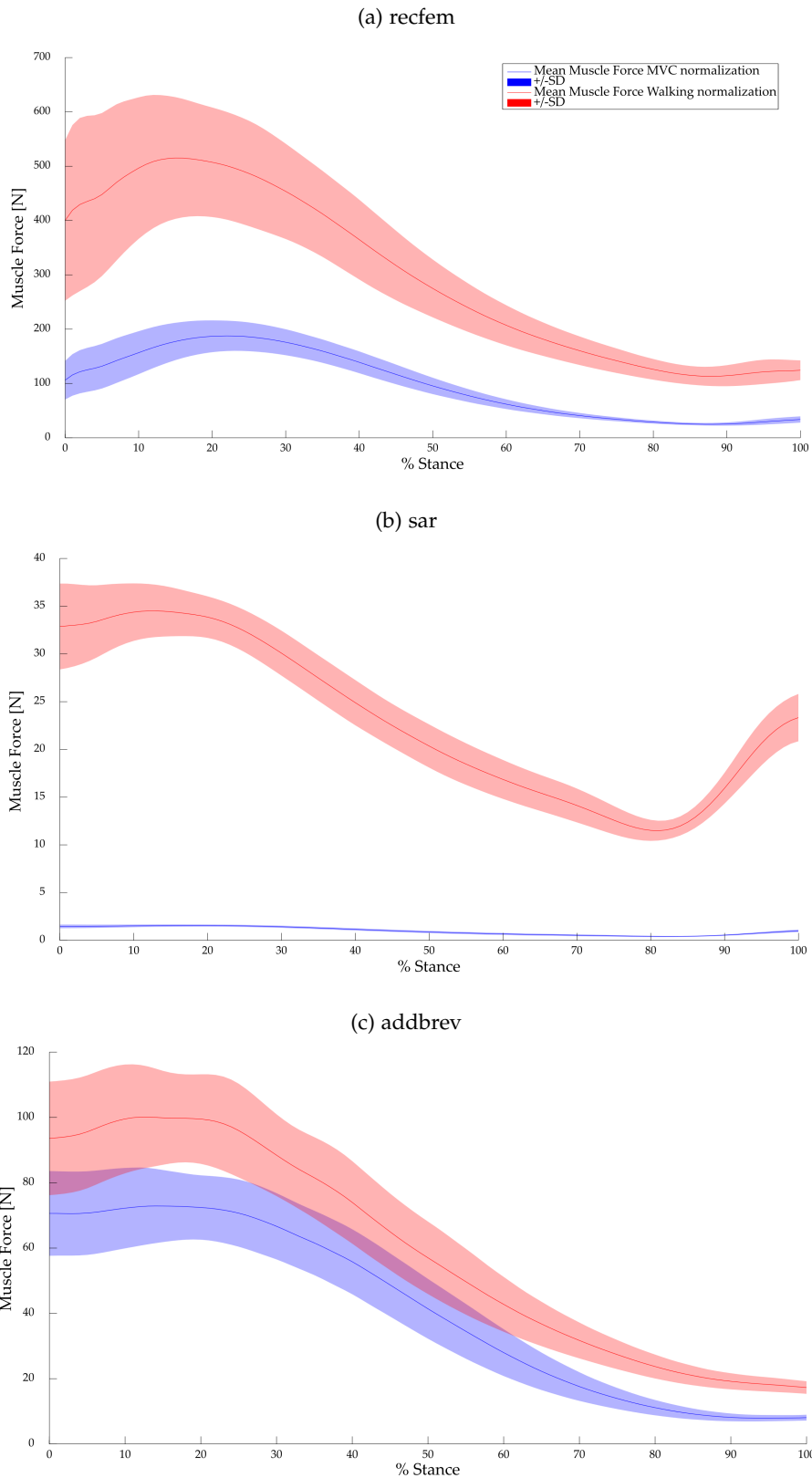


Figure 56: Comparison of Mean Muscle Forces estimated with CEINMS using MVC (blue) and walking (red) trials for normalization of input EMG signals.

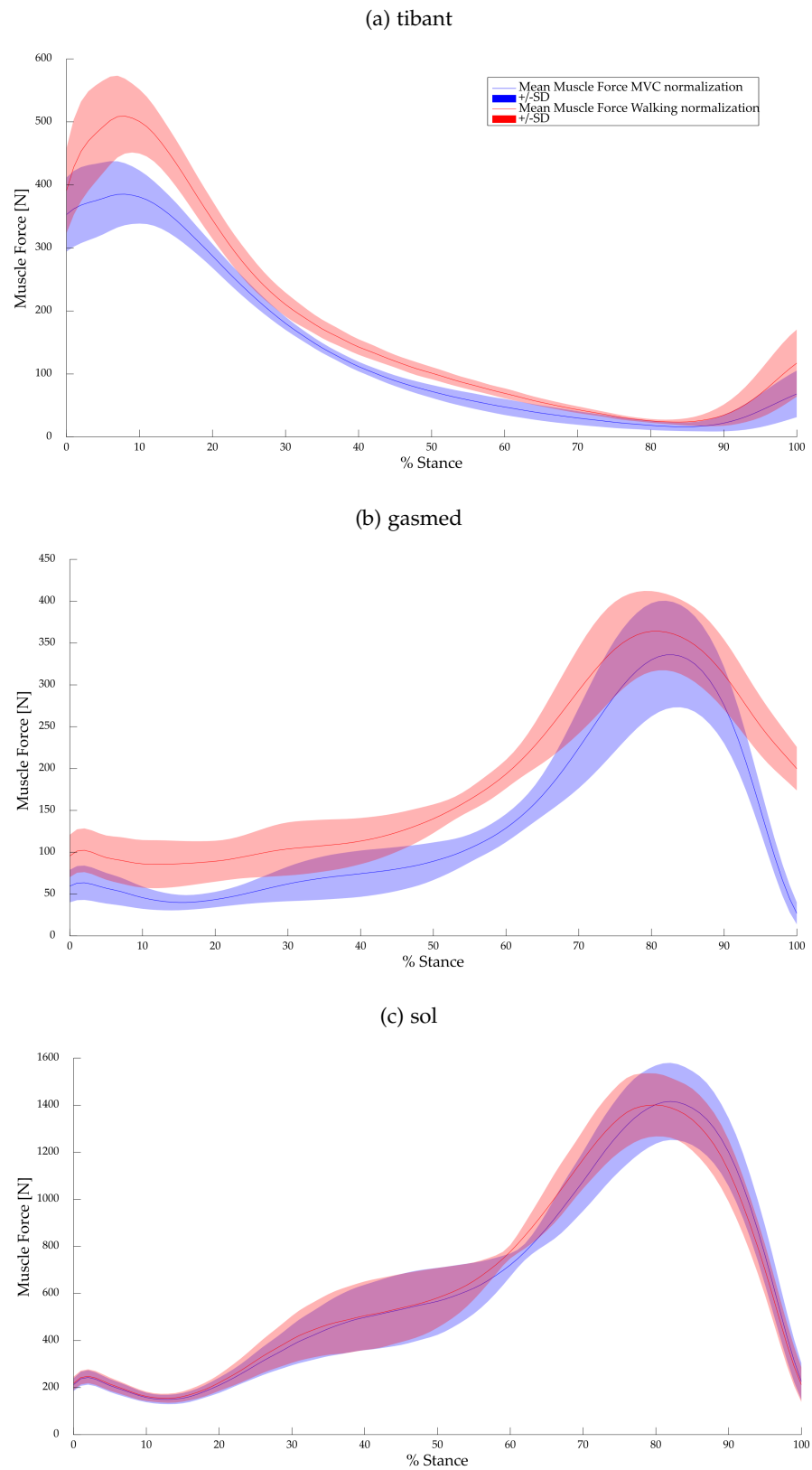


Figure 57: Comparison of Mean Muscle Forces estimated with CEINMS using MVC (blue) and walking (red) trials for normalization of input EMG signals.

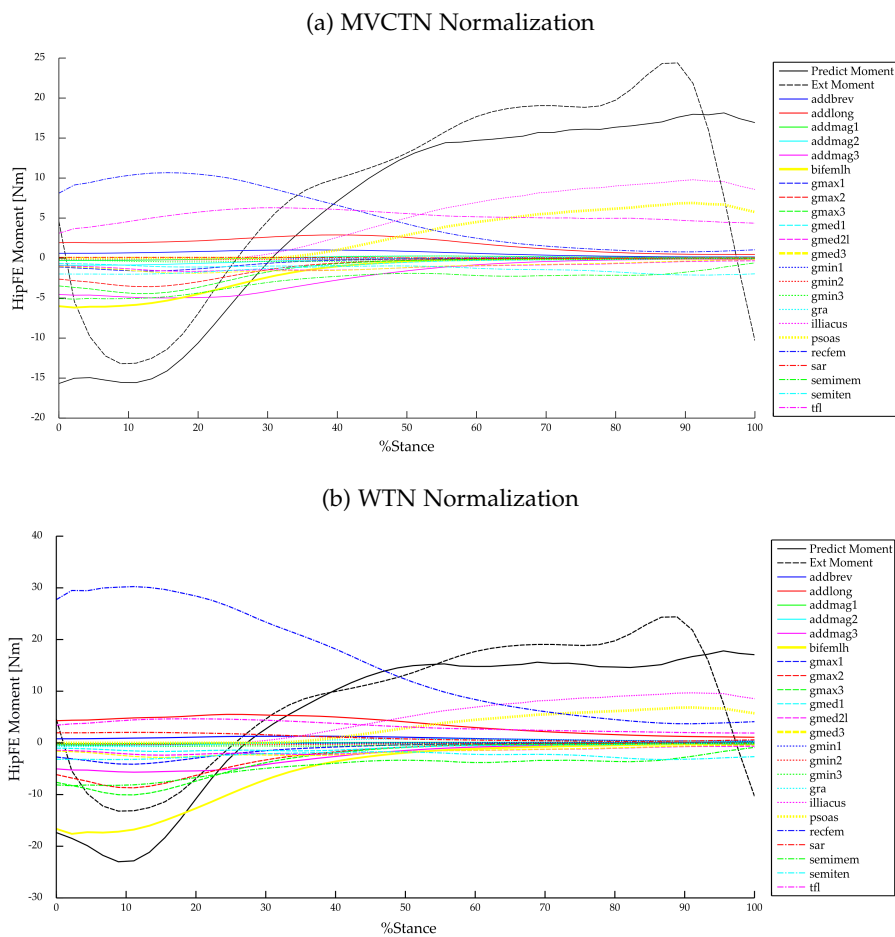


Figure 58: Example of Muscle Contributions to the net HipFE moment during a gait trial obtained with (a) MVCTN and (b) WTN normalization of input EMG signals.

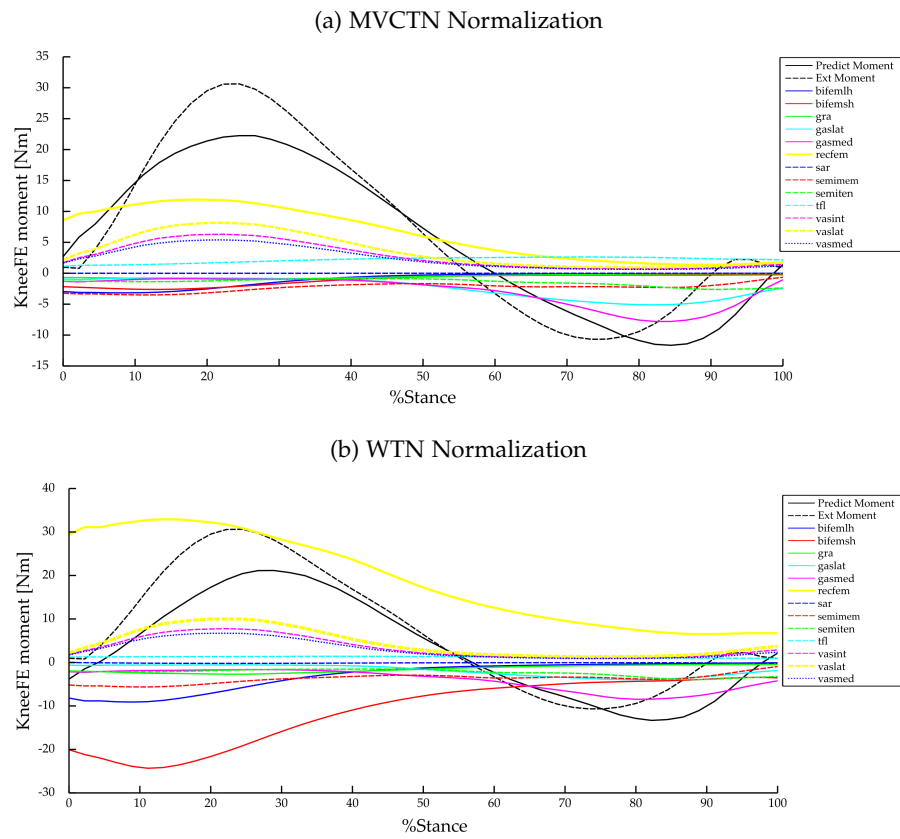


Figure 59: Example of Muscle Contributions to the net KneeFE moment during a gait trial obtained with (a) MVCTN and (b) WTN normalization of input EMG signals.

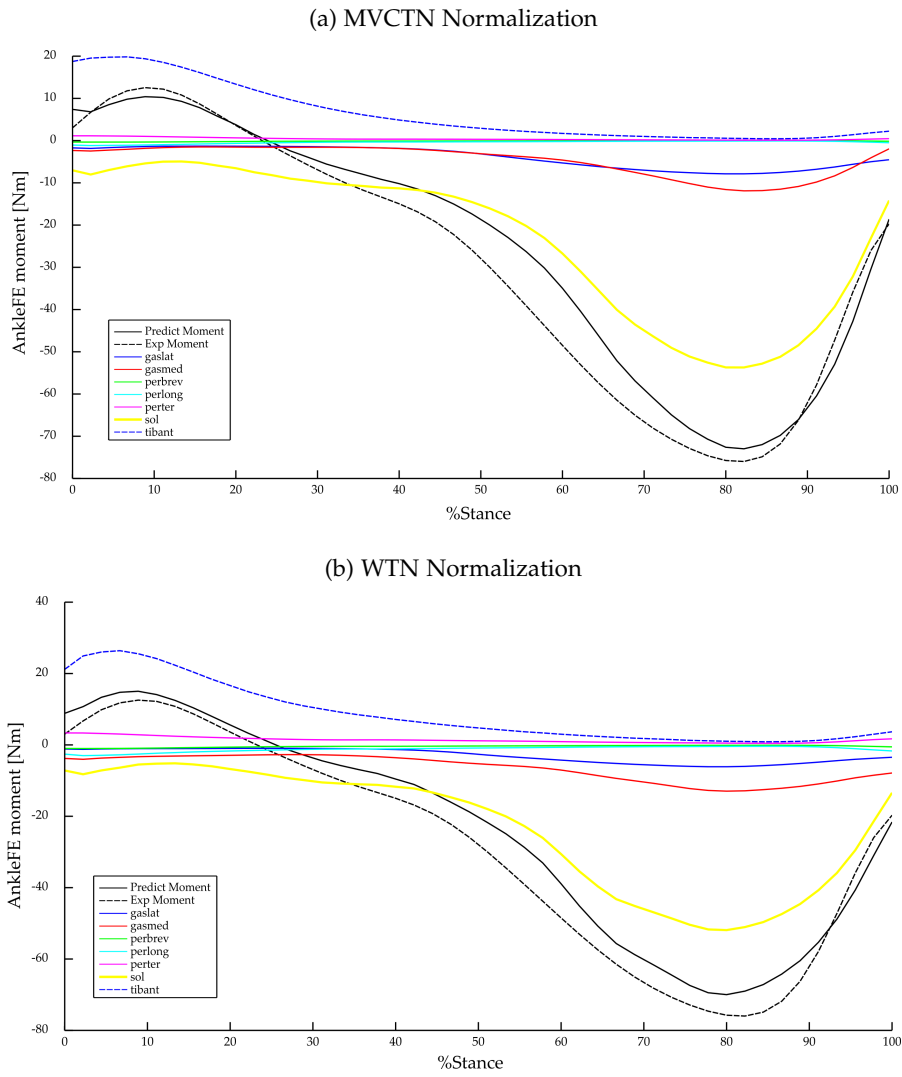


Figure 60: Example of Muscle Contributions to the net AnkleFE moment during a gait trial obtained with (a) MVCTN and (b) WTN normalization of input EMG signals.

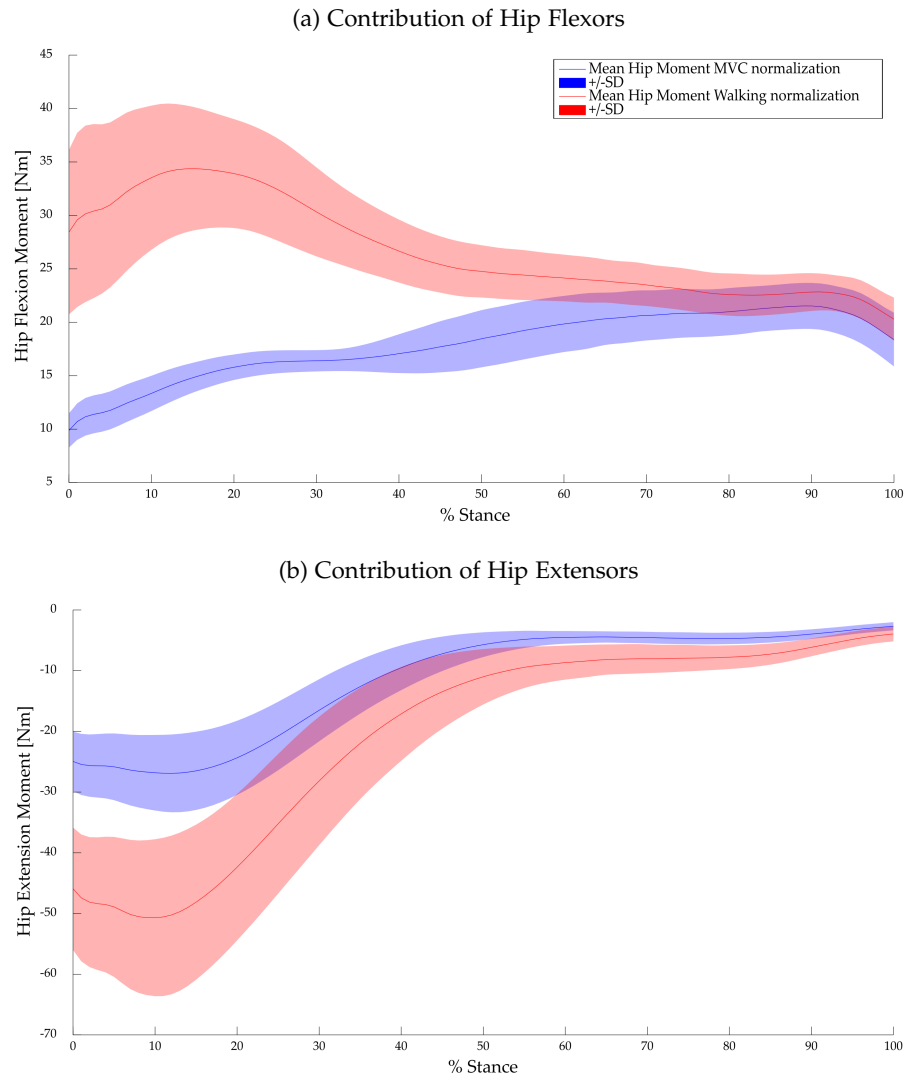


Figure 61: Mean Muscle Contributions of (a) hip flexors and (b) hip extensors to the net HipFE moment.

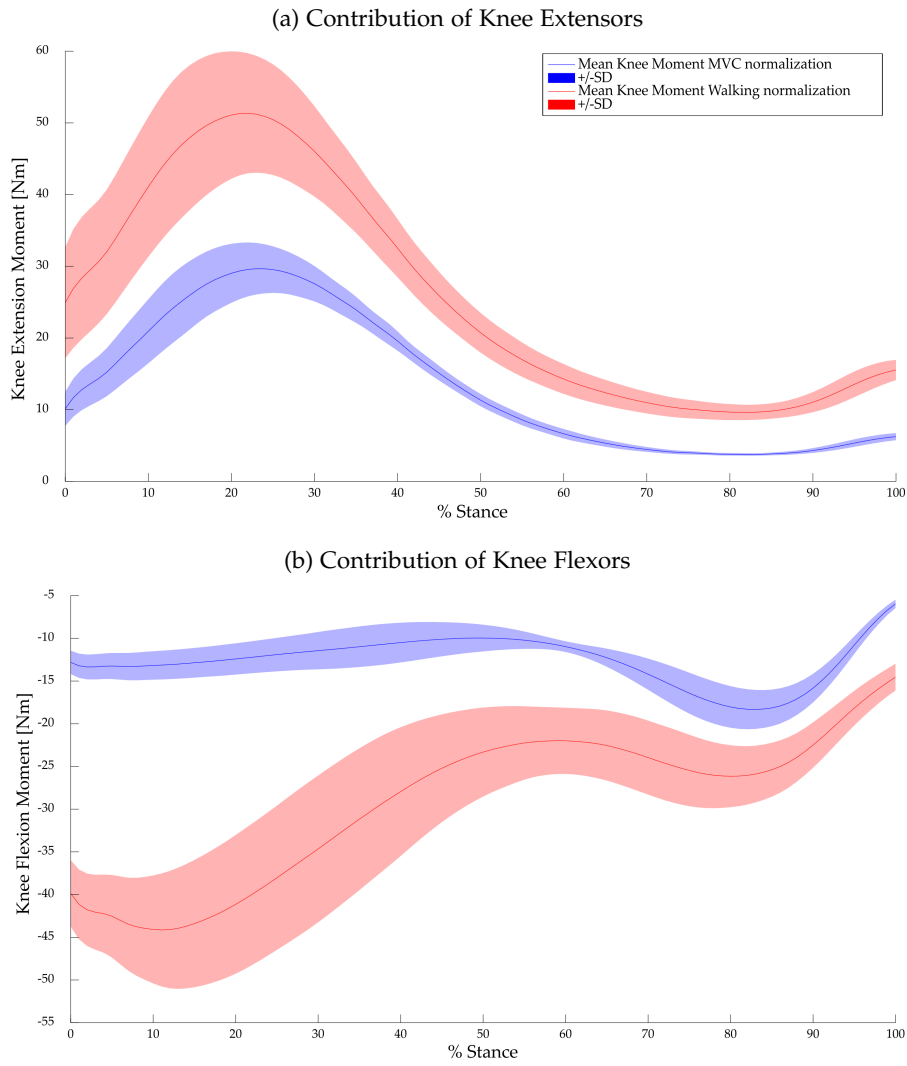
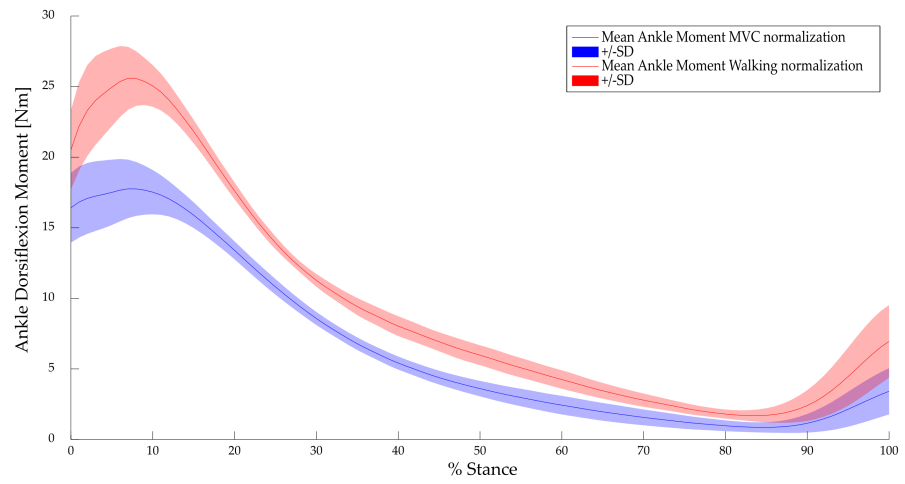


Figure 62: Mean Muscle Contributions of (a) knee extensors and (b) knee flexors to the net KneeFE moment.

(a) Contributions of Ankle Dorsiflexors



(b) Contributions of Ankle Plantar Flexors

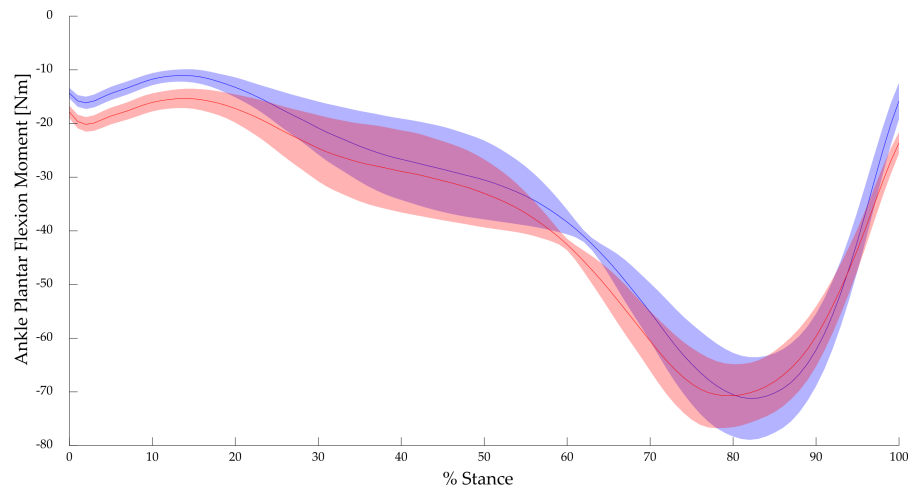


Figure 63: Mean Muscle Contributions of (a) ankle dorsiflexors and (b) ankle plantar flexors to the AnkleFE moment.

4.4.5 Discussion

This study represents an attempt towards the definition of a protocol for conducting MVC tests for the lower limb muscles, suitable for the application of EMG-driven multi-DOF NMS models in various clinical contexts. The previous work demonstrated the influence of the normalization technique used for input EMG signals on the NMS model, showing that the WTN approach can highly overestimate muscle forces. On the same time, it evidenced some limitations in the protocol used for obtaining MVC. Therefore, we aimed at overcoming those limitations with the intent of confirming previous findings and of generalizing the procedure to allow reproduction and comparison of results among multiple laboratories and research groups.

We proposed an alternative to the expensive isokinetic dynamometers commonly used (where available), and the dynamic tasks (e. g., running, sidestepping, crossover, Sartori et al. (2012a)) not feasible with patients, replacing the manual resistance of an expert operator exploited in the first study, with a steel cable and a padded ankle strap. We replicated the same processing and data analysis procedures contrived for the previous work.

Results are in line with those previously obtained in demonstrating a substantial gap between muscle forces when using the two normalization techniques, despite agreement in joint moments prediction. Therefore, they support the influence of normalized EMG input on EMG-driven multi-DOF NMS model results and the overestimation of muscle forces with the WTN method. Moreover, they provided evidences that an accurate prediction of joint moments can not be used to infer validity of muscle forces.

Improvements in the definition of MVC tasks were accomplished for the `PERLONG` and `TIBANT` muscles. In this study, indeed, a significant difference in the estimation of the peak EMG and, consequently, of muscle forces were obtained for both muscles. On the contrary, the same achievement did not occur for the posterior leg muscles, that maintained an high activation level during gait despite the use of the steel cable and the different task for the acquisition of their MVC. This result may be due to an ineffective testing position or it may be the case for this muscle group, known to greatly contribute during walking (Zajac et al., 2003; Anderson and Pandy, 2003; Arsenault et al., 1986). Further testing are needed to argue about this point. A related possible improvement that can be tested in a near future is to distinguish the tasks for the `gastrocnemii` muscles and the `soleus`, as their action is influenced differently by the knee angle (Konrad, 2005; Palastanga and Soames, 2011). However, for clinical applications, we need to consider that the total number of tasks must be constrained to the minimal.

Concerning this aspect, we can question if a MVC task for the sartorius muscle is necessary, since our results did not show a clear difference among performing it, as in this study, or not, as in the first case. The sartorius muscle has a very small influence on walking, but it contributes to several functional movements (e. g., hip and knee flexion, hip external rotation and abduction). It can be therefore normalized exploiting MVC tasks designed for other muscle groups, still reaching significant difference from the WTN (8% MVC during walking with the manual MVC protocol, Fig. 26). In this study, doing a specific MVC with the steel cable resulted only in a small variation, if compared with the first study (5% MVC during walking, Fig. 47). However, this can be a chance, and it requires to be tested with more subjects prior to not include a MVC test for the sartorius muscle in the protocol.

Besides, it is important to note that the use of the steel cable led to more marked differences among the two methods when looking at the muscle contributions to the net joint moments, if compared with those obtained adopting the manual MVC protocol of the first study. This can be seen from the single trial, comparing Fig. 58, 59 and 60 with Fig. 37, 38 and 39, and from the mean contributions of flexors and extensors muscles, especially for the knee joint. For the ankle joint, differences in the estimation of ankle dorsiflexors and plantar flexors contributions are mainly due to the improvement in the normalization of the TIBANT muscle.

In addition, this study revealed a more marked variation in the standard deviation among the two strategies if compared with previous results. This occurred particularly for the knee and hip extensors, and for the ankle dorsi and plantar flexors. Finally, global parameters resulting from the calibration process supported the discussion presented in the first study.

We can conclude that this work consolidated findings from the previous study. The proposed protocol can replicate results with significant improvements, allowing meantime a generalization of the acquisition procedure and its applicability in any clinical setting. Future works will include the enlargement of the dataset and the application of this methodology to a pathological population.

4.5 CONCLUSIONS AND FUTURE WORKS

Results from the two studies agree in demonstrating that EMG normalization is critical for the accuracy of EMG-driven multi-DOF NMS models predictions, and that validation based on joint moments can lead to a misleading assessment of muscle forces.

The two normalization strategies investigated for the input EMG signals yield completely different results in terms of muscle forces, and consequently, of muscle contributions to joint moments. Muscle forces

can not be measured, preventing a direct validation, therefore assessing their validity is not trivial. This is indeed a challenging common problem within the research community (Erdemir et al., 2007; Fregly, 2009; Hicks et al., 2015).

We showed that muscle-tendon model parameters resulting from the calibration process can represent a first warning of overfitting and non physiological behavior of the model. Indeed, significant differences in individual muscle parameters obtained with the WTN and MVCTN methods were noticed, being closer to physiological bounds in the first case. The MVCTN normalization seems to contribute in constraining parameters within their physiological range.

Results can be considered in line with previous studies saying that level of contractions larger than 50% MVC are required to calibrate a single DOF EMG to force model (Doorenbosch et al., 2005), and that unreliable normalization from MVC can be pointed as source of errors (Oliveira and Menegaldo, 2012). In contrast with the previous work of Barrett et al. (2007), instead, this investigation reveals that EMG normalization based only on walking trials (WTN) can lead to unreliable model results, and that it must be used with caution. A careful examination of calibration muscle-tendon parameters is suggested to assess confidence in the validity of results.

According to our findings, the WTN method is not recommended for calibration of a multi-DOF EMG-driven NMS model.

Consequently, there is a need for the definition of a protocol for MVC testing suitable for multiple DOFs applications being meanwhile feasible in the clinical practice. Some indications have emerged from the two studies concerning this point.

First, conducting MVC without any resistance are likely to be useless. Expensive isokinetic dynamometers are not always available in laboratories and they do not allow to span all DOFs in lower limb joints. Manual MVC are highly dependent on the level of resistance exerted by the operator, making this approach randomly effective. We therefore propose the use of a steel cable with a padded ankle strap as a mean to conform the level of resistance across laboratories and operators, and as an aid to guarantee that the maximum contraction is really reached in most occasions. Moreover, a simple dynamometer can be used in series with the steel cable to have reference force values, but mostly, as a motivational stimulator.

We compared results obtained normalizing EMG data by dividing for the maximum EMG value from gait trials with those achieved by means of two different protocols for performing MVC tests: the first based on an expert manual tester, and the second on the use of a steel cable. Resulting maximum EMG values show that higher level of contraction can be reached exploiting a steel cable, while the EMG-driven NMS model computations demonstrate that the proposed protocol can replicate results obtained with the intervention of an expert

manual tester. Still critical is the definition of a MVC task for the posterior leg muscles group (including *GASLAT*, *GASMED*, and *SOL*), which needs further testing.

Some limitations in the two studies have to be recognized. In a first instance, we restricted the calibration dataset to walking trials only, despite recommendations of different authors (Lloyd and Besier, 2003; Gerus et al., 2010), thinking to clinical needs (acquisition time reduction, unavailability of expensive dynamometers, patient motor impairments). Future works may consider to include other tasks in the calibration process to assess if they can contribute to improving calibration output. However, this implies knowing the external moment to the considered joints during the chosen tasks, which is usually possible having a dynamometer.

Secondly, the number of subjects may be questionable. However, our objective was not to validate a precise protocol, but instead to suggest guidelines that must be further investigated once that the problem has been recognized. The two studies aim at pointing out the relevance of the mentioned aspects, which haven't been examined yet with regards to multi-DOF EMG-driven NMS model applications.

A future direction to be pursued in a short time is testing the feasibility of the proposed MVCTN method with a pathological population. However, we must be aware of the difficulties in generalizing the methodology due to the individual nature of patients' motor impairments.

In summary, we can concluded that the importance of model calibration cannot be underestimated, and that moving from healthy subjects to patients, as well as from single to multiple DOFs, requires to rethink the methodology for data acquisition, and possibly, its validation, prior to make use of the estimated muscle forces for clinical purposes.

CONCLUSIONS

EMG-driven NMS modeling may have a great impact in the design of medical interventions and technologies. However, the state of the art is currently far from allowing the application of this approach in clinical practice. Single-DOF EMG-driven NMS models have been investigated in the literature, even for clinical studies, but the complexity implicit in their practical use still prevents their introduction into the clinical routine. The description of the overall workflow (Section 2.4) and of its main limitations (Section 2.5) may help in understanding the numerous issues that must be considered. Moving from single to multi-DOF is of great interest in a clinical context, where impairments usually compromise multiple joints. Nevertheless, the use of multi-DOF models increases even more the complexity of the problem. It is therefore not surprising that only one model considering multiple DOFs have been developed in the literature (Barrett et al., 2007; Sartori et al., 2012a). This model has been applied only to one healthy subject to demonstrate the improvements in the accuracy that can be achieved if compared with single-DOF models (Sartori et al., 2012a). However, no further investigations were afterwards provided to assess the quality of results in relation to the large number of variables that can influence the overall outcomes.

The work presented in this thesis represents a first effort towards a critical analysis of multi-DOF EMG-driven NMS models to evaluate their possible use in a clinical context.

With this objective, several issues have firstly arisen when attempting to replicate the workflow and to assess the accuracy of the proposed model in different acquisition settings. Comparing results obtained in different conditions is required to assess the reliability of the methodology, and only through an extensive use it can be truly verified and validated (Hicks et al., 2015), especially in clinical applications. As argued in Section 1.3, a methodology needs to be generalized and standardized to allow reproduction and comparison of results in different conditions. This means for example that it should not rely on acquisition setup and software, should not be operator-dependent, and any subject should be able to perform the designed protocol. Moreover, the processing procedures should be transparently reproducible and the selected parameters should be made available with the study results. This is even more important considering that it is not possible to directly use muscle forces for validation, as they cannot be measured. Thus perfect knowledge and the possibility to replicate the whole process are necessary steps to assess the quality of results. A

first shortcoming was therefore identified in the lack of tools to accomplish these tasks. With the intent to facilitate also other research groups in the use of EMG-driven NMS modeling, a great part of this research work was initially spent to generalize, standardize, and simplify the modeling workflow.

To this end, a software tool, named MOtoNMS, has been developed, freely available to the research community (Mantoan and Reggiani, 2014a) and described in *Chapter 3*. It is a complete, flexible, and user-friendly tool that allows to automatically process experimental motion data from different laboratories in a transparent and repeatable way, for their subsequent use in neuromusculoskeletal software. MOtoNMS generalizes data processing methods across laboratories, while meantime simplifying and speeding up the demanding modeling workflow. Therefore, with its support to several devices, a complete implementation of the processing procedures, its simple extensibility, the available user interfaces, and its free availability, it accomplishes an indispensable step towards an actual translation of NMS methods in daily and clinical practice.

In addition, we have also developed and made freely available to the community a tool for the batch processing of the musculoskeletal simulations within the OpenSim software (Section 2.4), including IK, ID and Muscle Analysis (Mantoan and Reggiani, 2014c). It automatizes the procedure, allowing the storing of setup and log files, as well as of plots representing the results for their subsequent visual inspection.

A second phase of this work was then dedicated to test the model in order to understand and address its limitations.

Several authors have tried to evaluate the accuracy of single-DOF EMG-driven NMS models (Koo et al., 2002; Koo and Mak, 2005; Menegaldo and De Oliveira, 2009; Oliveira and Menegaldo, 2012). Some of them assert that numerous methodological questions must be investigated as they are currently not solved, prior to move towards more complex applications, such as those that involved multijoint movements (Menegaldo and Oliveira, 2012). Furthermore, few studies have considered and faced the difficulties that can rise up when trying to adopt a new approach in the clinical field (Doorenbosch et al., 2005; Gerus et al., 2010).

Considering the concerns already highlighted for single-DOF models, and the few studies available so far on the impact that such a methodology may have in clinics (Section 1.2), we believe that multi-DOF EMG-driven models deserve a more in-depth analysis. A few roundabout solutions have been recently proposed to overcome limitations due to the scarce resolution of surface electromyography, such as an hybrid approach (Sartori et al., 2014), that combine EMG signals with optimization, or the use of muscle synergies (Sartori et al., 2013). However, current knowledge about multi-DOF and fully EMG-driven models is too limited to pass over without a better understanding of

its potentialities and limits. For these reasons, we have proposed a first investigation to ascertain accuracy and reveal some crucial aspects about the application of the only multi-DOF EMG driven model currently available in the literature.

We have started analyzing the sensitivity of model calibration and predictions to different EMG normalization strategies. The work addressed two main points: (i) the fact that it is hard to obtain confident values for peak EMGs in any condition, which is a recognized limitation related to the use of EMGs signals in a NMS modeling approach (Buchanan et al., 2004; Koo and Mak, 2005; Oliveira and Menegaldo, 2012); and (ii) the strategy used to obtain these maximum EMG values can be largely compromised when applied to impaired subjects (Doorenbosch et al., 2005). Exploring different contractile conditions and muscle recruitment strategies, as claimed by Lloyd and Besier (2003) and Gerus et al. (2010), is crucial but particularly difficult with patients. The same is when trying to obtain maximum efforts.

Therefore, we investigated the hypothesis of an ideal solution for clinical applications: considering only trials of walking both as calibration dataset and for the computation of maximum EMG values. We assessed the feasibility of this approach (WTN method), which was previously proposed also by Barrett et al. (2007). The two studies reported at *Chapter 4* agree in demonstrating first that validation based on joint moments can lead to a misleading assessment of muscle forces, confirming what already stated by other authors (Erdemir et al., 2007; Fregly, 2009; Chèze et al., 2012), and that this validation is not sufficient to guarantee a reliable application of the model. Second, the two studies allow to identify in the normalization of EMGs a critical factor for the accuracy of multi-DOF EMG-driven NMS models predictions, that can not be underestimated, as even previously remarked by Koo and Mak (2005) and Oliveira and Menegaldo (2012) regarding single-DOF models. In the specific, according to our findings, using only walking trials to compute the maximum EMG values by which normalize the processed EMG signals can bring inaccurate model results, and it is therefore not recommended for the calibration of a multi-DOF EMG-driven NMS model. Furthermore, results are in line with previous studies saying that an unreliable normalization from maximum voluntary contraction (MVC) can be a significant source of errors (Oliveira and Menegaldo, 2012).

Consequently, we have also provided some indications for the definition of a protocol for MVC testing, suitable for multiple DOFs applications, being meanwhile feasible in the clinical practice, and in any laboratory, as they use only basic and inexpensive instrumentation.

Finally, we showed that musculotendon model parameters resulting from the calibration process can represent a first warning of overfitting and non physiological behavior of the model. Therefore, a careful

examination of subject parameters is suggested as a first way to assess confidence in the validity of results.

In the end, the two studies highlighted the relevance of some methodological aspects, that have not been addressed before with regards to multi-DOF EMG-driven NMS model applications, but that cannot be neglected.

With the availability of instruments to facilitate the modeling workflow, the design of sensitivity studies able to account for the overall complexity of the problem becomes one of the fundamental challenges in the next future. More testing and analysis are indeed required to assess the influence of processing steps and calibration strategies. The evaluation of the effects that different filtering cut-off frequencies can have in the estimation of joint moments from inverse dynamics, and consequently on the calibration of the model, or the development of more precise methods to scale generic musculoskeletal models and determine subject-specific initial estimates of musculotendon parameters, are just some examples of required studies (Section 2.4). Different parameters constraints and calibration configuration may also be tested, especially with the aid of flexible software like CEINMS (Section 2.3). To overcome further and more specific issues related to clinical settings, some pathological cases may also be considered. However, generalization and validation of findings from clinical cases can result more difficult due to the specificity of patients' motor impairments.

We can conclude that moving from single to multiple DOFs, as well as from healthy subjects to patients, requires to rethink the methodology for data acquisition and elaboration, and to assess the influence of the processing of data through the whole process, as validation of predicted muscle forces is still challenging. Results of the calibration process, i. e., subject-specific musculotendon parameters, should be critically and deeply analyzed prior to argue about errors in the prediction of joint moments or correctness of estimated muscle forces. Usability and validation of a multi-DOF EMG-driven NMS model are strictly connected and have been addressed in this thesis. However, still a lot of work has to be done to boost its introduction into clinical practice.

BIBLIOGRAPHY

- F. C. Anderson and M. G. Pandy. Individual muscle contributions to support in normal walking. *Gait & Posture*, 17(2):159–169, 2003.
- A.B. Arsenault, D.A. Winter, and R.G. Marteniuk. Is there a normal profile of EMG activity in gait? *Medical and Biological Engineering and Computing*, 24(4):337–343, 1986.
- A. Barre and S. Armand. Biomechanical toolkit: Open-source framework to visualize and process biomechanical data. *Computer Methods and Programs in Biomedicine*, 114(1):80–87, 2014.
- R. S. Barrett, T. F. Besier, and D. G. Lloyd. Individual muscle contributions to the swing phase of gait: An EMG-based forward dynamics modelling approach. *Simulation Modelling Practice and Theory*, 15(9):1146–1155, 2007.
- M. G. Benedetti, A. Merlo, and A. Leardini. Inter-laboratory consistency of gait analysis measurements. *Gait & Posture*, 38(4):934–939, 2013.
- T. F. Besier, M. Fredericson, G. E. Gold, G. S. Beaupré, and S. L. Delp. Knee muscle forces during walking and running in patellofemoral pain patients and pain-free controls. *Journal of Biomechanics*, 42(7):898–905, 2009.
- N. E. Bezodis, A. I. T. Salo, and G. Trewartha. Excessive fluctuations in knee joint moments during early stance in sprinting are caused by digital filtering procedures. *Gait & Posture*, 38(4):653–657, 2013.
- S. S. Blemker, D. S. Asakawa, G. E. Gold, and S. L. Delp. Image-based musculoskeletal modeling: Applications, advances, and future opportunities. *Journal of Magnetic Resonance Imaging*, 25(2):441–451, 2007.
- L. A. Bolgla and T. L. Uhl. Reliability of electromyographic normalization methods for evaluating the hip musculature. *Journal of Electromyography and Kinesiology*, 17(1):102–111, 2007.
- T. S. Buchanan, M. J. Moniz, J. Dewald, and W. Z. Rymer. Estimation of muscle forces about the wrist joint during isometric tasks using an EMG coefficient method. *Journal of Biomechanics*, 26(4):547–560, 1993.
- T. S. Buchanan, D. G. Lloyd, K. Manal, and T. F. Besier. Neuromusculoskeletal modeling: estimation of muscle forces and joint moments and movements from measurements of neural command. *Journal of Applied Biomechanics*, 20(4):367–395, 2004.
- T. S. Buchanan, D. G. Lloyd, K. Manal, and T. F. Besier. Estimation of muscle forces and joint moments using a forward-inverse dynamics model. *Medicine and Science in Sports and Exercise*, 37(11):1911–1916, 2005.
- A. Burden. How should we normalize electromyograms obtained from healthy participants? what we have learned from over 25 years of research. *Journal of Electromyography and Kinesiology*, 20(6):1023–1035, 2010.
- A. Burden and R. Bartlett. Normalisation of EMG amplitude: an evaluation and comparison of old and new methods. *Medical Engineering & Physics*, 21(4):247–257, 1999.
- A. M. Burden, M. Trew, and V. Baltzopoulos. Normalisation of gait EMGs: a re-examination. *Journal of Electromyography and Kinesiology*, 13(6):519–532, 2003.

- A. Burnett, J. Green, K. Netto, and J. Rodrigues. Examination of EMG normalisation methods for the study of the posterior and posterolateral neck muscles in healthy controls. *Journal of Electromyography and Kinesiology*, 17(5):635–641, 2007.
- A. Cappozzo, F. Catani, U. Della Croce, and A. Leardini. Position and orientation in space of bones during movement: anatomical frame definition and determination. *Clinical Biomechanics*, 10(4):171–178, 1995.
- A. Cereatti, U. Della Croce, and A. Cappozzo. Reconstruction of skeletal movement using skin markers: comparative assessment of bone pose estimators. *Journal of NeuroEngineering and Rehabilitation*, 3:7, 2006.
- L. Chèze, F. Moissenet, and R. Dumas. State of the art and current limits of musculo-skeletal models for clinical applications. *Movement & Sport Sciences-Science & Motricité*, 2012.
- L. Chiari, U. Della Croce, A. Leardini, and A. Cappozzo. Human movement analysis using stereophotogrammetry- part 2: Instrumental errors. *Gait & Posture*, 21(2): 197–211, 2005.
- D. M. Corcos, G. L. Gottlieb, M. L. Latash, G. L. Almeida, and G. C. Agarwal. Electromechanical delay: An experimental artifact. *Journal of Electromyography and Kinesiology*, 2(2):59–68, 1992.
- M. Damsgaard, J. Rasmussen, S. T. Christensen, E. Surma, and M. de Zee. Analysis of musculoskeletal systems in the anybody modeling system. *Simulation Modelling Practice and Theory*, 14(8):1100 – 1111, 2006.
- R. B. Davis, III, S. Ounpuu, D. Tyburski, and J. R. Gage. A gait analysis data collection and reduction technique. *Human Movement Science*, 10(5):575–587, 1991.
- R. B. Davis, III, J. R. Davids, G. E. Gorton, III, M. Aiona, N. Scarborough, D. Oeffinger, C. Tylkowski, and A. Bagley. A minimum standardized gait analysis protocol: development and implementation by the Shriners Motion Analysis Laboratory network (SMALnet). In *Pediatric Gait, 2000. A new Millennium in Clinical Care and Motion Analysis Technology*, 2000.
- F. De Groote, A. Van Campen, I. Jonkers, and J. De Schutter. Sensitivity of dynamic simulations of gait and dynamometer experiments to hill muscle model parameters of knee flexors and extensors. *Journal of Biomechanics*, 43(10):1876–1883, 2010.
- C. J. De Luca. The use of surface electromyography in biomechanics. *Journal of Applied Biomechanics*, 13:135–163, 1997.
- L. F. De Oliveira and L. L. Menegaldo. Individual-specific muscle maximum force estimation using ultrasound for ankle joint torque prediction using an EMG-driven hill-type model. *Journal of Biomechanics*, 43(14):2816–2821, 2010.
- S. Del Din, E. Carraro, Z. Sawacha, A. Guiotto, L. Bonaldo, S. Masiero, and C. Cobelli. Impaired gait in ankylosing spondylitis. *Medical & Biological Engineering & Computing*, 49:801–809, 2011.
- S. Delp, A. Habib, A. Seth, and J. Hicks. [Internet]. opensim user guide. Available from: <http://simtk-confluence.stanford.edu:8080/display/OpenSim/User's+Guide>, 2012.
- S. L. Delp and J. P. Loan. A graphics-based software system to develop and analyze models of musculoskeletal structures. *Computers in Biology and Medicine*, 25(1): 21–34, 1995.

- S. L. Delp, J. P. Loan, M. G. Hoy, F. E. Zajac, E. L. Topp, and J. M. Rosen. An interactive graphics-based model of the lower extremity to study orthopaedic surgical procedures. *IEEE Transactions on Biomedical Engineering*, 37(8):757–767, 1990.
- S. L. Delp, F. C. Anderson, A. S. Arnold, P. Loan, A. Habib, C. T. John, E. Guendelman, and D. G. Thelen. Opensim: open-source software to create and analyze dynamic simulations of movement. *IEEE Transactions on Biomedical Engineering*, 54(11):1940–1950, 2007.
- A. R. Dempsey, D. G. Lloyd, B. C. Elliott, J. R. Steele, B. J. Munro, and K. A. Russo. The effect of technique change on knee loads during sidestep cutting. *Medicine and Science in Sports and Exercise*, 39:1765–1773, 2007.
- C. Disselhorst-Klug, T. Schmitz-Rode, and G. Rau. Surface electromyography and muscle force: Limits in sEMG–force relationship and new approaches for applications. *Clinical Biomechanics*, 24(3):225–235, 2009.
- C.J. Donnelly, D. G. Lloyd, B. C. Elliott, and J. A. Reinbolt. Optimizing whole-body kinematics to minimize valgus knee loading during sidestepping: implications for acl injury risk. *Journal of Biomechanics*, 45(8):1491–1497, 2012.
- C. A. M. Doorenbosch, A. Joosten, and J. Harlaar. Calibration of EMG to force for knee muscles is applicable with submaximal voluntary contractions. *Journal of Electromyography and Kinesiology*, 15(4):429–435, 2005.
- T. Dorn. [Internet]. C3D extraction toolbox. Available from: <https://simtk.org/home/c3dtoolbox>, 2011.
- T. W. Dorn, A. G. Schache, and M. G. Pandy. Muscular strategy shift in human running: dependence of running speed on hip and ankle muscle performance. *The Journal of Experimental Biology*, 215:1944–1956, 2012.
- J. Dunne. [Internet]. Opensim Documentation: Tools for Preparing Motion Data. Available from: <http://simtkconfluence.stanford.edu:8080/display/OpenSim/Tools+for+Preparing+Motion+Data>, 2013.
- W. B. Edwards, K. L. Troy, and T. R. Derrick. On the filtering of intersegmental loads during running. *Gait & Posture*, 34(3):435–438, 2011.
- A. Erdemir, S. McLean, W. Herzog, and A. J. van den Bogert. Model-based estimation of muscle forces exerted during movements. *Clinical Biomechanics*, 22(2):131–154, 2007.
- B. J. Fregly. Design of optimal treatments for neuromusculoskeletal disorders using patient-specific multibody dynamic models. *International Journal for Computational Vision and Biomechanics*, 2(2):145–155, 2009.
- B. J. Fregly, J. A. Reinbolt, K. L. Rooney, K. H. Mitchell, and T. L. Chmielewski. Design of patient-specific gait modifications for knee osteoarthritis rehabilitation. *IEEE Transactions on Biomedical Engineering*, 54(9):1687–1695, 2007.
- B. J. Fregly, M. L. Boninger, and D. J. Reinkensmeyer. Personalized neuromusculoskeletal modeling to improve treatment of mobility impairments: a perspective from european research sites. *Journal of NeuroEngineering and Rehabilitation*, 9:18, 2012.
- E. S. Gardinier, K. Manal, T. S. Buchanan, and L. Snyder-Mackler. Gait and neuromuscular asymmetries after acute ACL rupture. *Medicine and Science in Sports and Exercise*, 44(8):1490–1496, 2012.

- E. S. Gardinier, K. Manal, T. S. Buchanan, and L. Snyder-Mackler. Altered loading in the injured knee after acl rupture. *Journal of Orthopaedic Research*, 31(3):458–464, 2013.
- P. Gerus, G. Rao, T. S. Buchanan, and E. Berton. A clinically applicable model to estimate the opposing muscle groups contributions to isometric and dynamic tasks. *Annals of Biomedical Engineering*, 38(7):2406–2417, 2010.
- A. M. Gordon, A. F. Huxley, and F. J. Julian. The variation in isometric tension with sarcomere length in vertebrate muscle fibres. *The Journal of Physiology*, 184(1):170–192, 1966.
- D. E. Gordon Robertson, G. Caldwell, J. Hamill, G. Kamen, and S. Whittlesey. *Research methods in biomechanics*. Human Kinetics, 2004.
- G. E. Gorton, III, D. A. Hebert, and M. E. Gannotti. Assessment of the kinematic variability among 12 motion analysis laboratories. *Gait & Posture*, 29(3):398–402, 2009.
- K. P. Granata and W. S. Marras. An EMG-assisted model of trunk loading during free-dynamic lifting. *Journal of Biomechanics*, 28(11):1309–1317, 1995.
- A.C. Guimaraes, W. Herzog, M. Hulliger, Y.T. Zhang, and S. Day. Effects of muscle length on the EMG-force relationship of the cat soleus muscle studied using non-periodic stimulation of ventral root filaments. *Journal of Experimental Biology*, 193(1):49–64, 1994.
- S. R. Hamner, A. Seth, and S. L. Delp. Muscle contributions to propulsion and support during running. *Journal of Biomechanics*, 43(14):2709–2716, 2010.
- M. E. Harrington, A. B. Zavatsky, S. E. M. Lawson, Z. Yuan, and T. N. Theologis. Prediction of the hip joint centre in adults, children, and patients with cerebral palsy based on magnetic resonance imaging. *Journal of Biomechanics*, 40(3):595–602, 2007.
- H. Hatze. Estimation of myodynamic parameter values from observations on isometrically contracting muscle groups. *European Journal of Applied Physiology and Occupational Physiology*, 46(4):325–338, 1981.
- C. W. Heckathorne and D. S. Childress. Relationships of the surface electromyogram to the force, length, velocity, and contraction rate of the cineplastic human biceps1. *American Journal of Physical Medicine & Rehabilitation*, 60(1):1–19, 1981.
- W. Herzog. The relation between the resultant moments at a joint and the moments measured by an isokinetic dynamometer. *Journal of Biomechanics*, 21(1):5–12, 1988.
- J. L. Hicks, T. K. Uchida, A. Seth, A. Rajagopal, and S. L. Delp. Is my model good enough? best practice for verification and validation of musculoskeletal models and simulations of movement. *Journal of Biomechanical Engineering*, 137(2), 2015.
- J. S. Higginson, F. E. Zajac, R. R. Neptune, S. A. Kautz, and S. L. Delp. Muscle contributions to support during gait in an individual with post-stroke hemiparesis. *Journal of Biomechanics*, 39(10):1769–1777, 2006.
- J. S. Higginson, J. W. Ramsay, and T. S. Buchanan. Hybrid models of the neuromusculoskeletal system improve subject-specificity. *Proceedings of the Institution of Mechanical Engineers, Part H: Journal of Engineering in Medicine*, 226(2):113–119, 2012.
- A. V. Hill. The heat of shortening and the dynamic constants of muscle. *Proceedings of the Royal Society of London. Series B, Biological Sciences*, pages 136–195, 1938.

- A. L. Hof and J. W. van den Berg. EMG to force processing i: An electrical analogue of the hill muscle model. *Journal of Biomechanics*, 14(11):747–758, 1981.
- P. A. Huijing. Important experimental factors for skeletal muscle modelling: non-linear changes of muscle length force characteristics as a function of degree of activity. *European Journal of Morphology*, 34(1):47–54, 1995.
- I. Jonkers, C. Stewart, and A. Spaepen. The study of muscle action during single support and swing phase of gait: clinical relevance of forward simulation techniques. *Gait & Posture*, 17(2):97–105, 2003.
- M. P. Kadaba, H. K. Ramakrishnan, and M. E. Wootten. Measurement of lower extremity kinematics during level walking. *Journal of Orthopaedic Research*, 8(3):383–392, 1990.
- K. R. Kaufman. *Gait analysis in the science of rehabilitation*, pages 85–112. Diane Publishing Company, 1998.
- F. P. Kendall, E. K. McCreary, and P. G. Provance. *Muscles testing and function*. Williams & Wilkins, 1993.
- M. Khachani, R. Davoodi, and G. E. Loeb. Musculo-skeletal modeling software (MSMS) for biomechanics and virtual rehabilitation. In *Proceeding of American Society of Biomechanics Conference*, 2007.
- L. M. Knutson, G. L. Soderberg, B. T. Ballantyne, and W. R. Clarke. A study of various normalization procedures for within day electromyographic data. *Journal of Electromyography and Kinesiology*, 4(1):47–59, 1994.
- P. Konrad. *The ABC of EMG: a practical introduction to kinesiological electromyography*. Noraxon USA, Inc, Scottsdale, AZ, 2005.
- T. K. K. Koo and Arthur F. T. Mak. Feasibility of using EMG driven neuromusculoskeletal model for prediction of dynamic movement of the elbow. *Journal of Electromyography and Kinesiology*, 15(1):12–26, 2005.
- T. K. K. Koo, A. F. T. Mak, and L. K. Hung. In vivo determination of subject-specific musculotendon parameters: applications to the prime elbow flexors in normal and hemiparetic subjects. *Clinical Biomechanics*, 17(5):390–399, 2002.
- E. Kristianslund, T. Krosshaug, and A. J. van den Bogert. Effect of low pass filtering on joint moments from inverse dynamics: implications for injury prevention. *Journal of Biomechanics*, 45(4):666–671, 2012.
- K. H. E. Kroemer and W. S. Marras. Towards an objective assessment of the maximal voluntary contraction component in routine muscle strength measurements. *European Journal of Applied Physiology and Occupational Physiology*, 45(1):1–9, 1980.
- D. Kumar, K. S. Rudolph, and K. T. Manal. EMG-driven modeling approach to muscle force and joint load estimations: Case study in knee osteoarthritis. *Journal of Orthopaedic Research*, 30(3):377–383, 2012.
- B. Laursen, B. R. Jensen, G. Németh, and G. Sjøgaard. A model predicting individual shoulder muscle forces based on relationship between electromyographic and 3d external forces in static position. *Journal of Biomechanics*, 31(8):731–739, 1998.
- A. Leardini, Z. Sawacha, G. Paolini, S. Ingrassio, R. Nativo, and M. G. Benedetti. A new anatomically based protocol for gait analysis in children. *Gait & Posture*, 26(4):560–571, 2007.
- S. Lee and J. Son. [Internet]. Lee-Son’s toolbox. Available from: <https://simtk.org/home/lee-son>, 2012.

- G. Lichtwark, A. Habib, and R. Barrett. [Internet]. Matlab-Opensim Interfaces. Available from: https://simtk.org/home/matlab_tools, 2013.
- D. G. Lloyd and T. F. Besier. An EMG-driven musculoskeletal model to estimate muscle forces and knee joint moments in vivo. *Journal of Biomechanics*, 36(6):765–776, 2003.
- D. G. Lloyd and T. S. Buchanan. A model of load sharing between muscles and soft tissues at the human knee during static tasks. *Journal of Biomechanical Engineering*, 118(3):367–376, 1996.
- D. G. Lloyd and T. S. Buchanan. Strategies of muscular support of varus and valgus isometric loads at the human knee. *Journal of Biomechanics*, 34(10):1257–1267, 2001.
- D. G. Lloyd, T. S. Buchanan, and T. F. Besier. Neuromuscular biomechanical modeling to understand knee ligament loading. *Medicine and Science in Sports and Exercise*, 37(11):1939–1947, 2005.
- D. G. Lloyd, M. Reggiani, M. Sartori, and C. Pizzolato. [Internet]. CEINMS - Calibrated EMG-Informed NeuroMusculoSkeletal Model. Available from: <http://simtk.org/home/ceinms>, 2014.
- K. Manal and T. S. Buchanan. A one-parameter neural activation to muscle activation model: estimating isometric joint moments from electromyograms. *Journal of Biomechanics*, 36(8):1197–1202, 2003.
- K. Manal and T. S. Buchanan. An electromyogram-driven musculoskeletal model of the knee to predict in vivo joint contact forces during normal and novel gait patterns. *Journal of Biomechanical Engineering*, 135(2):021014, 2013.
- K. Manal, R. V. Gonzalez, D. G. Lloyd, and T. S. Buchanan. A real-time EMG-driven virtual arm. *Computers in Biology and Medicine*, 32(1):25–36, 2002.
- K. Manal, D. Kumar, K. S. Rudolph, and T. Buchanan. Joint loading during gait in those with medial compartment knee osteoarthritis and healthy controls. In *Proc. World Congress of Biomechanics*, page VI, 2010.
- A. Mantoan and M. Reggiani. [Internet]. Matlab MOtion data elaboration TOolbox for NeuroMusculoSkeletal apps (MOtoNMS). Available from: <http://simtk.org/home/motonms>, 2014a.
- A. Mantoan and M. Reggiani. *MOtoNMS - matlab MOtion data elaboration TOolbox for NeuroMusculoSkeletal applications - User Manual*, 2014b. Available from <http://goo.gl/Ukrw5B> and from <http://rehabenggroup.github.io/MOtoNMS/>.
- A. Mantoan and M. Reggiani. [Internet]. opensim preprocessing scripts. Available from: <https://github.com/RehabEngGroup/OpenSimProcessingScripts>, 2014c.
- S. T. McCaw, J. K. Gardner, L. N. Stafford, and M. R. Torry. Filtering ground reaction force data affects the calculation and interpretation of joint kinetics and energetics during drop landings. *Journal of Applied Biomechanics*, 29(6):804–809, 2013.
- S. M. McGill. A myoelectrically based dynamic three-dimensional model to predict loads on lumbar spine tissues during lateral bending. *Journal of Biomechanics*, 25(4):395–414, 1992.
- L. L. Menegaldo and L. F. De Oliveira. Effect of muscle model parameter scaling for isometric plantar flexion torque prediction. *Journal of Biomechanics*, 42(15):2597–2601, 2009.

- L. L. Menegaldo and L. F. Oliveira. The influence of modeling hypothesis and experimental methodologies in the accuracy of muscle force estimation using EMG-driven models. *Multibody System Dynamics*, 28(1):21–36, 2012.
- L. L. Menegaldo, L. F. de Oliveira, and K. K. Minato. EMGD-FE: an open source graphical user interface for estimating isometric muscle forces in the lower limb using an EMG-driven model. *Biomedical Engineering Online*, 13(1):37, 2014.
- H. S. Milner-Brown, R. B. Stein, and R. Yemm. Changes in firing rate of human motor units during linearly changing voluntary contractions. *The Journal of Physiology*, 230(2):371–390, 1973.
- Motion Lab Systems. [Internet]. The C3D File Format User Guide. Available from: http://www.c3d.org/pdf/c3dformat_ug.pdf, 2008.
- Motion Lab Systems. [Internet]. The 3D Biomechanics Data Standard. Available from: <http://www.c3d.org/>, 2014.
- R. R. Neptune, S. A. Kautz, and F. E. Zajac. Contributions of the individual ankle plantar flexors to support, forward progression and swing initiation during walking. *Journal of Biomechanics*, 34(11):1387–1398, 2001.
- M. F. Norcross, T. J. Blackburn, and B. M. Goerger. Reliability and interpretation of single leg stance and maximum voluntary isometric contraction methods of electromyography normalization. *Journal of Electromyography and Kinesiology*, 20(3):420–425, 2010.
- M. A. Nussbaum and D. B. Chaffin. Lumbar muscle force estimation using a subject-invariant 5-parameter EMG-based model. *Journal of Biomechanics*, 31(7):667–672, 1998.
- L. F. Oliveira and L. L. Menegaldo. Input error analysis of an EMG-driven muscle model of the plantar flexors. *Acta of Bioengineering and Biomechanics*, 14(3):75–81, 2012.
- Documentation OpenSim. [Internet]. gait2392 and 2354 models. Available from: <http://simtk-confluence.stanford.edu:8080/display/OpenSim/Gait+2392+and+2354+Models>, 2013.
- N. Palastanga and R. Soames. *Anatomy and Human Movement, Structure and function with PAGEBURST Access, 6: Anatomy and Human Movement*. Elsevier Health Sciences, 2011.
- M. G. Pandy. Computer modeling and simulation of human movement. *Annual Review of Biomedical Engineering*, 3(1):245–273, 2001.
- M. G. Pandy and T. P. Andriacchi. Muscle and joint function in human locomotion. *Annual Review of Biomedical Engineering*, 12:401–433, 2010.
- G. Paul and S. Wischniewski. Standardisation of digital human models. *Ergonomics*, 55(9):1115–1118, 2012.
- S. Piazza. Muscle driven forward dynamic simulations for the study of normal and pathological gait. *Journal of NeuroEngineering and Rehabilitation*, 3(1):5, 2006.
- J. R. Potvin and S. H. M. Brown. Less is more: high pass filtering, to remove up to 99% of the surface EMG signal power, improves EMG-based biceps brachii muscle force estimates. *Journal of Electromyography and Kinesiology*, 14(3):389–399, 2004.

- J. R. Potvin, R. W. Norman, and S. M. McGill. Mechanically corrected EMG for the continuous estimation of erector spinae muscle loading during repetitive lifting. *European Journal of Applied Physiology and Occupational Physiology*, 74(1-2):119–132, 1996.
- J. A. Reinbolt, A. Seth, and S. L. Delp. Simulation of human movement: applications using OpenSim. *Procedia IUTAM*, 2:186–198, 2011.
- D. J. Reinkensmeyer, P. Bonato, M. L. Boninger, L. Chan, R. E. Cowan, B. J. Fregly, M. M. Rodgers, et al. Major trends in mobility technology research and development: overview of the results of the nsf-wtec european study. *Journal of NeuroEngineering and Rehabilitation*, 9(22), 2012.
- B. D. Roewer, K. R. Ford, G. D. Myer, and T. E. Hewett. The impact of force filtering cut-off frequency on the peak knee abduction moment during landing: artefact or artifice? *British Journal of Sports Medicine*, 48(6):464–468, 2014.
- J. Rueterbories, E. G. Spaich, B. Larsen, and O. K. Andersen. Methods for gait event detection and analysis in ambulatory systems. *Medical Engineering & Physics*, 32(6):545–552, 2010.
- M. Sartori. *A Neuromuscular human-machine interface for applications in rehabilitation robotics*. PhD thesis, University of Padova, 2011.
- M. Sartori, M. Reggiani, D. Farina, and D. G. Lloyd. EMG-driven forward-dynamic estimation of muscle force and joint moment about multiple degrees of freedom in the human lower extremity. *PLOS ONE*, 7(12):e52618, 12 2012a.
- M. Sartori, M. Reggiani, E. Pagello, and D. G. Lloyd. Modeling the human knee for assistive technologies. *IEEE Transactions on Biomedical Engineering*, 59(9):2642–2649, 2012b.
- M. Sartori, L. Gizzi, D. G. Lloyd, and D. Farina. A musculoskeletal model of human locomotion driven by a low dimensional set of impulsive excitation primitives. *Frontiers in Computational Neuroscience*, 7(79), 2013.
- M. Sartori, D. Farina, and D. G. Lloyd. Hybrid neuromusculoskeletal modeling to best track joint moments using a balance between muscle excitations derived from electromyograms and optimization. *Journal of Biomechanics*, 47(15):3613–3621, 2014.
- L. Scheys, A. Spaepen, P. Suetens, and I. Jonkers. Calculated moment-arm and muscle-tendon lengths during gait differ substantially using mr based versus rescaled generic lower-limb musculoskeletal models. *Gait & Posture*, 28(4):640–648, 2008.
- L. M. Schutte, M. M. Rodgers, F. E. Zajac, and R. M. Glaser. Improving the efficacy of electrical stimulation-induced leg cycle ergometry: an analysis based on a dynamic musculoskeletal model. *IEEE Transactions on Rehabilitation Engineering*, 1(2): 109–125, 1993.
- A. Seth. [Internet]. Preprocess for Opensim. Available from: <https://simtk.org/home/opensim-utils>, 2008.
- Q. Shao, D. N. Bassett, K. Manal, and T. S. Buchanan. An EMG-driven model to estimate muscle forces and joint moments in stroke patients. *Computers in Biology and Medicine*, 39(12):1083–1088, 2009.
- L. M. Shutte. *Using musculoskeletal models to explore strategies for improving performance in electrical stimulation-induced leg cycle ergometry*. PhD thesis, Stanford University, 1992.

- D. Staudenmann, J. R. Potvin, I. Kingma, D. F. Stegeman, and J. H. van Dieën. Effects of EMG processing on biomechanical models of muscle joint systems: sensitivity of trunk muscle moments, spinal forces, and stability. *Journal of Biomechanics*, 40(4):900–909, 2007.
- D. Staudenmann, K. Roeleveld, D. F. Stegeman, and J. H. Van Dieën. Methodological aspects of SEMG recordings for force estimation—a tutorial and review. *Journal of Electromyography and Kinesiology*, 20(3):375–387, 2010.
- K. M. Steele, A. Seth, J. L. Hicks, M. S. Schwartz, and S. L. Delp. Muscle contributions to support and progression during single-limb stance in crouch gait. *Journal of Biomechanics*, 43(11):2099–2105, 2010.
- D. Testi, P. Quadrani, and M. Viceconti. Physiomespace: digital library service for biomedical data. *Philosophical Transactions of the Royal Society A: Mathematical, Physical & Engineering Sciences*, 2012.
- The Free Software Foundation. [Internet]. GNU General Public License. Available from: <http://www.gnu.org/licenses/gpl.html>, 2013.
- D. G. Thelen, A. B. Schultz, S. D. Fassois, and J. A. Ashton-Miller. Identification of dynamic myoelectric signal-to-force models during isometric lumbar muscle contractions. *Journal of Biomechanics*, 27(7):907–919, 1994.
- G Valente. *Subject-specific musculoskeletal models of the lower limbs for the prediction of skeletal loads during motion*. PhD thesis, University of Bologna, 2013.
- G. Valente, L. Pitto, D. Testi, A. Seth, S. L. Delp, R. Stagni, M. Viceconti, and F. Taddei. Are subject-specific musculoskeletal models robust to the uncertainties in parameter identification? *PloS one*, 9(11):e112625, 2014.
- A. J. Van den Bogert and J. J. De Koning. On optimal filtering for inverse dynamics analysis. In *Proceedings of the IXth biennial conference of the Canadian society for biomechanics*, pages 214–215, 1996.
- A. J. Van den Bogert, C. Janssen, and W. Herzog. Isometric properties of lower extremity muscles in cyclists determined by least-squares fitting of muscle models. In *Proceeding of XIVth ISB Conference*, pages 1382–1383, 1993.
- L. J. Van Ruijven and W. A. Weijts. A new model for calculating muscle forces from electromyograms. *European Journal of Applied Physiology and Occupational Physiology*, 61(5-6):479–485, 1990.
- M. Viceconti, C. Zannoni, D. Testi, M. Petrone, S. Perticoni, P. Quadrani, F. Taddei, S. Imboden, and G. Clapworthy. The multimod application framework: a rapid application development tool for computer aided medicine. *Computer Methods and Programs in Biomedicine*, 85(2):138–151, 2007.
- D. W. Wagner, V. Stepanyan, J. M. Shippen, M. S. DeMers, R. S. Gibbons, B. J. Andrews, G. H. Creasey, and G. S. Beaupre. Consistency among musculoskeletal models: caveat utilitor. *Annals of Biomedical Engineering*, 41(8):1787–1799, 2013.
- S. C. White and D. A. Winter. Predicting muscle forces in gait from EMG signals and musculotendon kinematics. *Journal of Electromyography and Kinesiology*, 2(4):217–231, 1992.
- C. R. Winby, D. G. Lloyd, and T. B. Kirk. Evaluation of different analytical methods for subject-specific scaling of musculotendon parameters. *Journal of Biomechanics*, 41(8):1682–1688, 2008.

- C. R. Winby, D. G. Lloyd, T. F. Besier, and T. B. Kirk. Muscle and external load contribution to knee joint contact loads during normal gait. *Journal of Biomechanics*, 42(14):2294–2300, 2009a.
- C. R. Winby, D. G. Lloyd, T. F. Besier, and T. B. Kirk. Muscle and external load contribution to knee joint contact loads during normal gait. *Journal of Biomechanics*, 42(14):2294–2300, 2009b.
- D. A. Winter. *Biomechanics and motor control of human movement*. John Wiley & Sons, 2009.
- J.J. Woods and B. Bigland-Ritchie. Linear and non-linear surface EMG/force relationships in human muscles: and anatomical/functional argument for the existence of both. *American Journal of Physical Medicine & Rehabilitation*, 62(6):287–299, 1983.
- G. T. Yamaguchi, A. G. U. Sawa, D. W. Moran, M. J. Fessler, and J. M. Winters. *A survey of human musculotendon actuator parameters*, pages 717–773. New York: Springer-Verlag, 1990.
- F. E. Zajac. Muscle and tendon: properties, models, scaling, and application to biomechanics and motor control. *CRC Critical Review of Biomedical Engineering*, 17:359–411, 1989.
- F. E. Zajac. Muscle coordination of movement: a perspective. *Journal of Biomechanics*, 26:109–124, 1993.
- F. E. Zajac, R. R. Neptune, and S. A. Kautz. Biomechanics and muscle coordination of human walking: part ii: lessons from dynamical simulations and clinical implications. *Gait & Posture*, 17(1):1–17, 2003.